

Republic of Iraq
Ministry of Higher Education
and Scientific Research



***NONLINEAR ANALYSIS OF CELLULAR
PLATE STRUCTURES WITH LINEARLY
VARYING DEPTH***

A Thesis

**Submitted to the College of Engineering
of the University of Babylon in Partial
Requirements of the Fulfillment
for the Degree of Master
of Science in Civil
Engineering**

By

MUNA-HATIM JABEER

Supervised by

**ASST. PROF.DR. NAMEER A.ALWASH
ASST. PROF. DR. MUSTAFA B.DAWOOD**

جمهورية العراق
وزارة التعليم العالي والبحث العلمي



التحليل الأخطي للمنشآت المخلوية ذات عمق متغير خطياً

رسالة

مقدمة إلى كلية الهندسة في جامعة بابل
كجزء من متطلبات نيل درجة الماجستير
في علوم الهندسة المدنية

من قبل

منى حاتم جابر

أشرف

الدكتور نمير عبد الامير علوش
الدكتور مصطفى بلاسم

بِسْمِ اللَّهِ الرَّحْمَنِ الرَّحِيمِ

وفوق كل ذي علم عليم

صدق الله العلي العظيم

المنشأ اللوحي الخلوي ذو الحواجز المتغيرة العمق يشيد من لوحين علوية و سفلية مفصولتين بحواجز طولية متغيرة العمق و عرضية مستقيمة. أن كفاءة هذا النوع من المنشآت تأتي من مقاومتها العالية وخفة وزنها. مثل هذه المنشآت تستعمل بكثرة في أرضيات الجسور , أجنحة الطائرات , قيعان السفن و الحالات الأخرى التي تكون فيها المقاومة العالية و خفة الوزن من العوامل التصميمية المهمة.

تم تطوير طريقة تشابه المشبكات المبسطة لتكون قادرة على التنبؤ بالسلوكية اللاخطية وحسب المقاومة القصوى لهذا النوع من المنشآت الخلوية. يتم تسليط الأحمال بصورة متزايدة للتعامل خطوة بخطوة مع كلا نوعي الاستجابة اللاخطية (اللاخطية الهندسية و اللاخطية المادية).

اللاخطية الهندسية تحصل نتيجة السلوكية ما بعد الانبعاج للشفة المنضغطة أو الحواجز أو كليهما. تم اعتماد مبدأ (فون كارمن) للعرض المؤثر لمتابعة سلوكية الشفة المنضغطة عند حدوث الانبعاج , بينما استخدمت طريقة (رو كي) بعد إدخال بعض التعديلات عليها لتكون ملائمة لتتبع التحمل الأقصى للحواجز الطولية و العرضية غير المتوازية والسلوكية ما بعد الانبعاج.

تم تبني مبدأ المفصل اللدن لتمثيل اللاخطية المادية التي تحصل نتيجة وصول الاجهادات في بعض المناطق القيمة إجهاد الخضوع لمادة المنشأ . إن الطريقة المقترحة تم برمجتها بواسطة برنامج خاص على الحاسوب تم تطبيقه على عدة أمثلة , حيث ظهر توافق جيد لنتائج الهطول الشاقولي و المقاومة القصوى كان الفرق بالنتائج يتراوح بين (٦% الى ٣٠%) بالهطول و(١.٦٧% الى ٥٠%) بالحمل للأمثلة المستخدمة.

ABSTRACT

A cellular plate structure for the linear varying depth is constructed of top and bottom flange plates separated by longitudinal non-prismatic and transverse prismatic webs. The efficiency of such form of construction arises from its high strength to weight ratio. It is widely used in bridge decks, aircraft wings, ship bottoms and other situations where strength and reduction of self-weight are important design objectives.

The simplified grillage approach is extended to investigate the nonlinear post-buckling behavior and ultimate strength of such structures. An incremental loading procedure is adopted to follow step by step both types of nonlinear responses (geometric and material nonlinearities).

The Geometric nonlinearity is due to the post-buckling behavior of the compression flange and/or panels. *Von Karman's* effective width concept is utilized to follow the post-buckling behavior of the compression flange panel. *Rockey's* approach for the ultimate load determination is used with some modifications to predict the post-buckling and ultimate strength of the linear varying depth web panel.

A plastic hinge approach is adopted to investigate the material nonlinearity which arises due to the occurrence of local yielding in the component plates.

Based on the suggested simplified method, a computer program is modified and applied to several examples. Results of vertical deflections and ultimate loads predicted by the proposed grillage method are found to be in good agreement. The differences at ultimate state about from (1% to 3%) in deflection and from (1.67% to 0%) in ultimate load in the examples considered herein.

LIST OF CONTENTS

<i>ACKNOWLEDGMENT</i>	<i>i</i>
<i>CONTENTS</i>	<i>ii</i>
<i>NOTATIONS</i>	<i>vi</i>
<i>ABSTRACT</i>	<i>iiix</i>

Chapter One *INTRODUCTION*

1- 1	<i>General</i>	<i>1</i>
1- 2	<i>Usage of Thin Walled Structures</i>	<i>1</i>
1- 3	<i>Characteristic Feature of Thin Walled Section</i>	<i>3</i>
1- 4	<i>Construction</i>	<i>3</i>
1- 5	<i>The Need For Simplified Analysis For Cellular</i>	<i>5</i>
	<i>Plate Structure</i>	
1- 6	<i>Objectives of The Present Study</i>	<i>5</i>

Chapter Two **REVIEW OF LITERATURE**

2-1	<i>Introduction</i>	
		1
2-2	<i>Application of Grillage Analogy To Linear</i>	
		1
		ii
	<i>Linear Analysis of Cellular Plate Structures</i>	
2-2	<i>Review of Literature OnNonlinear Analysis</i>	
		12
	<i>of Plate Structures</i>	

Chapter Three **EVALUATION OF SECTION PROPERTIES**

3-1	<i>Introduction</i>	17
3-2-1	<i>Flexural Rigidities</i>	
		17
3-2-2	<i>Torsional Rigidities</i>	
		19
3-2-3	<i>Shearing Rigidity</i>	
		24

۳-۲-۴	Warping Moment of Inertia	۲۴
-------	---------------------------	----

Chapter Four GRILLAGE ANALOGIES

۴- ۱	<i>Introduction</i>	۲۷
۴- ۲	<i>Inclusion of Warping Implicitly With Torsional Stiffness</i>	۲۷
۴- ۲- ۱	<i>Member with One End Restrained</i>	۲۹
۴- ۲- ۲	<i>Member with Two Ends Restrained</i>	۳۰
۴- ۳	<i>Grillage Analysis</i>	۳۱
۴- ۳- ۱	<i>Stiffness Matrix For Straight Member</i>	۳۱
۴- ۳- ۲	<i>Stiffness Matrix For Non-Prismatic Member</i>	۳۴

Chapter Five NONLINEAR BEHAVIOR OF CELLULAR PLATE

STABILITY ANALYSIS

۵- ۱	<i>Plate Stability</i>	۴۴
۵- ۱- ۱	<i>Material Nonlinearity</i>	۴۵
۵- ۱- ۲	<i>Geometric Nonlinearity</i>	۴۵
۵- ۱- ۳	<i>Necessary Assumptions</i>	۴۶

Post-Buckling Behavior of Compression

۴۷

Flange Panel

۵-۲-۱	<i>Introduction</i>	۴۷
۵-۲-۲	<i>Evaluation of Elastic Critical Stress</i>	۴۸
۵.۲.۳	<i>Post-Buckling Behavior</i>	۵۲
۵.۲.۳.۱	<i>Effective Width Expression</i>	۵۳
۵.۳	<i>Post-Buckling Behavior of Web Panel</i>	۵۶
۵.۳.۱	<i>Introduction</i>	۵۶
۵.۳.۲	<i>Evaluation of Elastic Critical Shearing Stress</i>	۵۷
۵.۳.۳	<i>Review of Failure Theories for Web Panels</i>	۶۰
۵.۳.۴	<i>Proposed interaction diagram</i>	۶۲
۵.۳.۵	<i>Rockey's Method</i>	۶۴
۵.۴	<i>Computational Technique</i>	۷۹
۵.۵	<i>Interpretation of Output</i>	۸۱
۵-۶	<i>Computer Program (NONLINEAR)</i>	۸۲
۵-۶	<i>Summary of The Present Study</i>	۸۲

Chapter Six APPLICATION AND DISCUSSION OF RESULTS

۶-۱	<i>Introduction</i>	۸۴
۶-۲	<i>Plated Structures Simply Supported at All Edges</i>	۸۴

7-3	<i>Plated Structures Fixed at All Edges</i>	94
7-4	<i>Cantilever Cellular Plated Structure</i>	102
7-3	<i>Plated Structures simply supported at</i>	
113	<i>All Edges</i>	

Chapter Seven

CONCLUSION AND RECOMMANDATION

7.1	<i>Conclusions</i>	117
7.2	<i>Recommendations</i>	119

LIST OF FIGURE

Fig. 1-1

Cellular box girder

2

Fig. 1-2 *Torsional behavior of thin-walled members*

4

Fig ३- १	<i>Details of cellular plate structure</i>	
		११
Fig ३- २	<i>Shear flow in cellular plate structure</i>	२१
Fig ३- ३	<i>Determination of the sectorial area (ω) for</i>	
	<i>uniform multi closed section</i>	२६
Fig ३- ४	<i>Determination of the sectorial area (ω) for</i>	
	<i>non-uniform multi closed section</i>	२६
Fig ०- १	<i>Bi-linear stress-strain relation used for</i>	४६
	<i>transforming measured strains to stresses</i>	
Fig ०- २	<i>A plate under uniform uniaxial stress</i>	००
Fig ०- ३	<i>Stability of single plate with simply</i>	०२
	<i>Supported edges</i>	
Fig ०- ४	<i>Nonlinear stress distribution in buckled</i>	०४
	<i>Plate replaced by assumed uniform stress</i>	
Fig ०- ०	<i>Modes of failure of plate girder</i>	६३
Fig ०- ६	<i>Interaction digram between shear and</i>	६४
	<i>bending effect for web</i>	

<i>Fig 2- 7</i>	<i>Stage in web behavior up to collapse</i>	<i>77</i>
<i>Fig 2- 8</i>	<i>State of stress in web at post-buckling stage</i>	<i>78</i>
<i>Fig 2- 9</i>	<i>Free body diagram of compression flange</i>	<i>79</i>
<i>Fig 2- 10</i>	<i>Unsymmetrical section for the grillage member</i>	<i>77</i>

ACKNOWLEDGEMENT

﴿In The Name of Allah the Most Gracious, The Most Merciful﴾

*Before every thing and after every thing, praise is to be to my generous God (**Allah**) for providing me the willingness and strength to accomplish this work.*

*I would like to express my sincere appreciation and deepest gratitude to Ass. Prof. **Dr. Nameer A. Alwash** and Ass. Prof. **Dr. Mustafa Balasim**, who I had the honor of working under their supervision, for their guidance, valuable suggestions and continuous encouragement through all stages of this research.*

*I would like to express my sincere thanks with deepest respect to **Dr. Ammar Yaser Ali** the head of the civil engineering department.*

*Appreciation and thanks are due to, **Sadjad Amir Hemzah AL-Jowary** I, also wish to express my deepest thanks for all my friends who supported me thought the preparation of this work.*

I wish also to express my deepest thanks to all the staff of the civil engineering department.

Finally, the research extends her sincere gratitude to her parents and family for their patience endurance.

NOTATION

a	Half length of a cellular plate structure.
b	Half width of cellular plate structure.
a	Length of plate element.
A_f	Cross sectional area of flange.
A_{FC}, A_{FT}	Cross sectional areas of compression and tension flanges, respectively.
A_j	Area enclosed by the median line of the entire cross section of cell j.
A_{mn}	Amplitude of deflection of a plate.
A_v	Effective shear area of grillage beam element.
A_w	Cross sectional area of the web.
B	Width for the grillage member.
b	Width for the plate element.
B_e	Effective width of a cell due to shear lag effect.
b_e	Effective width of compression flange due post-buckling behavior.
b_{ey}	Effective width of compression flange(at yield).
C_c	Position of plastic hinge at the compression flange.
C_t	Position of plastic hinge at the tension flange.
d₁, d₂	Depth of a cellular plate structure (distance between Centerline of the flange) at the start and end of the grillage member respectively.
D_x, D_y	Flexural rigidities in x and y directions, respectively.

D_{xy}, D_{yx}	Torsional rigidities in x and y directions, respectively.
E	Modulus of elasticity.
$\{F'\}$	Force vector in local coordinate.
G	Total depth of cellular structure.
h	Clear distance between upper and lower flanges.
I	Second moment of area of a grillage beam element
J	Torsional constant of a grillage beam element
K	Coefficient of buckling.
$[K], [K']$	Stiffness matrix in global and local coordinates.
L	Length of a grillage beam element.
M_f	Plastic moment of resistance provided by flange alone.
M_{pfc}	Plastic moment capacity of the compression flange.
M_{pft}	Plastic moment capacity of the tension flange.
M'_{pfc}	Reduced plastic moment capacity of the compression flange.
M'_{pft}	Reduced plastic moment capacity of the tension flange.
M^*_{pc}	Non-dimensional strength parameter compression flange.
M^*_{pt}	Non-dimensional strength parameter of the tension flange.
M_{pw}	Plastic moment of resistance of the web plate acting alone.
M_{ult}	Ultimate moment capacity
N_x, N_y	Membrane normal forces (per unit width) in the x and y Directions, respectively.
N_{xy}, N_{yx}	Membrane shearing forces (per unit width) in the x and y Directions, respe

$\{P\}$	Applied accumulated incremental load vector.
$\{\Delta P\}$	Applied incremental load vector.
$[T]$	Transformation matrix.
t_{fc}	Thickness of compression flange.
T_{bm}	Torsion bimoment
t_{ft}	Thickness of tension flange.
t_w	Thickness of the exterior webs in x and y directions.
t_{wx}	Thickness of the interior webs in x directions.
t_{wy}	Thickness of the interior webs in y directions.
U	Total strain energy.
U_b	Strain energy due to bending.
U_s	Strain energy due to transverse shear.
U_s	Strain energy due to transverse shear.
U_w	Strain energy due to warping.
V	Shearing force.
V_c	Shearing capacity of the web corresponding to the plastic Moment of resistance provided by flange (M_F).
V_s	Shearing capacity of the web associated with applied Moment up to (M'_s).
V_{ult}	Ultimate shearing capacity of the web.
V_{yw}	Shearing force required to make the web fully plastic.
W	Transverse deflection of plate.
$\{X\}$	Accumulated incremental displacement vector.
λ	Distance from the neutral axis to the centerline of the compression flange.
$\{\Delta X\}$	Incremental displacement vector.
$\{\Delta'\}$	Displacement vector in local coordinate.

θ	Rate of twist.
ν	Poisson's ratio.
$\sigma, \bar{\sigma}$	Direct (normal) stresses acting on two orthogonal planes
σ_{cf}, σ_{tf}	Average normal stresses in the compression and tension flanges, respectively.
σ_x	Normal stress in the x direction.
$\sigma_{x(cr)}$	Critical buckling stress of the compression flange.
σ_t	Membrane tensile stress.
σ_t^y	Membrane tensile stress that cause yielding in the web.
σ_{yf}	Yield stress of the flange material.
σ_{yw}	Yield stress of the web material.
τ	Shearing stress.
τ_{cr}	Critical shearing stress.
ϕ	Angle of inclination between the local and global axes of a grillage beam.
Φ, Φ_r	Inclination of the compression and tension flanges, respectively, when applying a virtual displacement.

Note: Other notations (not listed here) are defined as they appear in the text.

ABBREVIATIONS

AASHTO	American Association of Steel Highway and transportation Official.
AISC	American Institute of Steel Construction.
AISI	American Iron and Steel Institute.
ASCE	American Society of Civil Engineers
ASME	American Society of Mechanical Engineers.
LRFD	Load and Resistance Factor Design.
SSRC	Structure Stability Research Council

APPEDEX B Sample of data file for Plated Structure Fixed at All Edges

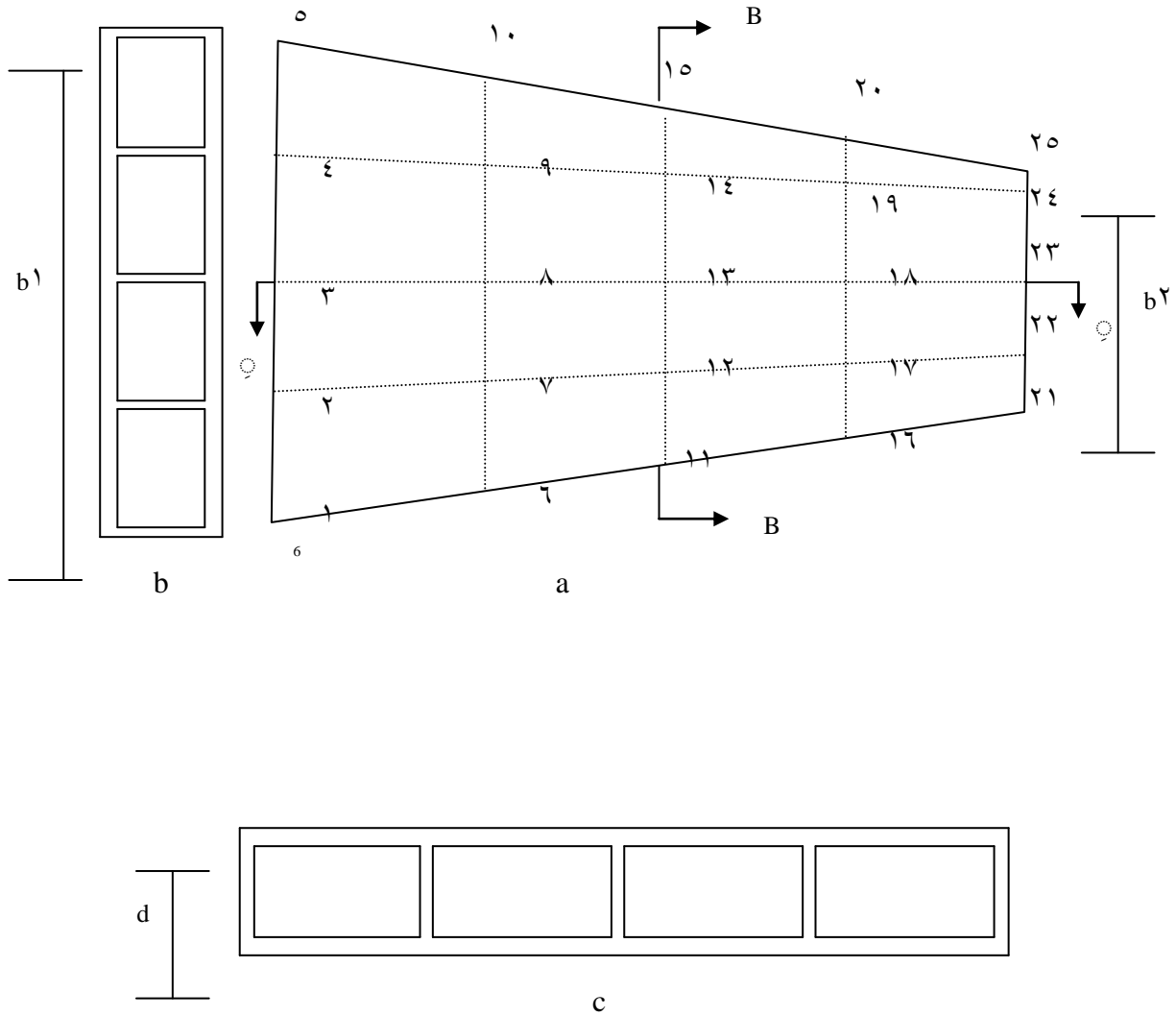
Fixed at ξ Edges		

Tf,Tw,D \backslash ,D γ / Inc,Fy/ NCM,NCH,ND,NL,Ls		
1.	1.	0.0 1.000
0.0	2.40	
ξ	ξ	1 1 2.000
No. of Riest. D.O.F / No. of Loaded Node		
7.4		9
Node No./ D.O.F./D.O.Ries.		
1	1	.
1	2	.
1	3	.
1	4	.
2	1	.
2	2	.
2	3	.
2	4	.
.	.	.
.	.	.
.	.	.
20	1	.
20	2	.
20	3	.
20	4	.
Loaded Node/D.O.F/ Load Value		
7	3	-1.0000
8	3	-1.0000
9	3	-1.0000
.	.	.
.	.	.
.	.	.
.	.	.
Modulus of Elasticity/ Poisson Ratio		
2.00000		.3

Where:

- Inc* = No. of Increment
- Fy* = Yield Stress of Steel
- NCM* = No. of Cell in Y Direction
- NCH* = No. of Cell in X Direction
- ND* = No. of Division Per Cell in Y Direction
- NL* = No. of Division Per Cell in X Direction
- Ls* = Length of Straight Member
- D \backslash ,D γ* = depth in the first and last end

Appendix (c)



a-Plan b-Section (B-B) c-Section(A-A)

Cellular plate structure for linear varying width

Chapter One

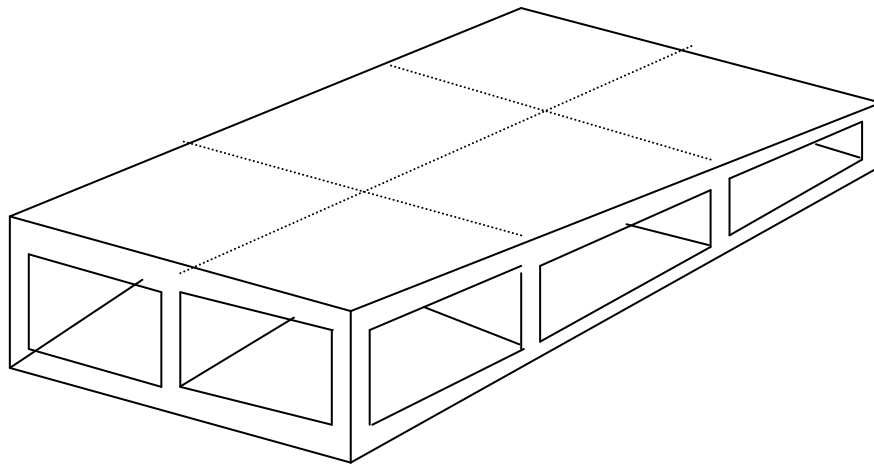
INTRODUCTION

1- 1 General

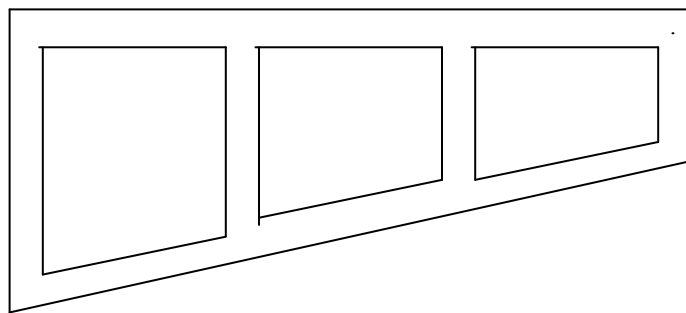
Thin-walled structures are made from thin plates joined along their edges. Thin-walled cellular structures consist of top and bottom flange plates, separated by a combination of longitudinal and transverse webs. The depth of the longitudinal webs may be varied as shown in fig.(1.1). The thickness of plate is small compared with the other dimensions and with the overall length of the member. Thin-walled structures which provide high stiffness and strength with relative small weight, are often used in many modern engineering construction. The property of these structures is that they are really light compared with alternative structures. Therefore they are used in long span bridges and other structures where weight and cost are of prime consideration. According to that using thin-walled cellular plates is that the materials are concentrated at the locations of stresses concentration. The top and bottom flanges take predominantly the flexural stresses while webs take the transverse shearing stresses.

1- 2 Usage of thin walled structures

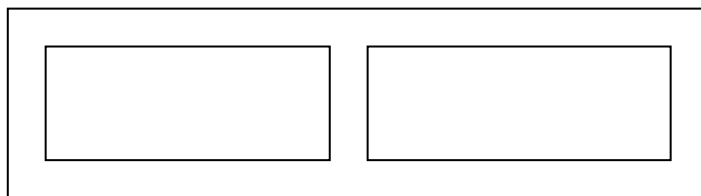
The multi-cellular plate structures represent an efficient form of construction. They are suitable and used in many structures, such as bridge decks, air craft wings, ship bottoms and any situations needing high strength to weight ratio. Utilizing the high strength for both bending and torsion and their light weight, they are used in large storage tanks and wide-span shells.



(a) cellular box girder with varying depth



(b) Longitudinal cell.



(c) Transverse cell.

Fig.(1. 1):cellular box girder

1- ۳ Characteristic Features of Thin Walled Section

The most important feature of thin-walled sections is their response to the torsional loading. For the solid and thick-walled sections, out-of-plane warping is usually small and secondary stress arising from warping restraint. Therefore it can be neglected. The applied torsion is assumed to be resisted entirely by a system of pure Saint-Venant shear stress. For the thin-walled sections, out-of-plane warping displacements resulting from torsional loading generally much larger. Open sections are more susceptible than closed sections in this regard. If these relatively much larger warping displacements are restrained, a system of longitudinal normal stresses (producing bimoment) is setting up. These may not be necessarily local in effect and may extend for a considerable distance from the point of restraint. Complementary warping stresses are also created which have the effect of modifying the transverse distribution of shear stress due to pure shear Fig. (1-۳).

1- ۴ Construction

Methods of construction of cellular plate structures depend on many factors such as the type and size of the structure and thickness of the plate. Generally, flanges and webs are composed of several weld or rivet connected pieces of plate. Webs may be made of flat plates with double angle section at top and bottom for connection with flanges or they have bent edges to become like wide channels Z- section or I- sections to facilitate the connection with flanges.

The procedure of construction, webs in the two directions are connected together and fixed to one of the flanges by means of welding rivets or bolts. The other flange is connected to the web piece by riveting to the protruding

plates at top of webs. The flange plates are assumed rigidly fixed to the webs plate for full interaction. .

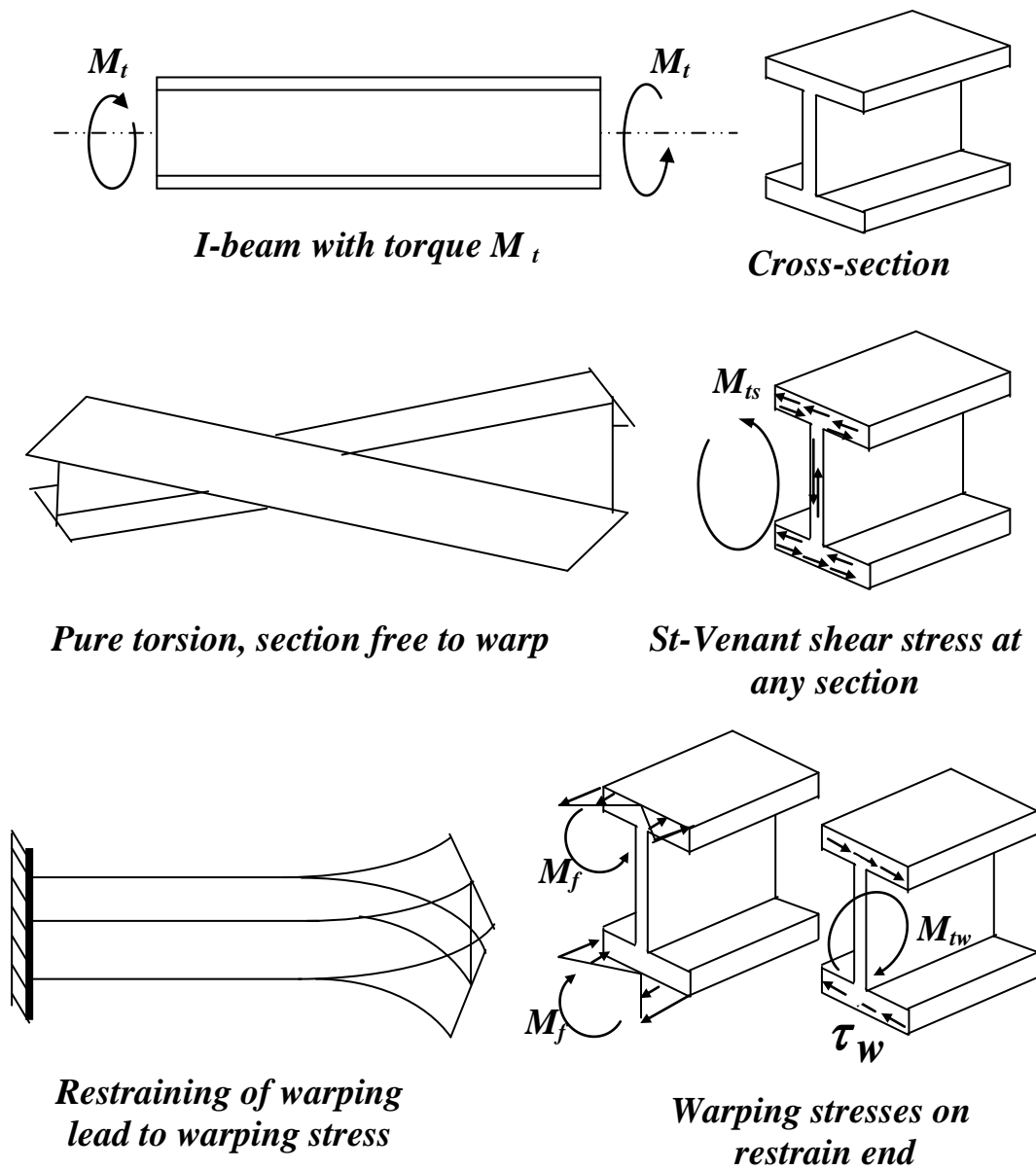


Figure (1- 7) Torsional Behavior of Thin-Walled Members

1- 0 The Need For Simplified Analysis For Cellular Plate Structure

The analysis of multi-cellular structures is complex because of the variety of structural geometry, and support conditions. In the last years, the development of finite element method and the availability of large capacity digital computers, make the analysis easier for plate structures of arbitrary geometry and boundary conditions and subjected to any loading conditions. Moreover, effects and modifying factors (such as shear lag, biaxial effect and composite actions) can be included in the analysis.

For solution of a cellular structure, the three-dimensional plate element programs require large computer capacity and considerable computing time and effort for data preparation (especially for those problems that deal with the analysis of structures in the nonlinear range and in the investigation of collapse load). Certainly, at the initial design stages when the designer is trying to optimize the proportion of the structure analysis, the cost involved in using the finite elements may become unfavorable.

There is a real need for a simplified computer method as an alternative to the finite element methods for use at the preliminary design stages and for quick and inexpensive analysis of plate structures insuring that the errors are not considerable. However, once the designer has established a reasonably efficient structure by repeated analysis using a simplified method, a final check by a sophisticated finite element method may be carried out.

1- 7 Objectives of the Present Study

The present study deals with the static (linear and non-linear) analysis of steel cellular plate structures with webs having varying depths. Such structures are constructed by two plate separated by vertical webs in each direction. These structures have varying depth in longitudinal direction as shown in fig. (1-1). For linear static grillage analysis of plate structures (such as cellular plate structures), the more accurate torsional properties of straight and non-prismatic thin-walled multi-cell members is obtained by including the effect of warping restraints. The effect of torsional warping may be significant in the behavior of structures made of thin-walled members.

The widely used grillage analogy method is a simplified discretization approach for the linear analysis of cellular plate structures. This method is extended to investigate the non-linear analysis and ultimate load behavior of cellular plate structures. In this grillage simulation a proper treatment with post-buckling and elastic-plastic analysis of cellular plate structures.

The cellular plate structures are assumed to fail under the action of high bending stresses, high shearing stresses or due to interaction between the two types of stresses. The analysis of ultimate load behavior of cellular plate structures deals with the effects of non-linearity arising from both material and geometric non-linearity. The effect of material non-linearity in the proposed grillage method is controlled by adopting analogy, A plastic hinge approach .

The geometric non-linearity arises from the problem of buckling in the compression flange and/or web panels which are taken into account by implementing *Von-Karman's* approach (effective width concept). Different assumptions regarding the effective width of compression flange are reviewed.

An incremental loading procedure is adopted and the results are presented to indicate the rate of convergence of the solution. The computer programs have been developed to perform static linear and non-linear analysis of the

problem. A numerical method is presented to evaluate the required sectional properties of closed sections, which are the main part of the problem.

1. ✓ Thesis Layout

The thesis consists of seven chapters.

Chapter one is the present introduction.

Chapter two presents a general review of literature on the use of different methods for analyzing the cellular plate structure.

Chapter three covers the evaluation of the elastic section properties required to analyze cellular plate structure as a two dimensional grillage.

Chapter four provides guidelines on the application of the grillage analogy in the nonlinear behavior of steel cellular plate structure.

Chapter five presents the nonlinear behavior and collapse load investigation of a steel cellular plate structure non-prismatic due to instability of the compression flange panels and/or the web panels and also due to the occurrence of local yielding in the highly stressed component plates.

Chapter six includes some exemplar models, which are analyzed using the suggested grillage method.

Chapter seven gives conclusions and suggests recommendations for future research related to this subject.

Chapter Two

REVIEW OF LITERATURE

2.1 Introduction

As mentioned in the previous chapter, the use of thin-walled sections has been increasing rapidly in many engineering structures. The cellular plate structure can be analyzed by various simplified and sophisticated methods. Some of these methods have been developed to be applied to non-linear analysis of cellular plate Structures.

In the review of previous works on the method of grillage for the analysis of cellular plate structure with varying depth, it is found that there was a very limited amount of studies on the analytical or numerical solution for the behavior of cellular plate structure with linear varying depth in the non-linear range and at ultimate load for me. In this chapter, the application of the grillage analogy for linear and non-linear analysis to general plate structures is reviewed.

2.2 Application of Grillage Analogy to Linear Analysis of Cellular Plate Structures

The use of grillage analogy to cellular plate structure has been well approved by published literatures. The study of **Husain** (1974)⁽²⁰⁾ was the

first one to idealize a cellular plate structure (aircraft cantilever cellular wing) as a grillage of orthogonally connected beams. He did not take into account the effect of transverse shear deformation of the webs and the shear lag phenomenon in the cover plates on the behavior of the structure. The grillage structure consisted of beams with flexural and torsional rigidities. The flexural rigidity of a grillage member was derived from the partitioning web together with attached top and bottom cover plates (as an I-section), while the torsional rigidity was derived from the torsional rigidities of the adjacent cell (as closed rectangular section). The deflections by the grillage analogy compared favorably with the available results and with a plane stress finite element. The method proposed by **Husain** presented a simple solution to the cellular plate structures with parallel webs.

Sawko and **Willcock** (1974)⁽¹⁰⁾ extended **Husain's** method to the analysis of cellular plate structure having variable section depth in the longitudinal direction. Several transverse webs (or diaphragms) were used to take into account the transverse shear rigidity. By comparing the grillage analogy with model test results, they concluded that cellular plate structures with several transverse webs could be analyzed by the grillage analogy including the effect of transverse shear distortions of cells.

Smyth and **Srinivasan** (1971)⁽¹¹⁾ applied the grillage analogy for the analysis of cellular bridge deck, which was trapezoidal in cross section and made of prestressed concrete. By comparing the grillage analogy results with model test and the equivalent space frame results, the grillage gave quit good results for the longitudinal action but required supplementary information for the transverse action (due to neglecting cell distortion).

Hambly and **Pennels** (1975)⁽¹²⁾ discussed the grillage analogy in the analysis of concrete cellular bridge decks having skew plan geometry and rectangular or trapezoidal cross sections. They discussed in details the

effect of cell distortion in cellular bridge decks. A method for calculating the torsional rigidity of the grillage members was proposed by considering the effect of shear flow in the top, bottom slabs and side webs only as one cell by neglecting the rather small shear flows in the intermediate webs. They have been the first to consider the effect of shear lag in calculating the flexural (or bending) rigidity of grillage beams through adopting the principle of effective flange width. The result of the analysis compared favorably with the result by the folded plate theory.

Evans and *Shanmugam* (1979)⁽³¹⁾ used the grillage approach for the analysis of steel cellular plate structures. In case where the spacing of webs in one direction is more than twice the spacing of webs in the other direction they proposed the use of intermediate (or fictitious) members between the main members to increase the accuracy of the grillage structure in idealizing the cellular plate structure and to avoid the incorrect assessment of effective widths of flanges. The intermediate fictitious members consisted of top and bottom flanges only (without web). In calculating the torsional constant of the grillage members, they proposed the same method by *Husain*⁽³⁰⁾. Like other investigators, they also neglected the effect of Poisson's ratio in calculating the flexural (or bending) rigidities of the grillage members. Thus, in the grillage idealization, the cellular structure is found to be more flexible when the results are compared with the finite element method.

Jaeger and *Bakht* (1982)⁽³²⁾ provided guidance on idealization of various types of bridge decks. In cellular structures, they suggested to neglect the interior webs or diaphragms and treat the whole cross section as a single cell for calculating the torsional constant. The value of the torsional constant for this single cell section was then distributed to the main grillage members in the section (almost the same suggestion by *Hambly* and *Pennels* (1972)⁽³³⁾

Mohammed (1994)⁽²⁸⁾ used various types of grillage analogy approaches for analyzing steel cellular plate structures with parallel webs and diaphragms. He also suggested to use effective modulus of elasticity $E^* = E / (1 - \nu^2)$ in calculating the flexural rigidity of the beams of the equivalent grillage. Thus, more rigidity (or stiffness) was given to the grillage. The results obtained by the grillage meshes compared favorably with the orthotropic plate method, the finite element method and with available experimental results.

Mohsin (1990)⁽²⁹⁾ extended **Mohammed** (28) work to analyze steel cellular plate structures with non-parallel webs and diaphragms, which are usually used in aircraft wing and some bridge decks and approaches. He also used three alternatives of grillage meshes to represent the cellular plate structure. Grillage analysis results were compared with orthotropic plate method and with finite element method.

Fairooz (1990)⁽³⁰⁾ analyzed a cellular bridge deck curved in plan by a grillage analogy. The cellular decks contained circumferential curved webs and radial straight webs (or diaphragms). The substitute grillage consisted of orthogonally connected curved and straight beams. Warping restraint effects were not included. The results showed a good agreement compared with the results by the three-dimensional shell elements.

Hasan (1991)⁽³¹⁾ presented a simplified space grillage analogy for the analysis of spherical cellular domes consisting of top and bottom plates with a grid of orthogonally connected arch webs. A method for calculating closed sections under restrained warping was suggested. Also, a method of interpretation of the result from the grillage outputs is presented.

Husain, Al-Ausi and Al-Azawi (1999)⁽³²⁾ presented a linear analysis of cellular and ribbed plate structures curved in plane including implicitly the effect of warping restraints. A more accurate torsional stiffness of straight and curved thin walled members was obtained by including the effect of

warping restraints. *Timoshenko's* concept ⁽¹¹⁾ of torsional warping was utilized for studying the torsional behavior of straight and curved thin-walled members. Results of solutions for straight and curved members were presented and compared with results from other studies and available results .

Methak, Al-Fatlawy (2001) ⁽¹²⁾ presented a linear analysis of plate structures with linear varying depth including implicitly the effect of warping restraints. A more accurate torsional stiffness of straight and non-prismatic thin walled members was obtained by including the effect of warping restraints. *Timoshenko's* concept ⁽¹¹⁾ of torsional warping was utilized for studying the torsional behavior of straight and non-prismatic thin-walled members. Results of solutions for straight and non-prismatic members were presented and compared with results from the finite element method using *NASTRAN* program.

2.2 Review of Literature On Nonlinear Analysis of Cellular Plate Structures

Fusjita and Yoshida (1977) ⁽¹³⁾ investigated the collapse due to buckling of arbitrarily shaped stiffened plated structures (such as cellular plate structures) used in ship design. An analytical method was formulated using an incremental finite element method with inclusion of elastic-plastic and large deflection non-linearities. In addition to the use of the triangular plate elements for plates and beam elements for stiffeners, beam elements were also used for components where girder behavior was predominated, thereby reducing the number of degree of freedom.

Shanmugam and Evans (1981) ⁽¹⁴⁾ suggested an extension to the grillage analogy, used for linear analysis of steel cellular plate structures, for analysis in the non-linear range and at collapse. The structures were assumed to have failed under the action of high bending stress only.

Regarding buckling of compression flange panels, these panels were assumed to be simply supported under uniaxial or biaxial compression and their post buckling behavior was controlled by implementing the effective width approach. An incremental loading procedure is adopted during which there would be continuous updating of the stiffness matrix.

Evans et al. (1989)⁽³³⁾ suggested development to the application of finite element method to the analysis of large deflection elastic –plastic behavior of plated structure. The analysis was applicable to structures with thin plates, which would operate in the post-buckling range. Therefore, the method took into account the effect of geometrical non-linearity arising from the plate buckling and the effect of material non-linearity due to the spread of yield during the approach to collapse. A four-noded rectangular element with five degrees of freedom per node was adopted for the solution. These degrees of freedom are three translational displacements plus two rotations around the two perpendicular axes in the plane of the plate. The drilling rotation (normal to the plane of the plate) was ignored.

Abdel Rahman and *Hinton* (1986)⁽³⁴⁾ presented a novel approach for linear and nonlinear finite element analysis of reinforced and prestressed concrete cellular slabs based on slab-beam model. The model consisted of *Mindlin* thick plate element to represent the upper and lower flanges and *Timoshenko* deep beam element to represent the webs or beam stiffeners. They assumed that the stiffeners are monolithically connected to the plate in order to produce identical displacement fields at the junction between the plate and the beam. This requirement is automatically satisfied by the presented model since the displacement functions used with *Mindlin* plate formulation and those adopted in *Timoshenko* beam formulations are related with each other. A computer program (*PLASAN*) was coded to implement the suggested idealization using various nonlinear solution

techniques. The results obtained from this program are compared with the available experimental results.

Harding (1990)^(٤٠) summarized the work undertaken by him and his colleagues, on the behavior of steel plated structures relating to bridges and offshore rings. His work demonstrated the power of the existed non-linear finite element programs in examining the non-linear behavior of structural component and how the results of organized parametric study can be used to formulate design guidance. The study showed the effects of using longitudinal and/or transverse stiffeners in the flanges or in the webs. It has clearly shown that these stiffeners affected considerably the local buckling of the component plates as well as the failure load.

Mashal (1991)^(٤١) used the grillage analogy to analyze cellular plate structures with parallel webs and diaphragms in their non-linear range and at collapse. Using the effective width approach represents the post-buckling behavior of the compression flange panel. The method proposed by **Rocky et al**^(٤٢) (for ultimate analysis of stiffened plate structures) was applied to represent the non-linear behavior of the web panels of the cellular plate structure. The result of vertical deflection and collapse load by the proposed simplified method showed good agreement when compared with those obtained from the finite element method using **NASTRAN** program.

Aldaami (2000)^(٤٣) used a spherical grillage analogy for thin-walled cellular and ribbed spherical domes. Linear and non-linear static and free vibration analyses were presented. The cellular dome consisted of double metal plate having a spherical shape and separated by meridian and hoop diaphragms. The flexibility and stiffness matrices of thin walled curved beams was given, warping restrain effect was taken into consideration. The results were compared with result obtained from the finite flat shell element

Al-Azawi (۲۰۰۱)^(۶) used the grillage method for both linear and nonlinear analysis of cellular plate structure curved in plan. Regarding the linear analysis, warping restrained effects was included. While in the nonlinear analysis, he extends *Mashal's* work to analyze cellular structure curved in plane. Also, the elastic buckling stresses in curved compression flange panels were evaluated by including the effect of the geometric curvature using the finite difference method in polar coordinates. Comparison of the results given by the proposed grillage method with the finite element method using (*NASTRAN*) package program verified the accuracy of the proposed method.

Younis M.H(۲۰۰۱)^(۹) used the grillage analogy to analysis of thin wall cellular plate structures with non-parallel webs and diaphragms in the nonlinear range. Both types of nonlinear response (material and geometrical nonlinearities) were considered. The post-buckling behavior of the compression flange panels was traced by depending on the effective width concept presented by *Von Karman*.^(۹) The result of vertical deflection and collapse load by the proposed simplified method showed a good agreement when compared with those obtained from the finite element method using *MSC/NASTRAN* program. The shape of the structure (as shown in Appendix C).

Al-Jowari S.A(۲۰۰۲)^(۹) used the grillage analogy for the analysis of horizontally curved cellular plate structures in the linear and nonlinear range. Both types of nonlinear response (material and geometrical nonlinearities) were considered. The post-buckling behavior of the compression flange panels was traced by depending on the effective width concept presented by *Von Karman*.^(۹) The result of vertical deflection and collapse load by the proposed simplified method showed a good

agreement when compared with those obtained from the finite element method using *NASTRAN* program.

From the preceding literature review, one can notice that no study is found that deals with the non-linear behavior of cellular plates with varying depth using grillage method and such problem will be considered in the present study.

Chapter Three

EVALUATION OF ELASTIC SECTION PROPERTIES

3.1 Introduction

In the present study the grillage analogy is used for analyzing cellular plate structures with web having varying depths.. The accuracy of this method depends largely on the proper evaluation of the section rigidities of the grillage members. Furthermore, the grillage analogy gives the designer a good appreciation and a feeling of how the actual structure behaves.

This chapter shows the techniques of grillage idealization of non-prismatic (linearly varying depth). The formulae for evaluation of different types of rigidities of the grillage elements are presented in this chapter.

3.2 Flexural Rigidities

Generally, two factors must be considered in calculating the flexural rigidities of the grillage members. These factors are the shear lag and poisson's ratio effects. A brief review of literature pertaining to the evaluation of flexural rigidities is presented herein as follows:

In representing a cellular plate structure by an equivalent plane grillage, many investigations (19, 20, and 21) considered the cross section of the grillage member as an I-section in calculating the moment of inertia (or second moment of area).

Basu and Dawson (1970) proposed the following equations for calculating the values of D_x and D_y for rectangular cellular plate structures

having top and bottom flanges of equal thickness, longitudinal webs with equal thickness and without transverse diaphragms

$$D_x = \frac{Et \nu_{xy} d^2}{2(1 - \nu_{xy} \cdot \nu_{yx})} \quad (3-1)$$

$$D_y = \frac{Et_1 d^2}{2(1 - \nu_{xy} \cdot \nu_{yx})} \quad (3-2)$$

where: -

$$\left. \begin{aligned} \nu_{xy} &= 1 - \frac{I t_x d}{6 t_{fc} B_x} \\ \nu_{yx} &= \nu \end{aligned} \right\} \quad (3-3)$$

all relevant notations are shown in Fig.(3-1)

Crisfield and *Twemlow* (1971)⁽³⁴⁾ proposed the following equations for calculating the flexural rigidities in(X and Y)direction for a rectangular cellular plate structure having flanges of equal thickness($t_{fc} = t_{ft}$), web thickness (t_x)and diaphragm thickness (t_y):

$$D_x = \frac{E}{(1 - \nu^2)} \frac{t_{fc} \cdot d^2}{2} + \frac{E \cdot t_x \cdot d^3}{12B_x} \quad (3-4)$$

$$D_y = \frac{E}{(1 - \nu^2)} \frac{t_{fc} \cdot d^2}{2} + \frac{E \cdot t_y \cdot d^3}{12B_y} \quad (3-5)$$

Cusens and *Pama* (1970)⁽³⁷⁾ suggested the following formula for calculating the flexural rigidity for a cellular plate structure having two unequal flange thickness (t_{fc} and t_{ft}) and web thicknesses ($t_x = t_y$):

$$D_x = \frac{E't_{ft}^3}{12} - \frac{E^*t_x^3}{6B_x} \left(e_{x1} - \frac{t_{ft}}{2} \right)^2 \left(e_{x2} - \frac{t_{ft}}{2} \right) + \frac{E^*t_x^3}{6B_x} \left(h + \frac{t_{ft}}{2} - e_{x1} \right)^2 \quad (3-7)$$

$$+ E't \left(h + \frac{t_{ft}}{2} - e_{x2} \right) + \left(h + \frac{1}{2}(t_{ft} + t_{fc}) \right) + \frac{E't_{fc}^2}{2} \left(h + \frac{t_{ft}}{2} - \frac{2t_{fc}}{3} \right)$$

$$E' = \frac{E}{1-\nu^2} \quad (3-7)$$

$$E^* = \frac{E}{\left(1 - \nu^2 \frac{t_x t_y}{B_x B_y} \right)} \quad (3-8)$$

where e_{x2} is the distance from the neutral axis of the cellular deck to the centerline of the upper flange in x-direction and other notations are shown in Fig.(3-1).

As discussed by *Cusens* and *Pama*⁽³⁷⁾ formula (3-7) is unwise (or clumsy) for practical use and only becomes of value if the vertical webs are particularly thick and closely spaced. *Jaeger* and *Bakth* (1972)⁽³⁸⁾ suggested to neglecting the effect of Poisson's ratio and the effect of the webs in calculating D_x and D_y and proposed the following formula:

$$D_x = D_y = E(t_{fc} \cdot e_{x1}^2 + t_{ft} \cdot e_{x2}^2) \quad (3-9)$$

9)

where e_x' and e_x , the distances from the neutral axis of the section to the centerlines of the lower and upper flanges respectively.

Mohammed (1994) derived the following formula for calculating D_x and D_y for a rectangular plate structure having two equal thicknesses ($t_{fc} = t_{ft}$) web thickness (t_x) and diaphragm thickness (t_y): -

$$D_x = \frac{E' t_{fc} d^2}{2} + \frac{E t_x d^3}{12 B_x} \quad (3-1)$$

$$D_y = \frac{E' t_{ft} d^2}{2} + \frac{E t_y d^3}{12 B_y} \quad (3-2)$$

These formulas are simple and satisfactorily accurate.

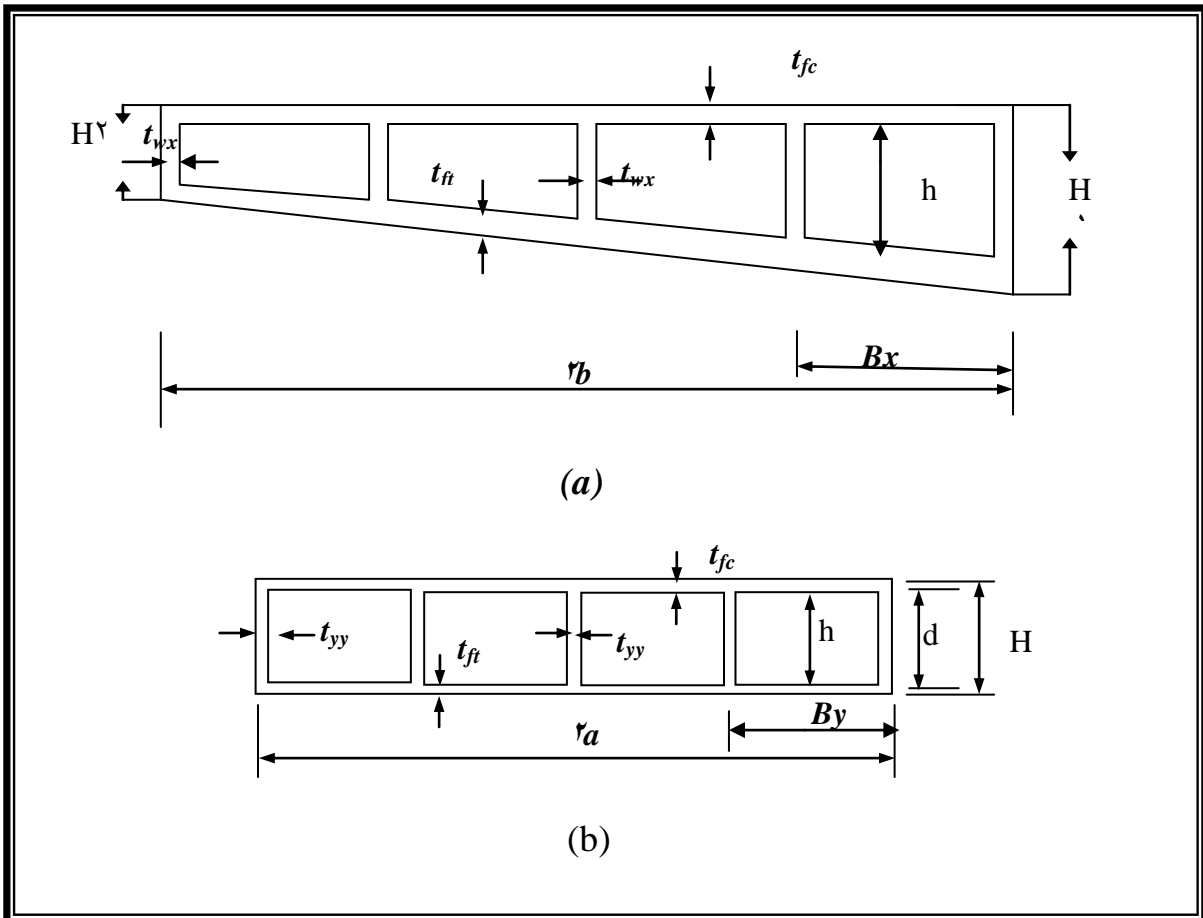


Figure (3-1) Details of cellular plate structure
 (a) Longitudinal section (b) Transverse section

3.2.2 Torsional Rigidities

As a cellular plate structure is twisted a network of shear flows develops around the flanges and webs, as shown in Fig. (3-2). Shear flow at any intermediate web represents the difference between the shear flows of adjacent cells. When the substitute grillage is twisted in the same manner of the cellular plate structure, the grillage torques are represented by the couples arising from the opposite shear flows in the top and bottom flanges, while the grillage shear force is directly represented by the shear flow in the webs.

Timoshenko and *Goodier* (1901) gave a procedure for the calculation of the torsional constant (J) of a cellular section under pure torsion and free to warp. The basic assumption used for establishing the torsional constant for a multi-cell is considering the shear flow in the walls, as shown in Fig. (3-2) and employing the membrane analogy. Fig. (3-2) shows the distribution of the shear flows in n -cells section. The n -independent shear flows are taken as unknown.

For three typical cell i, j and k the angle of twist per unit length θ (rate of twist) of the intermediate cell (j) is:

$$\theta_j = \frac{1}{2GA_j} \left[-q_i \int_w \frac{ds}{t} + q_j \int_c \frac{ds}{t} - q_k \int_w \frac{ds}{t} \right] \quad (3-2)$$

(3-2)

where:

$\int_w \frac{ds}{t}$ = the integral along the common webs of cells (i & j) and (j & k)

$\int_c \frac{ds}{t}$ = the contour integral around the cell (j)

A_j = the enclosed area of the cell (j)

The authors assumed that each cell rotates at the same rate of twist as for the whole section (θ), therefore:

$$\theta_1 = \theta_2 = \theta_3 = \dots = \theta_i = \theta_j = \theta_k = \dots = \theta_{n-1} = \theta_n \quad (3-13)$$

According to the membrane analogy, the twisting moment (M_t) in a cell is equal to twice the shear flow (q) in the wall of the cell times the area (A) inclosed by the median line of the cell:

$$M_t = 2 \cdot q \cdot A \quad (3-14)$$

Also, noting that:

$$M_t = G \cdot J \cdot \theta \quad (3-15)$$

Then:

$$J = \frac{2 \cdot q \cdot A}{G \cdot \theta} \quad (3-16)$$

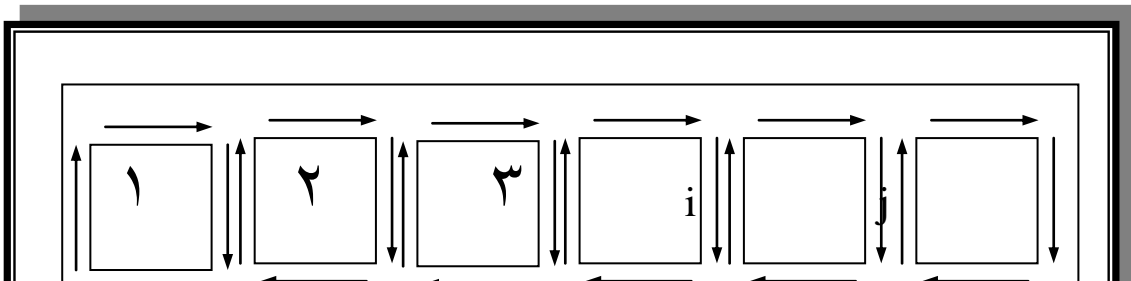
Husain (1974)⁽¹⁰⁾ proposed that the cellular plate structure is assumed to act as a series of independent closed tubes running in both longitudinal and transverse directions. The torsional constant for each cell is calculated from **Bredt's** formula:

$$J_i = \frac{4 \cdot A_i^2}{\int \frac{ds}{t}} \quad (3-17)$$

(17)

The torsional constant of the whole section (in any direction) is the summation of the torsional constants of the independent cells in that direction, as follows:

$$J = \sum_{i=1}^n J_i \quad (3-18)$$



Crisfield and *Twemlow* (1971)⁽²⁴⁾ and, *Hambly* and *Pannells* (1975)⁽²⁵⁾ calculated the torsional constant (per unit width) for a structure having unequal flange thickness ($t_{fc} \neq t_{ft}$) by using equation (3-14) and neglecting the contribution of the interior webs and dividing the result by two (as the torque acts in two direction in a cellular plate while it acts in one directions in a grillage):

$$J = \frac{2 \cdot t_{fc} \cdot t_{ft} \cdot d^2}{t_{fc} + t_{ft}} \quad (3-19)$$

A number of investigators (12,21,29...) suggested that the torsional rigidity of the full cellular section may be approximated by considering the whole inclosed section as a single box and the torsional rigidity may be obtained from *Bredt's* formula for a single closed section using equation (3-14). This approximation is justified by the fact that for a multi-cell structure the net shear flow through the interior webs is negligible and only the shear flow around the outer webs and top and bottom flanges is of prime significance.

Mohammed (1994)⁽²⁶⁾ suggested the following formulas to express the torsional constant for exterior and interior cells of a multi-cell section having equal flange thickness ($t_{fc} = t_{ft}$):

For exterior cells:

$$J_n = \frac{4 \cdot A_n^2}{\frac{2B}{t_{fc}} + \frac{d}{t_x} + \frac{d}{\beta t'}} \quad (3-20)$$

20)

For interior cells: -

$$J_n = \frac{2 \cdot A_n^2}{\frac{B}{t_{fc}} + \frac{d}{\beta t'}} \quad (3-21)$$

where

$$\beta = \left(\frac{2b}{d} \right) \left(\frac{t'}{t_{fc}} \right) \cdot 10 \quad (3-22)$$

22)

B = width of cell (c/c)

t' = Thickness of the web in X or Y directions.

The factor (β) is suggested such that the calculated torsional constant will be identical to the value by the exact torsion theory of cellular sections shown by *Timoshenko* and *Goodier*. *Al-Sherrawi* (1990) (1) benefited equation (3-22) to transform equation (3-21) into the following form:

$$4 \cdot A_j^2 = -J_i \frac{A_j}{A_i} \int_w \frac{ds}{t} + J_j \oint \frac{ds}{t} - J_k \frac{A_j}{A_k} \int_w \frac{ds}{t} \quad (3-23)$$

23)

Each of the n -cells can provide one equation in terms of the torsional constant of the cell and its adjacent cells and the solution of the resulting n independent linear equations gives the values of the torsional constant (J),

J_1, J_2, \dots, J_n). Then the torsional constant for the whole section (J) is calculated from equation (3-18).

Mashal (1994)⁽¹⁶⁾ modified the formulae presented by Mohammed (1994)⁽¹⁷⁾ to be suitable for a cellular section with unequal flange thickness ($t_{fc} \neq t_{ft}$) as follows:

For exterior cells:

$$J_n = \frac{4.A_n^2}{\frac{B(t_{fc} + t_{ft})}{2.t_{fc}.t_{ft}} + \frac{d}{t_{xt}} + \frac{d}{\beta t'}} \quad (3-19)$$

(3-19)

For interior cells:

$$J_n = \frac{2.A_n^2}{\frac{B(t_{fc} + t_{ft})}{2.t_{fc}.t_{ft}} + \frac{d}{\beta t'}} \quad (3-20)$$

where

$$\beta = \left(\frac{2b}{d} \right) \left(\frac{t'}{\sqrt{t_{fc}.t_{ft}}} \right) \cdot 10 \quad (3-21)$$

(3-21)

In the present study the torsional constant for a single cell cross-section can be evaluated by Eq. (3-19). For a multi-cell cross-section (with n cells) which is undergoing Saint-Venant torsion the rate of twist (θ) for each cell is the same, so a set of simultaneous equations in the shear flow constants ($q_{sv1}, q_{sv2}, q_{sv3}, q_{sv4}, \dots$) can be obtained. Therefore for the i th

cell (recalling Eq. (3-12) with new arrangement) the following expression may be written:

$$2A_i = \left(-\psi_{i-1} \int_w \frac{ds}{t} + \psi_i \int_i \frac{ds}{t} - \psi_{i+1} \int_w \frac{ds}{t} \right)$$

where

$$\psi_i = \frac{q_{svi}}{G\theta'}$$
 for the cell i

$$\psi_{i-1} = \frac{q_{svi}}{G\theta'}$$
 for the left cell

$$\psi_{i+1} = \frac{q_{svi}}{G\theta'}$$
 for the right cell

For a cellular section, the torsional constant (J_i) to each cell is:

$$J_i = 2A_i \psi_i$$

and the torsional constant for the whole section is:

$$J_t = \sum_{i=1}^n J_i$$

3.2.3 Shearing Rigidity

In a cellular plated structure having few or no transverse diaphragms, the vertical (or transverse) shearing forces developed across a cell causes the flanges and the webs to flex independently out of plane. This pattern of deformation is referred to as distortion. The effect of distortion may become pronounced in cellular sections with relatively thin webs. The shearing rigidity is (GA_v), where A_v is taken to be the full area of the web. The effect of shearing rigidity on deformation is usually very small.

3.2.4 Warping Moment of Inertia

Warping moment of inertia ($I\omega$) and the sectorial moment of area ($S\omega$) are evaluated as follows:

$$I\omega = \int \omega^2 dA \quad (3-27)$$

$$S\omega(s) = \int_0^s \omega(s) dA \quad (3-28)$$

The sectorial area (ω) can be estimated for the uniform thin-walled cellular box section (having two axes of symmetry) as shown in Fig.(3.3). In non-uniform thin-walled box section (where no axes of symmetry exist), the sectorial area diagram can be expected to be as shown in Fig.(3.4).

The warping displacement u of any portion of the wall relative to the origin of the wall peripheral s -coordinate is given by (3.29):

$$\bar{u} = u - u_o = \frac{1}{G} \int \frac{q_{sv}}{t} ds - \theta \int r_s ds \quad (3-29)$$

where r_s is the normal radius from the shear center to the tangent at the point considered and q_{sv} is the shear flow and θ is the twist per unit length by assuming that the origin of the peripheral coordinates coincides with a point of zero warping, then u_o vanishes and equation (3-29) becomes :

$$u = \frac{1}{G} \int \frac{q_{sv}}{t} ds - \theta \int r_s ds \quad (3-30)$$

In agreement with *Vlasov's* original analysis, it is here assumed that the transverse distribution of warping displacement u is fully described by the warping function or (sectional area). Since the degree of warping is directly

proportional to the rate of twist θ , warping displacement at any point may be conveniently defined in the following way: -

$$u = -\omega\theta \tag{3-31}$$

By introducing Eq. (3-31) into Eq. (3-30) the following expression is obtained for the warping:-

$$\omega = \int r_s ds - \frac{1}{G\theta} \int \frac{q_{sv}}{t} ds \tag{3-32}$$

This Eq. may be written as: -

$$\omega = \int (r_s - \frac{\psi}{t}) ds \tag{3-33}$$

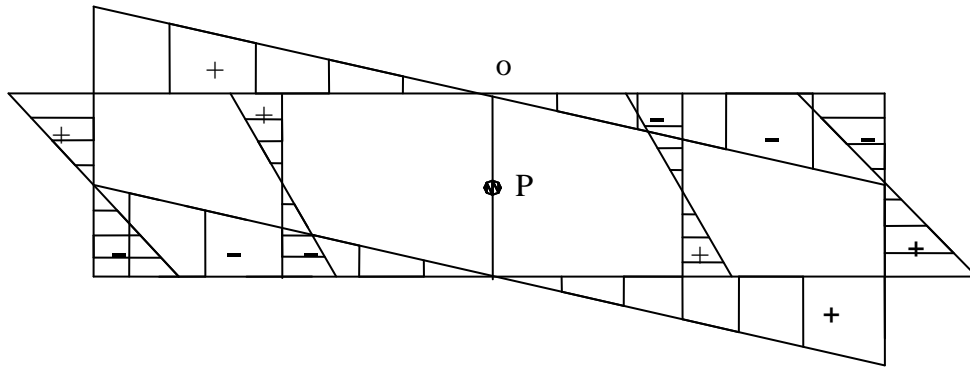


Fig.(3. 3) Determination of the sectorial area (ω) for uniform multi-cell closed section.

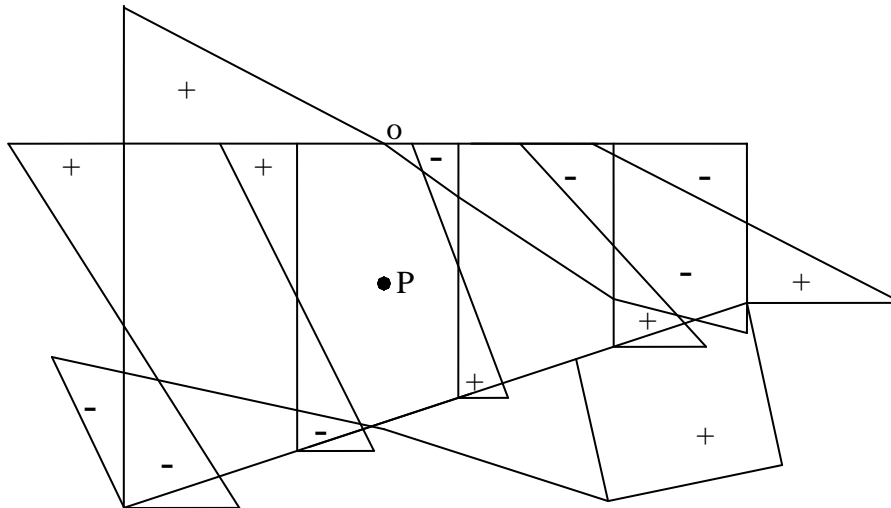


Fig. (۳. ۴) Determination of the sectorial area(ω) for non-uniform(tapered) multi-cell closed section.

Chapter Four

GRILLAGE ANALOGY

4-1 Introduction

Grillage analogy is used in this study for analyzing cellular plate structures with lineary varying depth and diaphragms in the linear and non-linear range. The method involves conversion of the three –dimensional cellular plate into a plane grillage of discrete rigidly connected beams in two-dimensional arrangement. In thin-walled members, in which warping deformations are usually relatively large, the effect of warping restraint may become significant and should be fully considered in the analysis. Free warping due to pure St.-Venant's torsion is identical at every cross-section along the beam and proportional with the rate of twist of the beam (see Fig (1-2)). The distribution of warping deformation along the beam is varied and, thus additional axial direct (or normal) stresses and complementary shearing stresses will be created. These axial stresses differ from the more familiar stress resultants, such as axial forces and bending moments, in that they cannot be determined from equilibrium conditions alone.

The main aim of this chapter is to provide guidelines on the applicability of the grillage analogy to the non-linear analysis and ultimate load investigation of steel cellular plate structures with lineary varying depth. Elastic analysis of thin-walled non-prismatic plate structures in plane includes both implicitly and explicitly the effects of warping restraints.

ε.۲ Inclusion of Warping Implicitly with Torsional Stiffness

In the mathematical derivation that follows, various expressions are derived for the angle of twist and its rate of change, by applying *Timoshenko's* concept of torsional warping for straight members with open and closed section and various boundary conditions. Using the following expression for the total torque:

$$T = T_{sv} + T_w \quad (\xi-۱)$$

where

T = the total torque

T_{sv} = the Saint-Venant torque ($GJ\theta$)

T_w = the warping torsional moment ($EI_w\theta''$)

Substituting these expressions into Eq.(ξ-۱) the following differential equation of torsion with warping restraint will be obtained:

$$\frac{T}{GJ} = \theta - a^2 \frac{d^2\theta}{dx^2} \quad (\xi-۲)$$

where

θ = is the rate of twist, and x is the longitudinal axis and

$$a^2 = EI_w / GJ.$$

This is a non-homogeneous second-order ordinary differential equation (*Timoshenko's* differential equation for non-uniform torsion). The general solution of Eq. (ξ-۲) is (۳۲):

$$\theta = A.e^{-x/a} + B.e^{x/a} + \frac{T}{GJ} \quad (\xi-۳)$$

The constants A and B are to be found from the boundary conditions. The general boundary conditions for torque and bimoment are shown in table (ξ-۱)

Table (4-1) Boundary conditions for thin-walled beam

Boundary	Deformation	Force
Fixed end	$\phi = \phi' = 0$	$T_{sv} = \cdot$
Free end	-----	$T_{bm} = \cdot$
Hinge	$\phi = 0$	$T_{bm} = \cdot$

4.2.1 Member with One End Restrained

By applying the following boundary conditions; when $X=0$ (the fixed end), the axial displacement $u=0$, consequently, the rate of twist $\theta=0$ ($u = -\theta(\int_s (r - \frac{\psi}{t}) ds$). Also, at $X=L$ (the free end) the axial (or normal) stress $\sigma_x=0$ or, according to expression that $\sigma = E\omega \cdot (d\theta/dX)$ (4), then the constants are:

$$A = \frac{T}{GJ} \left(\frac{-L}{e^a + e^{-a}} \right) \quad (4-5)$$

$$B = \frac{T}{GJ} \left(\frac{-L}{e^a + e^{-a}} \right) \quad (4-6)$$

Thus,

$$\theta = \frac{T}{GJ} \left(1 - \frac{\cosh \frac{L-x}{a}}{\cosh \frac{L}{a}} \right) \quad (4-7)$$

The maximum displacement at $x=L$, is:

$$\phi_{x=L} = \int_0^L \theta \cdot dx = \frac{T \cdot L}{GJ} \left(1 - \frac{a}{L} \cdot \tanh \frac{L}{a} \right) \quad (4-8)$$

whereas in pure torsion (with no warping restraint):

$$\phi = \frac{T.L}{GJ} \quad (\xi-8)$$

Comparing Eq. ($\xi-8$) with Eq. ($\xi-7$), hence with warping restraint being included implicitly, the modified torsional constant is:

$$\bar{J} = \frac{J}{\left(1 - \frac{a}{L} \cdot \tanh \frac{L}{a}\right)} \quad (\xi-9)$$

It will be noticed $\bar{J} > J$ (indicating an increase in torsional stiffness due to warping restraint). Moreover, as the length (L) increases, $\bar{J} \rightarrow J$.

$\xi.2.2$ Member with Two Ends Restrained

By applying the following boundary conditions; when $x=0$ and $x=L$, the axial displacement $u=0$. Consequently, the rate of twist $\theta=0$, this follows from formula ($\gamma-31$). Then, the constants are:

$$A = \frac{T}{GJ} \left(\frac{-e^{-\frac{L}{2a}}}{e^{\frac{L}{2a}} + e^{\frac{L}{2a}}} \right) \quad (\xi-10)$$

$$B = \frac{T}{GJ} \left(\frac{-e^{-\frac{L}{2a}}}{e^{\frac{L}{2a}} + e^{\frac{L}{2a}}} \right) \quad (\xi-11)$$

Then,

$$\theta = \frac{T}{GJ} \left(1 - \frac{\cosh \frac{L-x}{2a}}{\cosh \frac{L}{2a}} \right) \quad (\xi-12)$$

$$\phi_{x=L} = \int_0^L \theta \cdot dx = \frac{T.L}{GJ} \left(1 - \frac{2a}{L} \cdot \tanh \frac{L}{2a} \right) \quad (\xi-13)$$

Comparing Eq. (4-14) with Eq (4-13), hence with warping restraint being included implicitly, the modified torsional constant is

$$\bar{J} = \frac{J}{\left(1 - \frac{2a}{L} \cdot \tanh \frac{L}{2a}\right)} \quad (4-15)$$

Also, here $\bar{J} > J$ and $\bar{J} \rightarrow J$ as L increases.

4-2 Grillage Analysis

A plane grillage is two-dimensional structure consisting of rigidly connected longitudinal and transverse members intersecting at a right angles with straight radial members representing the transverse diaphragms.. The matrix techniques applied to the analysis of the grillage are the stiffness (or displacement) method and the flexibility (or force) method . The stiffness matrix method is based on the assemblage of member stiffnesses. The ease of programming and the convenience in the application of the stiffness method on the computer have made it widely used. Also, this method is more suitable for the analysis of large structures than the flexibility method.

4-2-1 Stiffness Matrix For Straight Member

The total strain energy of a deformed beam can be written in the form:

$$U = U_b + U_t + U_w \quad (4-16)$$

where U_b is the contribution by the bending to the element strain energy, and U_t and U_w are the contributions to the element strain energy by torsion and bimoment, respectively (4-16).

The total strain energy can be expressed by:

$$U = \frac{EI}{2} \int_0^L (v'')^2 dx + \frac{GJ}{2} \int_0^L (\phi')^2 dx + \frac{EI_w}{2} \int_0^L (\phi'')^2 dx \quad (4-17)$$

The assumed displacement fields $v(x)$ and $\phi(x)$ corresponding to the translation and torsional degree of freedom are:

$$v = a_1 + a_2 x + a_3 x^2 + a_4 x^3 \quad (\xi-17)$$

$$\phi = b_1 + b_2 x + b_3 x^2 + b_4 x^3 \quad (\xi-18)$$

The degrees of freedom considered at both ends of the element are:

$$\left\{ v_1, \left(\frac{dv_1}{dx} \right), \phi_1, \left(\frac{d\phi_1}{dx} \right), v_2, \left(\frac{dv_2}{dx} \right), \phi_2, \left(\frac{d\phi_2}{dx} \right) \right\}$$

Then, by solving Eqs. (ξ-17) and (ξ-18) for the ends degrees of freedom the following results can be obtained:

$$v = (1 - 3x^2 + 2x^3) v_1 + (x - 2x^2 + x^3) L \left(\frac{dv_1}{dx} \right) + (3x^2 - 2x^3) v_2 + (-x^2 + x^3) L \left(\frac{dv_2}{dx} \right) \quad (\xi-19)$$

and

$$\phi = (1 - 3x^2 + 2x^3) \phi_1 + (x - 2x^2 + x^3) L \left(\frac{d\phi_1}{dx} \right) + (3x^2 - 2x^3) \phi_2 + (-x^2 + x^3) L \left(\frac{d\phi_2}{dx} \right) \quad (\xi-20)$$

By making use of the Eqs. (ξ-19) and (ξ-20) and carrying out the integration of Eq. (ξ-16), then the total strain energy may be written in matrix form as:

$$U = \frac{1}{2} \{\Delta\}^T \cdot [K_B] \cdot \{\Delta\} + \frac{1}{2} \{\Delta\}^T \cdot [K_T] \cdot \{\Delta\} + \frac{1}{2} \{\Delta\}^T \cdot [K_W] \cdot \{\Delta\} \quad (\xi-21)$$

where:

$$\Delta = \{\phi_1, v_1', v_1, \phi_1', \phi_2, v_2', v_2, \phi_2'\} \quad (\xi-22)$$

$[K_B]$ = the contribution of bending to the stiffness matrix.

$[K_T]$ = the contribution of St. Venant torsion to the stiffness matrix.

$[K_W]$ = the contribution of bimoment to the stiffness matrix.

Eq. (ξ-21) may be written as:

$$a1 = H2^2 .B1 + 2H5.H2B2 + H5^2 .B3$$

$$a2 = H1.H2.B1 + H1.H5.B2 + H3.H2.B2 + H3.H5.B3$$

$$a3 = H1^2 .B1 + 2H1.H3.B2 + H3^2 .B3$$

$$a4 = H2.H4.B1 + H6.H2.B2 + H4.H5.B2 + H6.H5.B3$$

$$a5 = H2.H4.B1 + H5.H4.B2 + H2.H6.B2 + H5.H6.B3$$

$$a6 = H4^2 .B1 + 2H4.H6.B2 + H1^2 .B3$$

$$a7 = -a2$$

$$a8 = H1^2 .B1 - H1.H3.B2 - H1.H3.B2 - H3^2 .B3$$

$$a9 = -a7$$

$$a10 = -a8$$

$$H1 = \frac{C}{B} - C$$

$$H2 = A - \frac{C.L}{B}$$

$$H3 = \frac{C}{B^2} - C$$

$$H4 = C.L - A$$

$$H5 = 1 - \frac{1}{B} - \frac{C.L}{B^2}$$

$$H6 = \frac{1}{B} + C.L - 1$$

$$H7 = \frac{C^2}{B} - \frac{C^2}{B^2}$$

$$H8 = \frac{C + A.C}{B^2} - \frac{C}{B}$$

$$H9 = C - C.A - \frac{C}{B}$$

$$H_{10} = C.A + \frac{C2.L - C - A.C}{B} + \frac{C - C^2.L}{B}$$

$$A = \ln(1 + C.L)$$

$$B = 1 + C.L$$

$$C = \frac{I_2 - I_1}{I_1.L}$$

$$B_1 = 2.C.I_1.(1 - \frac{1}{B^2})$$

$$B_2 = 2.C^3.I_1.(1 - \frac{1}{B})$$

$$B_3 = C^4.I_1.A$$

$$R = \frac{2.C - C^2.L}{B} + \frac{C^2.L - C - C.A}{B^2} + C.A - C$$

The twisting stiffness matrix will be as follows :

$$\begin{aligned}
b_4 = & -M1^2.C1.L^2 + M1.M3\left(\frac{C1}{2} - \frac{C1.t^2}{2}\right) + M1.M7.\left(\frac{1}{3} - \frac{t^3}{3}\right) - \\
& M1.M3.\left(\frac{C1}{2} - \frac{C1.t^2}{2}\right) - M3^2.\left(\frac{C1}{3} - \frac{C1}{3}\right) - M3.M7.\left(\frac{1}{3} - \frac{t^3}{3}\right) - M1.M7.\left(\frac{1}{3} - \frac{t^3}{3}\right) \\
& - M3.M7.\left(\frac{t^4}{4} - \frac{1}{4}\right) - M7^2.\left(\frac{1}{3} - \frac{t^3}{3}\right)
\end{aligned}$$

$$\begin{aligned}
b_5 = & -M1.M2.C1.L^2 - M3.M2.\left(\frac{C1}{2} - \frac{C1.t^2}{2}\right) - M7.M2.\left(\frac{1}{3} - \frac{t^3}{3}\right) - \\
& M1.M5.\left(\frac{C1}{2} - \frac{C1.t^2}{2}\right) - M3.M5.\left(\frac{C1}{3} - \frac{C1}{3}\right) - M7.M5.\left(\frac{1}{3} - \frac{t^3}{3}\right) - M1.M8.\left(\frac{1}{3} - \frac{t^3}{3}\right) \\
& - M3.M8.\left(\frac{t^4}{4} - \frac{1}{4}\right) - M7.M8.\left(\frac{1}{3} - \frac{t^3}{3}\right)
\end{aligned}$$

$$\begin{aligned}
b_6 = & M1^2.C1.L^2 + M3.M1.\left(\frac{C1}{2} - \frac{C1.t^2}{2}\right) + M1.M7.\left(\frac{1}{3} - \frac{t^3}{3}\right) + M1.M3.\left(\frac{C1}{2} - \frac{C1.t^2}{2}\right) \\
& + M3^2.\left(\frac{C1}{3} - \frac{C1}{3}\right) + M7.M3.\left(\frac{1}{3} - \frac{t^3}{3}\right) + M1.M7.\left(\frac{1}{3} - \frac{t^3}{3}\right) + M3.M7.\left(\frac{t^4}{4} - \frac{1}{4}\right) \\
& + M7^2.\left(\frac{1}{3} - \frac{t^3}{3}\right)
\end{aligned}$$

$$\begin{aligned}
b_7 = & M1.M4.C1.L^2 + M1^2.\left(\frac{C1}{2} - \frac{C1.t^2}{2}\right) + M1.M9.\left(\frac{1}{3} - \frac{t^3}{3}\right) + M4.M2.\left(\frac{C1}{2} - \frac{C1.t^2}{2}\right) \\
& + M1.M2.\left(\frac{C1.t^3}{3} - \frac{C1}{3}\right) + M9.M2.\left(\frac{1}{3} - \frac{t^3}{3}\right) + M7.M4.\left(\frac{1}{3} - \frac{t^3}{3}\right) + M1.M7.\left(\frac{t^4}{4} - \frac{1}{4}\right) \\
& M7.M9.\left(\frac{1}{3} - \frac{t^3}{3}\right)
\end{aligned}$$

$$\begin{aligned}
b_8 = & M2.M4.C1.L^2 + M2.M1.\left(\frac{C1}{2} - \frac{C1.t^2}{2}\right) + M2.M9.\left(\frac{1}{3} - \frac{t^3}{3}\right) + \\
& M4.M5.\left(\frac{C1}{2} - \frac{C1.t^2}{2}\right) + M1.M5.\left(\frac{C1.t^3}{3} - \frac{C1}{3}\right) + M9.M5.\left(\frac{1}{3} - \frac{t^3}{3}\right) + M8.M4.\left(\frac{1}{3} - \frac{t^3}{3}\right)
\end{aligned}$$

$$+ M8.M1.\left(\frac{t^4}{4} - \frac{1}{4}\right) + M8.M9.\left(\frac{1}{3} - \frac{t^3}{3}\right)$$

$$b9 = M1.M4.C1.L^2 + M1.M2.\left(\frac{C1}{2} - \frac{C1.t^2}{2}\right) + M1.M9.\left(\frac{1}{3} - \frac{t^3}{3}\right) +$$

$$M4.M3.\left(\frac{C1}{2} - \frac{C1.t^2}{2}\right) + M1.M3.\left(\frac{C1.t^3}{3} - \frac{C1}{3}\right) + M9.M3.\left(\frac{1}{3} - \frac{t^3}{3}\right) +$$

$$M7.M4.\left(\frac{1}{3} - \frac{t^3}{3}\right) + M7.M1.\left(\frac{t^4}{4} - \frac{1}{4}\right) + M7.M9.\left(\frac{1}{3} - \frac{t^3}{3}\right)$$

$$b10 = M4^2.C1.L^2 + M4.M2.\left(\frac{C1}{2} - \frac{C1.t^2}{2}\right) + M4.M9.\left(\frac{1}{3} - \frac{t^3}{3}\right) +$$

$$M4.M1.\left(\frac{C1}{2} - \frac{C1.t^2}{2}\right) + M1^2.\left(\frac{C1.t^3}{3} - \frac{C1}{3}\right) + M9.M1.\left(\frac{1}{3} - \frac{t^3}{3}\right) +$$

$$M9.M4.\left(\frac{1}{3} - \frac{t^3}{3}\right) + M9.M1.\left(\frac{t^4}{4} - \frac{1}{4}\right) + M9^2.\left(\frac{1}{3} - \frac{t^3}{3}\right)$$

$$M1 = \frac{C1}{t} - C1$$

$$M2 = \beta - \frac{C1.L}{t}$$

$$M3 = \frac{C1}{t^2} - C1$$

$$M4 = C1.L - \beta$$

$$M5 = 1 - \frac{1}{t} - \frac{C1.L}{t^2}$$

$$M6 = \frac{1}{t} + C1.L - 1$$

$$M7 = \frac{C1^2}{t} - \frac{C1^2}{t^2}$$

$$M8 = C1 + \frac{\beta.C1}{t^2} - \frac{C1^2}{t}$$

$$M9 = C1 - C1.\beta - \frac{C1}{t}$$

$$M9 = C1 - C1.\beta - \frac{C1}{t}$$

$$M10 = C1.\beta + \frac{C1^2.L - C1 - C1.\beta}{t} + \frac{C1 - C1^2.L}{t}$$

$$C1 = \frac{J2 - J1}{J1.L}$$

$$\beta = \ln(1 + C1.L)$$

$$t = 1 + C1.L$$

$$R1 = \frac{2.C1 - C1^2.L}{t} + \frac{C1^2.L - C1 - C1.\beta}{t^2} + C1.\beta - C1$$

Finally, the warping stiffness matrix becomes:

$$K_w = EI_w / R2^2 \begin{bmatrix} w1 & & & & & & & & & & \text{Symm.} \\ 0 & 0 & & & & & & & & & \\ 0 & 0 & 0 & & & & & & & & \\ w2 & 0 & 0 & w3 & & & & & & & \\ w4 & 0 & 0 & w5 & w6 & & & & & & \\ 0 & 0 & 0 & 0 & 0 & 0 & & & & & \\ 0 & 0 & 0 & 0 & 0 & 0 & 0 & & & & \\ w7 & 0 & 0 & w8 & w9 & 0 & 0 & w10 & & & \end{bmatrix}$$

$$w1 = S1^2.X1 + S1.S3.X2 + S3^2.X2 + S3.S5.X3$$

$$w2 = S1.S2.X1 + S1.S5.X2 + S3.S2.X2 + S3.S5.X3$$

$$w3 = S2^2.X1 + S5.S2.X2 + S2.S5.X2 + S5^2.X3$$

$$w4 = -S1^2.X1 - 2.S1.S3.X2 - S3^2.X3$$

$$w5 = -w2$$

$$w6 = -w4$$

$$w7 = S1.S4.X1 + S1^2.X2 + S4.S3.X2 + S1.S3.X3$$

$$w8 = S2.S4.X1 + S1.S2.X2 + S4.S5.X2 + S1.S5.X3$$

$$w9 = -w7$$

$$w_{10} = S_4^2 \cdot X_1 + 2 \cdot S_4 \cdot S_1 \cdot X_2 + S_1^2 \cdot X_3$$

$$R_2 = \frac{2 \cdot C_2 - C_2^2 \cdot L}{\alpha} + \frac{C_2^2 \cdot L - C_2 - C_2 \cdot D}{\alpha^2} + C_2 \cdot D - C_2$$

$$S_1 = \frac{C_2}{\alpha} - C_2$$

$$S_2 = D - \frac{C_2 \cdot L}{\alpha}$$

$$S_3 = \frac{C_2}{\alpha^2} - C_2$$

$$S_4 = C_2 \cdot L - D$$

$$S_5 = 1 - \frac{1}{\alpha} - \frac{C_2 \cdot L}{\alpha^2}$$

$$S_6 = \frac{1}{\alpha} + C_2 \cdot L - 1$$

$$S_7 = \frac{C_2^2}{\alpha} - \frac{C_2^2}{\alpha^2}$$

$$S_8 = C_2 + \frac{D \cdot C_2}{\alpha^2} - \frac{C_2^2}{\alpha}$$

$$S_9 = C_2 - C_2 \cdot D - \frac{C_2}{\alpha}$$

$$S_{10} = C_2 \cdot D + \frac{C_2 \cdot L - C_2 - D \cdot C_2}{\alpha} + \frac{C_2 - C_2^2 \cdot L}{\alpha}$$

$$X_1 = 2 \cdot C_2^3 \left(1 - \frac{1}{\alpha}\right)$$

$$X_2 = 2 \cdot C_2^3 \left(\frac{1}{\alpha} - 1\right)$$

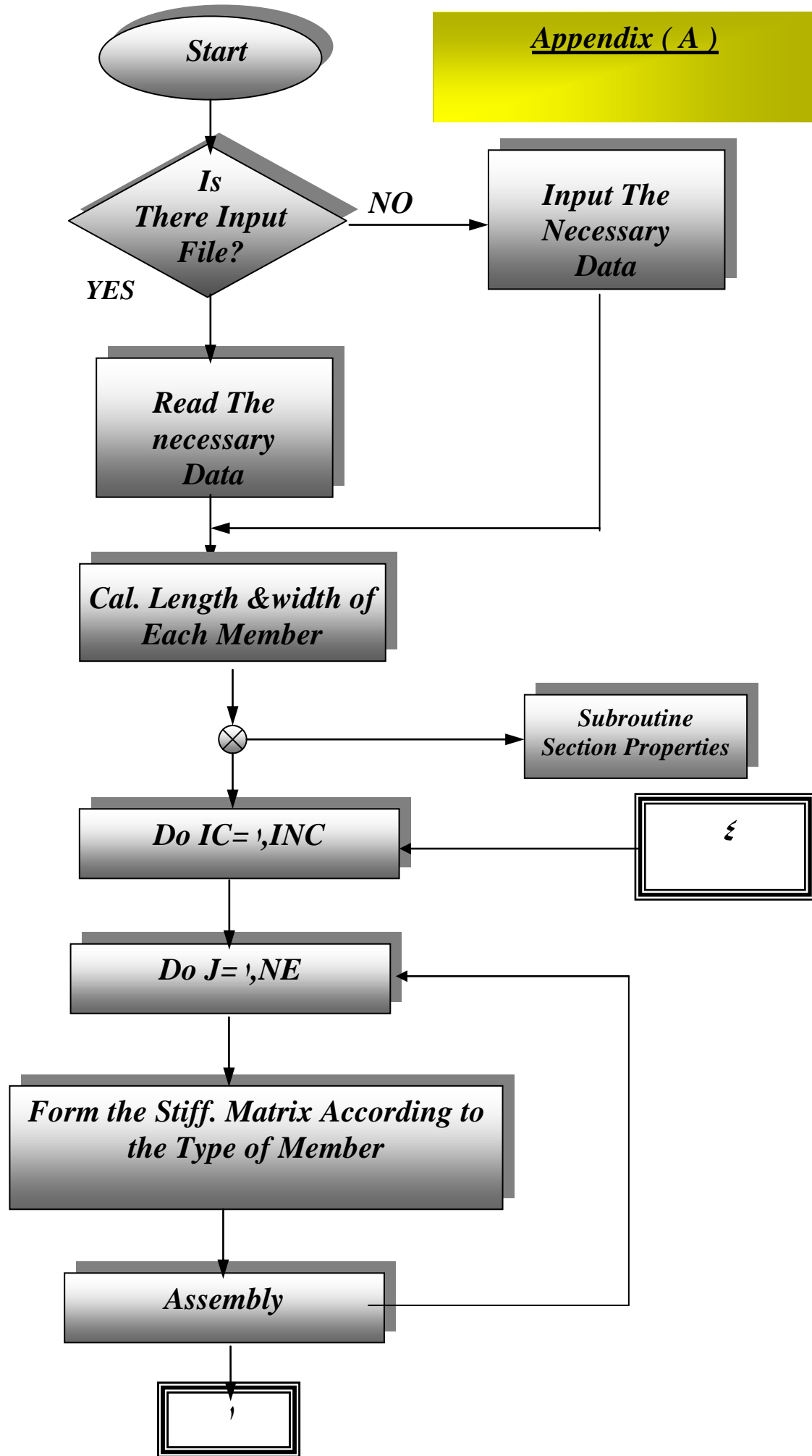
$$X_3 = C_2^4 \cdot D$$

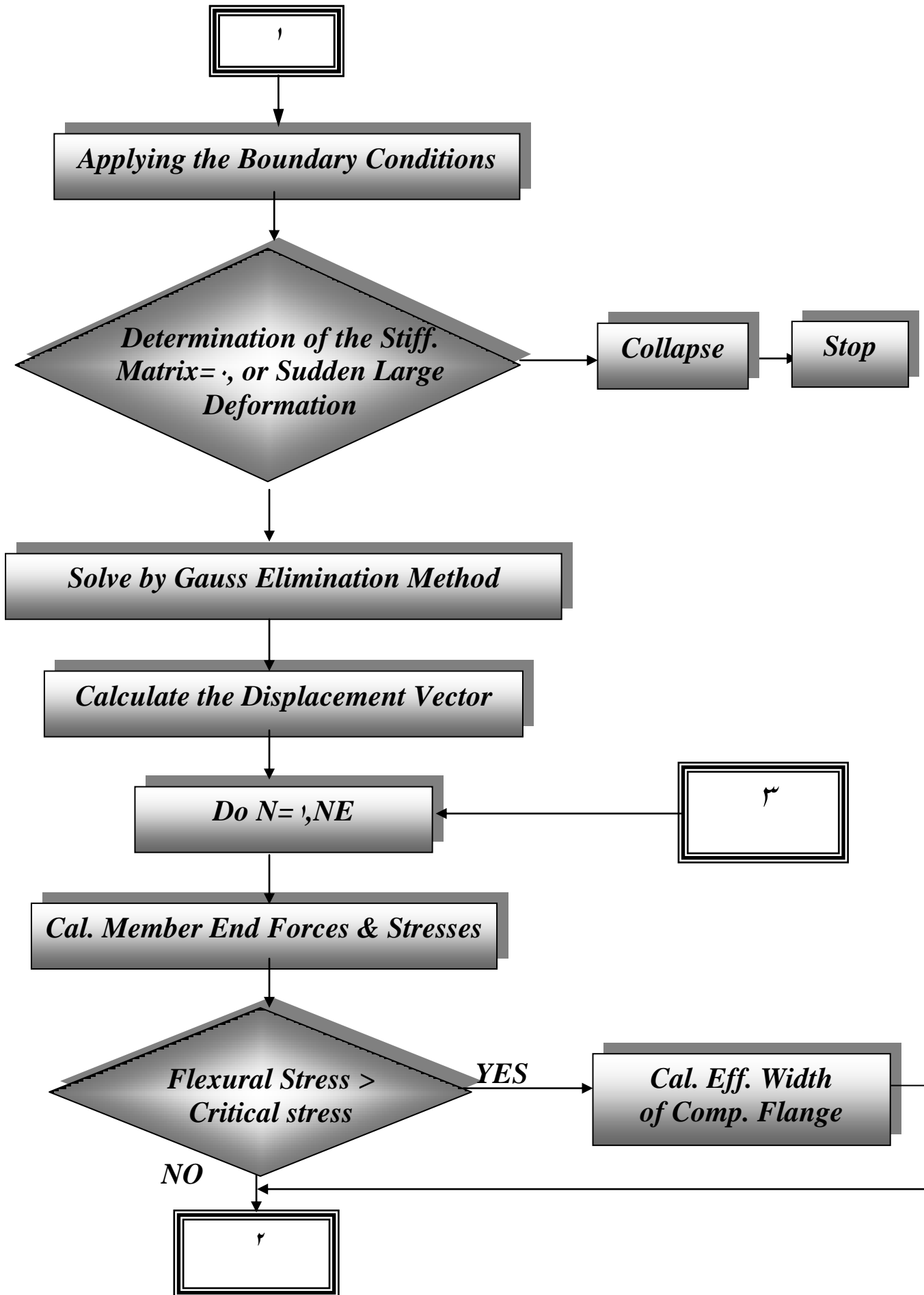
$$C_2 = \left(\frac{I_w 2 - I_w 1}{I_w 1 \cdot L}\right)$$

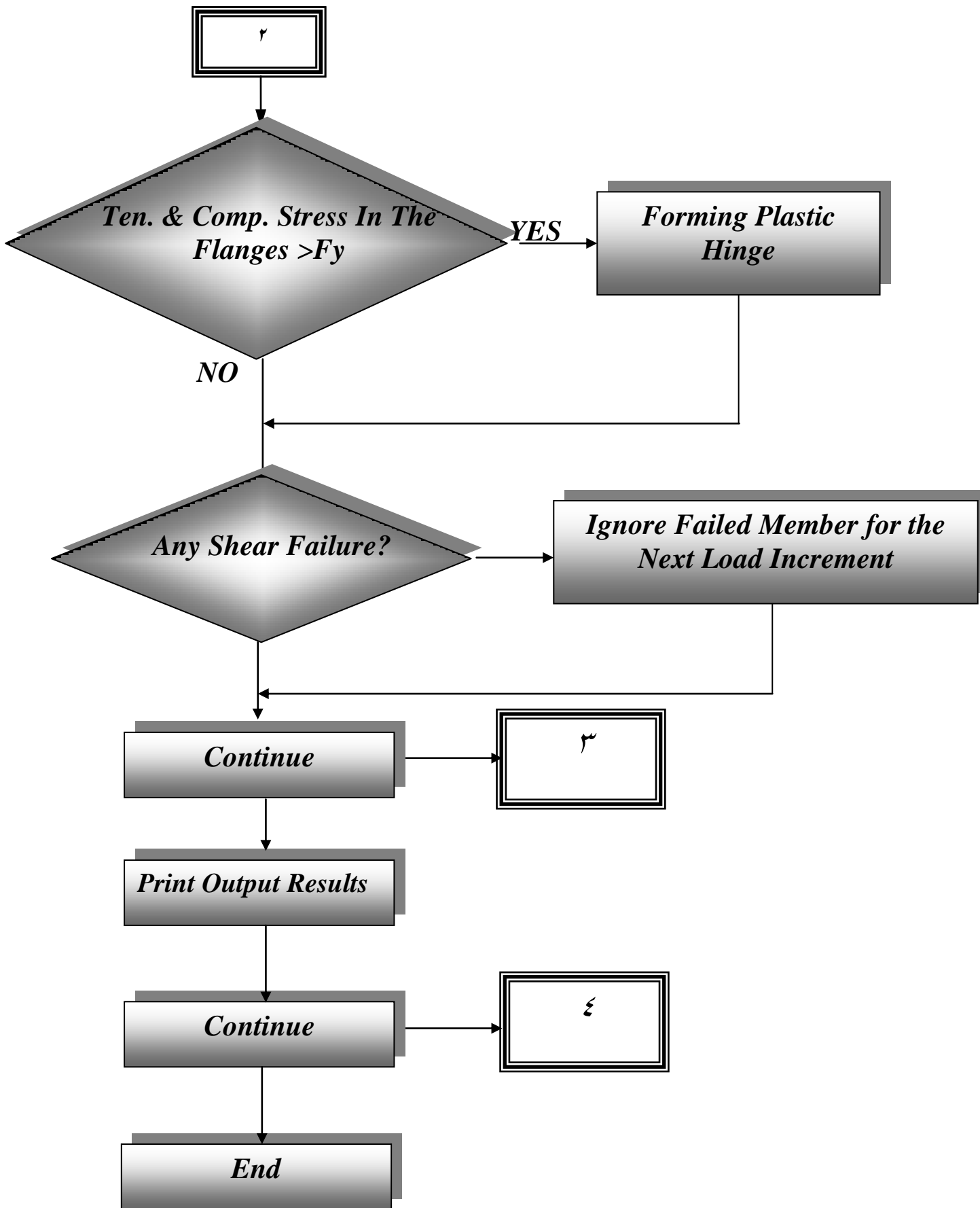
$$\alpha = 1 + C_2 \cdot L$$

$$D = \ln(1 + C_2 \cdot L)$$

$$D = (1 + c_2 \cdot L)$$







CHAPTER FIVE

NONLINEAR BEHAVIOR OF CELLULAR PLATE STRUCTURES

5.1 Introduction

The objective of this chapter is to provide the theoretical basis for the nonlinear analysis and ultimate load investigation of cellular plate structures with linear-varying depth and with or without diaphragms. A simple analysis method is presented, which is capable to predict the collapse load of cellular plate structures with a good degree of accuracy. This method consists of the extension of the grillage approach into the nonlinear range and at the collapse of the multi-cell structure.

As mentioned previously, steel or aluminium cellular plate structures are fabricated as an assemblage of individual plates forming the top and bottom cover plates and the longitudinal and transverse partitioning webs. This construction allows the structures to have high strength to weight ratio. So, this type of structure will be well suited to bridge decks, aircraft wings, ship bottoms and other situations where strength and reduction of self-weight are important design objectives. To maximize the saving in self-weight, the component plates are designed to be of thin proportions. Accordingly, they will have a low elastic critical (or buckling) stress and will normally operate in the post-buckling range. Thus, advantage must be taken for their post-buckling reserve of strength concerning the nonlinear

analysis. The present study takes into account the effects of the two basic type of nonlinearly (material and geometric nonlinearities) to represent the nonlinear behavior of the component plates used in the construction of cellular plate structures.

5.1.1 Material Nonlinearity

The effect of material nonlinearity is incorporated in the nonlinear analysis when the material properties vary with the growth of stress in the material; i.e. the constitutive laws are functions of the current stresses in the material. This variation is a consequence of the occurrence and spread of local yielding in component plates of the cellular plate structure.

In the present study, as the material yields (reaching the yield stress), a hypothetical hinge (plastic hinge) concept is adopted in which the structural model softens under increasing loads due to increasing spread of plasticity for the whole structure. The experimental study made by *Ova Lagerqvist* (1973) on steel girders with modulus of elasticity $E = 206 \text{ GPa}$ showed that the plastic modulus of elasticity is $E = 0.6 \text{ GPa}$ as shown in Fig.(5-1). This value is used in the present study.

5.1.2 Geometric Nonlinearity

This type of nonlinearity is introduced when deflections in the individual thin plates become large enough to activate membrane forces in the plane of the plate panels. When the membrane compressive stresses (acting upon the compression flange) reach the critical limit, the flange will buckle. Also, the webs (which are assumed to sustain constant shearing stresses in any cross in the analysis of cellular plate structures) will buckle when the shearing stress reaches the critical limit. So, while dealing with the nonlinear behavior and ultimate load investigation of the thin –walled

structures (like the cellular plate structure), it becomes important to consider the post-buckling behavior of the compression flange as well as the web panels.

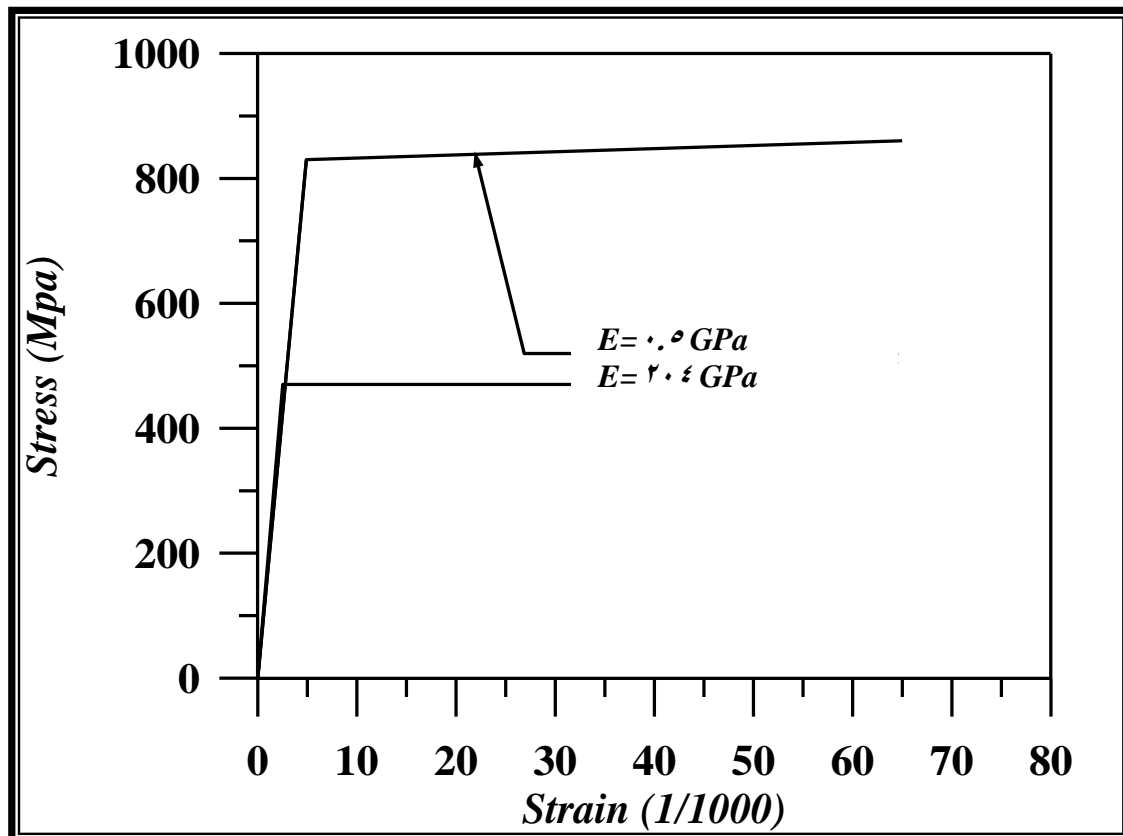


Figure (2-1) Bi-linear stress-strain relation used for transforming measured strains to stresses⁽¹⁷⁾

2.1.3 Necessary Assumptions

Regarding the present work, the following assumptions will be made to deal with the grillage simulation of the post-buckling and elastic-plastic behavior of steel cellular plate structures with linear-varying depth:

- 1-The material of the plate is homogeneous and isotropic (the effect of strain hardening is neglected).
- 2-Concerning the critical stress evaluation of rectangle compression flange the following assumptions will be considered:

- a- Since each grillage member represents the state of stress in one direction only, thus for simplicity, the critical stress (in each direction of the grillage structure) will be calculated as if the compression flange is under uniform uniaxial stress acting at that direction.
- b- The boundary edges for the compression flange panels are assumed to be simply supported (as the flexural rigidity of the thin flange plate is very small).
- ƴ- Regarding the evaluation of the shear buckling coefficients of the web panels, the boundary edges of these panels are assumed to be partially restrained according to the parametric study presented by *Lee and Yoo* (1991)⁽⁶⁴⁾. Also, the web panels are assumed to be under constant shearing stresses.
- ε- The effects of residual stresses due to welding and fabrication are neglected
- All plate panels are assumed to be flat (without geometrical imperfections).

5.2 Post-Buckling Behavior of Compression Flange Panel

5.2.1 Plate Stability

Membrane (or in-plane) forces may be acting on a thin plate in this case. The middle surface of the plate is subjected to in plane stresses. When the plate deflects (by any means), these forces will have components in the transverse (or lateral) direction and will cause moments on the section of the plate. The deflection will decrease or increase according to the tensile or compressive type of the membrane forces.

The theoretical treatment of local buckling of thin flat plates under the action of membrane forces (in the plane of the middle surface of the plate)

is based on the governing differential equation of the buckled plate, which is given as follows:

$$\nabla^4 w = \frac{1}{D} \left[N_x \frac{\partial^2 w}{\partial x^2} + 2N_{xy} \frac{\partial^2 w}{\partial x \partial y} + N_y \frac{\partial^2 w}{\partial y^2} \right] \quad (5.1)$$

where:

$$\nabla^4 w = \left[\frac{\partial^4 w}{\partial x^4} + 2 \frac{\partial^4 w}{\partial x^2 \partial y^2} + \frac{\partial^4 w}{\partial y^4} \right] \quad (5.2)$$

w = the deflection of a point in the middle surface in the direction z , perpendicular to the xy -plane.

N_x, N_y = the membrane (or in plane) normal forces (per unit width) in the x and y directions, respectively.

N_{xy} = the membrane shearing force (per unit width).

$$D = \frac{Et^3}{12(1-\nu^2)}$$

t = thickness of the plate.

The plate remains flat until the compressive stress, which is assumed to be uniformly distributed over the width of the plate, exceeds the elastic critical stress, then the plate may buckle causing geometric nonlinearity.

5.2.2 Evaluation of Elastic Critical Stress

Based on the assumption (2-a) in section (5.1.3), the differential equation defining equilibrium of a buckled flat plate under uniform uniaxial compressive stress is expressed by substituting ($N_x = -\sigma_x \cdot t$) into Eq. (5.1) as follows (2):

$$\frac{\partial^4 w}{\partial x^4} + 2 \frac{\partial^4 w}{\partial x^2 \partial y^2} + \frac{\partial^4 w}{\partial y^4} = \frac{\sigma_x \cdot t}{D} \cdot \frac{\partial^2 w}{\partial x^2} \quad (5.3)$$

where:

σ_x = the uniform compressive stress in the x-direction (Fig(5-2)).

In order to evaluate the elastic critical stress utilizing the second assumption cited in Section (5.1.3), a simply supported flat rectangular plate subjected to uniform uniaxial compressive stress is considered, as shown in Fig(5-2). Accordingly, the deflected surface $w(x, y)$ of the buckled plate is expressed in double Fourier half-range sine series ⁽⁵⁾ ,:

$$w(x,y) = \sum_{m=1}^{\infty} \sum_{n=1}^{\infty} A_{mn} \cdot \sin\left(\frac{m\pi x}{a}\right) \cdot \cos\left(\frac{n\pi y}{b}\right) \quad (5.4)$$

where:

A_{mn} = the amplitude of the deflection.

m, n = the number of half-waves in the x and y direction , respectively.

By substituting into Eq.(5.3) and equating the coefficients of identical terms, then the critical values of (σ_x) are:

$$\sigma_x = \frac{D\pi^2}{t \cdot a^2} \left(m + \frac{n^2 \cdot a}{m \cdot b^2} \right)^2 \quad (5.5)$$

From which:

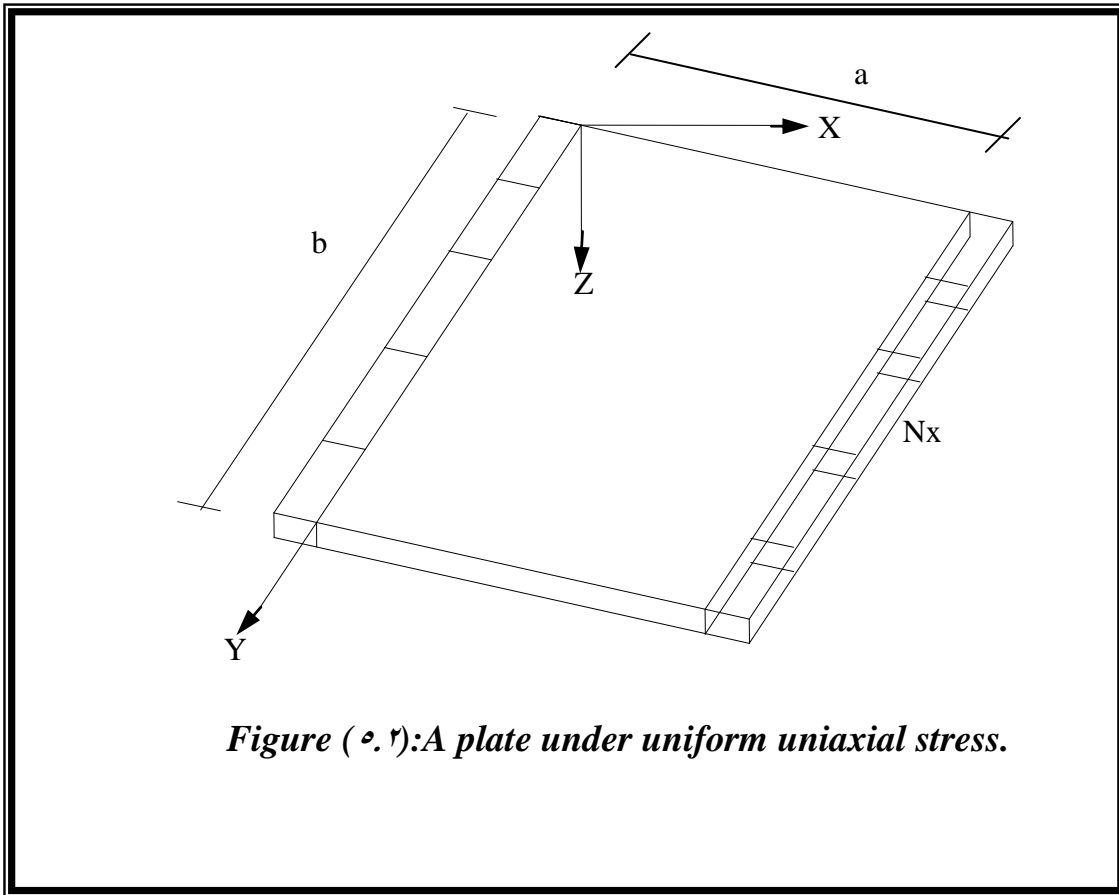
$$\sigma_x = \frac{D\pi^2}{t \cdot b^2} \left(\frac{m \cdot b}{a} + \frac{n^2 \cdot a}{m \cdot b} \right)^2 \quad (5.6)$$

According to Eq.(5.6), it is obvious that the smallest value of (σ_x) will be obtained by taking (n) equal to (1). The physical meaning of this, is that the plate buckles in such a way that there can be several half-waves in the

□ □ □

□ □

□



□

x- direction (the direction of compression) and only one half-wave along the perpendicular y-direction. Thus, the expression for the critical value of the compressive stress becomes ^(5.1);

$$\sigma_{x(cr)} = \frac{D\pi^2}{t.b^2} \left(\frac{m.b}{a} + \frac{a}{m.b} \right)^2 \quad (5.1)$$

then:

$$\square \sigma_{x(cr)} = K \cdot \frac{D \cdot \pi^2}{t \cdot b^2} \quad (5.8)$$

$$\sigma_{x(cr)} = K \cdot \frac{D \cdot \pi^2}{t \cdot b^2} \quad (5.8)$$

where the buckling coefficient(**K**) is expressed as follows:

$$K = \left(\frac{m \cdot b}{a} + \frac{a}{m \cdot b} \right)^2 \quad (5.9)$$

Along the x-direction, the number of half-waves (**m**) that yields the minimum value of ($\sigma_{x(cr)}$) is found by taking the first derivative of ($\sigma_{x(cr)}$) in Eq.(5.7) with respect to (**m**) and putting this derivative equal to zero, as follows:

$$\frac{d\sigma_{x(cr)}}{dm} = \frac{2D\pi^2}{t \cdot b^2} \left(\frac{m \cdot b}{a} + \frac{a}{m \cdot b} \right) \left(\frac{b}{a} - \frac{a}{m^2 \cdot b} \right) = 0$$

Form with a real value of (**m**) is:

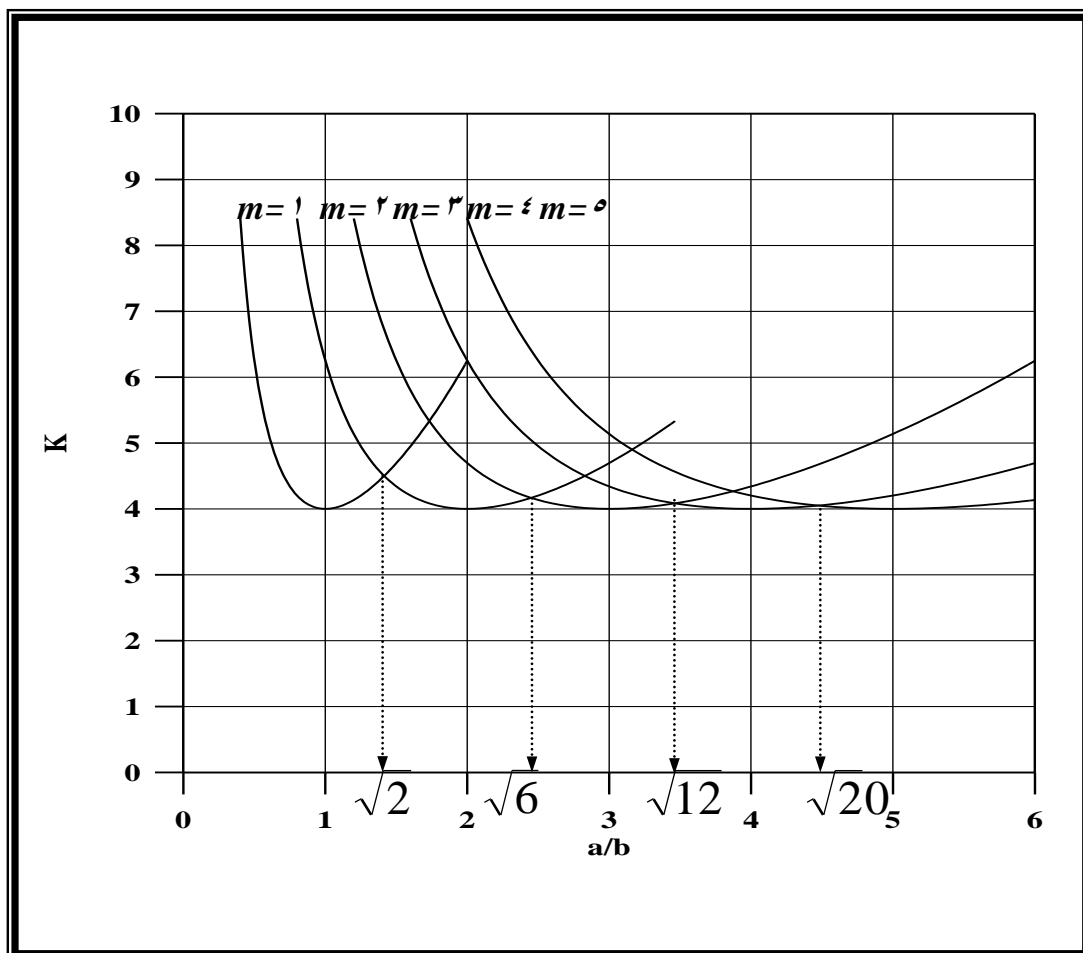
$$m = \frac{a}{b}$$

So, the minimum value of the buckling coefficient (**Kmin**) is calculated by substituting ($m = a/ b$) into Eq.(5.7);then:

$$\sigma_{x(cr)} = \frac{4D\pi^2}{t \cdot b} \quad (5.10)$$

Equation (5.10) is valid if (a/ b) is an integer, while for non-integer values, Eq.(5.7) is used(for $m = 1, 2, 3, \dots$).

In order to evaluate the stability of single plates with simply supported boundary conditions and subjected to uniform uniaxial compressive stress, *Timoshenko and Gere (1961)*^(A1) presented the following buckling curves that showed the relationship between the buckling coefficient (K) and aspect ratio (a/b) with various values of (m). Regarding the present study, the buckling coefficient (K) for various aspect ratios is calculated from Fig.(5-3) depending on Eq. (5.9).



Figure(5-3) Stability of single plate with simply supported edges^(5.3)

5.3 Post-Buckling Behavior

Beyond the critical stress, the compression flange enters into the nonlinear range due to post-buckling during which the distribution of the normal stress across the width of the flange will be nonuniform.

Von Karman et al. (1932)^(A9) argued that; when buckling occurs in a rectangular plate, the central portion of the plate deflects, and tends to shed away some of the compressive stress while, in contrast, the portion of the plate nearer the edges accepts higher stress and remain almost straight.

Accordingly, the distribution of the longitudinal compressive stress across the flange plate becomes nonuniform. Based on this, *Von Karman et al.*^(A9) made their bold assumption that the central strip of the plate can be thought to be completely ineffective, and the nonlinear post-buckling longitudinal stress in the plate is approximated by a uniform stress (equal to the edge stress σ_e) over two strips at the edges, each strip has width $(b_e/2)$, as shown in Fig. (0-1); where (b_e) is the effective width of the plate. Thus, the in-plane load may increase beyond the critical (or buckling) stress, provided that the effective width of the plate is steadily decreased.

0.2.3.1 Effective Width Expression

The evaluation of the effective width of a buckled plate is the primary focus of the ultimate strength discussion^(VY). So, a reliable effective width is needed for stiffened plate elements in pure compression (like compression flange in grillage analogy). Different empirical formulas are available for the determination of the effective width. An important early method for calculating the effective width is attributed to *Von Karman et al.* (1932)^(A9). According to this method, the following expression was suggested:

$$b_e = b \left(\frac{\sigma_{cr}}{\sigma} \right)^{0.5} \quad (0.11)$$

where:

b_e = the effective width of the plate.

b = the actual width of the plate.

σ_{cr} = the critical buckling stress.

σ = the applied compressive stress across the width of the plate

σ ($\sigma > \sigma_{cr}$).

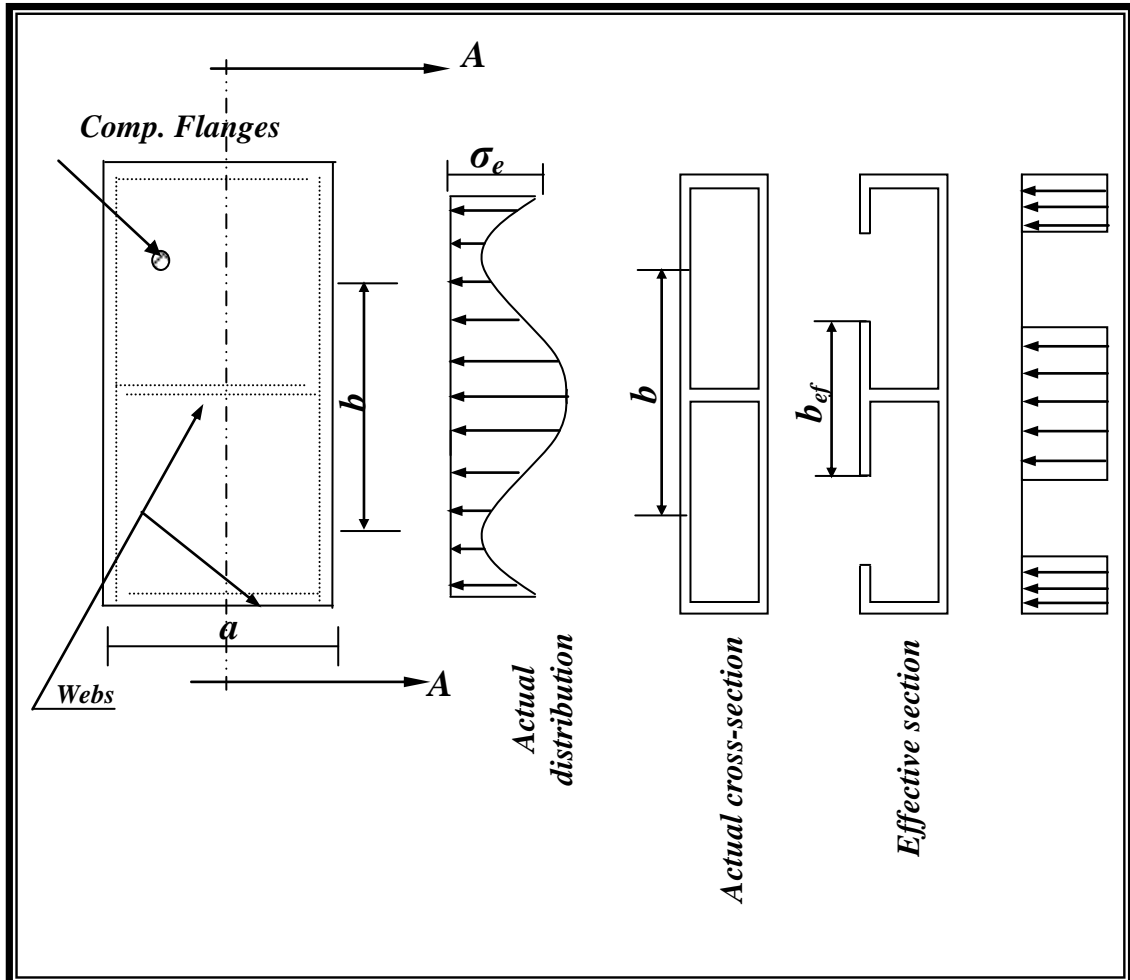


Figure (٥- ٤): Nonlinear stress distribution in buckled plate replaced by assumed uniform stress distribution acting on the compression flange

Many investigators have suggested somewhat more accurate expressions than *Von Karman's* equation. *Marguerre* ^(٥٨) gave the following expression for the effective width of a plate with simple boundary condition:

$$b_e = 0.5b \left(\frac{1 + \sigma_{cr}}{\sigma_m} \right) \quad (0.12)$$

where $\sigma_m = \frac{\sigma_1 + \sigma_2}{2}$ is the mean stress in the edge of the plate.

Winter (1947)⁽⁹⁷⁾ proposed an empirical correction to *Von Karman* formula, and suggested the following expression to predict the effective width of a buckled plate:

$$b_e = b \left(\frac{\sigma_{cr}}{\sigma} \right)^{0.5} \left(1 - 0.25 \left(\frac{\sigma_{cr}}{\sigma} \right)^{0.5} \right) \quad (0.13)$$

Koiter (97) gave, for all edge conditions, the following approximation to evaluate the effective width:

$$b_e = b \left[1.2 - 0.65 \left(\frac{\sigma_{cr}}{\sigma_m} \right)^{\frac{2}{5}} + 0.45 \left(\frac{\sigma_{cr}}{\sigma_m} \right)^{\frac{4}{5}} \right] \left(\frac{\sigma_{cr}}{\sigma_m} \right)^{\frac{2}{5}} \quad (0.14)$$

Cox (97) suggested that for plates with clamped edges, the effective width could be represented by the approximate formula:

$$b_e = b \left[0.14 + 0.86 \left(\frac{\sigma_{cr}}{\sigma_m} \right)^{\frac{1}{2}} \right] \quad (0.15)$$

Faulkner (1978)⁽⁷⁷⁾ proposed the following empirical formula:

$$b_e = 1.05b \left(\frac{\sigma_{cr}}{\sigma} \right)^{0.5} \left(1 - 0.27 \left(\frac{\sigma_{cr}}{\sigma} \right)^{0.5} \right) \quad (0.16)$$

Shanmugam and *Evans* (1981)⁽⁷⁹⁾, *Evans* and *Shanmugam* (1984)⁽⁷⁷⁾ recommended using *Winter's* formula for the effective width of the compression flange panel. *Shanmugam* and *Evans* (1981)⁽⁷⁹⁾ clarified that the loss in effective width for the equivalent grillage member begins to become significant when a compression flange panel is subjected to a stress

equal to 1.5 times its buckling stress. Also, they suggested that the reference stress for each grillage member be taken as the average of the calculated nodal stresses of the member. This suggestion is considered in the present study.

Several recent studies (*Kalyanaraman and Rao* (1994)⁽⁴⁴⁾, *Schafer and Peköz* (1994)⁽⁴⁵⁾, *Marsh* (1994)⁽⁴⁶⁾ and *Ranby* (1994)⁽⁴⁷⁾) have shown that the expression suggested by *Von Karman* overrates the ultimate load resistance, while *Winter's* formula (which is used in *Eurocode 3 Part 1.2* (1990)⁽⁴⁸⁾ and *AISI* (1991)⁽⁴⁹⁾ in a slightly modified form) is sufficiently accurate and confidently recommended for use as follows:

$$\text{For } \left(\frac{\sigma_{cr}}{\sigma} \right)^{0.5} < 0.673$$

$$b_e = b \left(\frac{\sigma_{cr}}{\sigma} \right)^{0.5} \left(1 - 0.22 \left(\frac{\sigma_{cr}}{\sigma} \right)^{0.5} \right) \quad (5.17)$$

otherwise, $b_e = b$

Regarding the present work, Eq.(5.17) is used for evaluating the effective widths of compression flange panel at the beginning and the end of the grillage member.

5.2 Post-Buckling Behavior of Web Panel

5.2.1 Introduction

The primary functions of the web plate in a plate girder to maintain the relative distance between the top and bottom flanges and resist the introduced shearing force. In practical thin plate girders, the web plates carries (90%) or more of the applied transverse shear and that, although the flange resists most of the bending moment, the web may carry a considerable part. When the applied loads are increased the combination of stresses (shear and bending) acting on the web may initiate buckling, yielding, or both buckling and yielding. Then, as the applied loads are further increased the web must carry an even greater shearing force

(because the flanges cannot carry considerable shearing force). In order to do this, the web must reduce its share of the bending moment. Thus, the flanges have to carry not only the increase in bending moment from the applied loads but also that what the web sheds off in order to carry the increase in shearing force. This phenomenon is known as **Load Shedding** (59).

Web behavior in the post buckling range and at collapse has been studied by many investigators (63,68,69...). The most well known approach is the so-called "**Rockey's approach**" which is the resultant of many studies carried out by professor **Rockey** and his colleagues in **Cardiff** (74,75). Many researchers (67,68) have recommended to use this approach to predict the post buckling behavior of the web panels till collapse. In the present study, **Rockey's** (67) method, with some modifications, is utilized in the grillage simulation of the nonlinear analysis of cellular plate structures linear-varying depth for predicting the post-buckling behavior for the web panels.

5.3.2 Evaluation of Elastic Critical Shearing Stress

Tests indicate that a stiffened web panel may still have a tendency to buckle even when vertical stiffeners are incorporated into the design. This is because the combination of diagonal tension and diagonal compression can cause closely spaced buckles to form across a diagonal (69).

In order to accurately calculate the elastic buckling strength of the web panel, the boundary conditions need to be properly determined. The elastic shear buckling stress of a rectangular web plate was given by **Timoshenko** and **Gere** (1971) (67) as follows:

$$\tau_{cr} = K \frac{\pi^2 \cdot E}{12(1 - \nu^2)} \left(\frac{t_w}{h} \right)^2 \quad (5.18)$$

where:

K = the shear buckling coefficient.

E = The modules of elasticity.

ν = Poisson's ratio.

h = the depth of web panel (clear distance between upper and lower flanges).

t_w = the thickness of the web panel.

The shear buckling coefficient (K) depends upon the boundary conditions and aspect ratio of the web panel (B/h), where (B) is the unstiffened length of the web panel (clear spacing between transverse stiffeners). Although the real boundary condition at the flange-web juncture is somewhere between simple and fixed, the boundary condition for a mathematical solution has been arbitrarily assumed, mainly due to the lack of means to evaluate it in a rational manner⁽⁶⁴⁾.

Basler and **Thürlimann** (1969)⁽¹³⁾, **Porter et al.** (1970)⁽¹⁰⁾ and **Rockey et al.** (1974)⁽¹⁷⁾ assumed that the web panel is simply supported at the flange-web juncture, while **Chern** and **Ostapenko** (1979)⁽¹⁹⁾ obtained the elastic buckling strength by assuming that the juncture behaves like a fixed supported.

Sharp and **Clark** (1971)⁽⁸⁾ assumed intuitively that the boundary condition lies halfway between the simply supported and fixed condition. **AISC** (1989)⁽²⁾ and **AASHTO** (1997)⁽¹⁾ specification followed **Basler's** procedure, in which the boundary condition of web panels at the juncture is conservatively assumed to be simple.

A study by **Let et al.** (1997)⁽¹⁵⁾ suggested simple design equations to determine shear buckling coefficients that represent various boundary condition. According to this study, the boundary condition at the flange-web juncture is closer to a fixed condition. They reported that the relative flange rigidity expressed in terms of the ratio of the flange thickness to the

web thickness (t_f/t_w) affects the overall ultimate strength by influencing the elastic buckling strength. **Bradford** (1997)^(1v) also pointed out that **AASHTO** assumption underestimated the shear buckling strength. He developed a local buckling design chart for shear buckling coefficients for plate girders that represented more accurately the field condition. The local buckling chart by **Bradford** gives values of shear buckling coefficients very close to that suggested by **Lee et al.** (1997)^(or).

Lee and Yoo (1998)^(o2) confirmed the validity of the design equations by **Lee et al.** (1997)^(or) and recommended them for use in the investigation of the ultimate shearing strengths of web panels. They also concluded that the assumption of the boundary condition at the flange-web juncture being simply supported gives much too conservative shearing strength for many web panels. Using **NASTRAN** computer program, they conducted nonlinear analyses by three-dimensional finite element models on a transversely stiffened plate girder web panel subjected to pure shear. The results obtained from these analyses showed that the boundary condition at juncture is much closer to a fixed supported. Accordingly, they suggested that the shear buckling coefficient (**K**) could be calculated as follows:

Form **Timoshenko and Gere** (1971)⁽⁸⁷⁾ and **SSRC Guide** (1988)⁽⁸²⁾:

1- For plates simply supported at all edges;

$$K_{ss} = 4 + 5.34 \left(\frac{h}{B} \right)^2 \quad \text{for } \frac{B}{h} < 1 \quad (0.19a)$$

$$K_{ss} = 5.34 + 4 \left(\frac{h}{B} \right)^2 \quad \text{for } \frac{B}{h} \geq 1 \quad (0.19b)$$

2- For plates where two opposite edges are simply supported and the others fixed;

$$K_{sf} = 5.34 \left(\frac{h}{B} \right)^2 + 2.31 \left(\frac{h}{B} \right) - 3.44 + 8.39 \left(\frac{h}{B} \right) \text{ for } \frac{B}{h} < 1 \quad (0.20a)$$

$$K_{sf} = 8.98 + 5.61\left(\frac{h}{B}\right)^2 - 1.99\left(\frac{h}{B}\right)^3 \quad \text{for } \frac{B}{h} \geq 1 \quad (5.20b)$$

The shear buckling coefficient (k) of a web panel according to the previously mentioned study by *Lee et al.* (1997)⁽⁵⁷⁾ is;

$$K = K_{ss} + \frac{4}{5}(K_{sk} - K_{ss}) \left[1 - \frac{2}{3} \left(2 - \frac{t_f}{t_w} \right) \right] \quad \text{for } \frac{1}{2} < \frac{t_f}{t_w} < 2 \quad (5.21a)$$

$$K = K_{ss} + \frac{4}{5}(K_{sf} - K_{ss}) \quad \text{for } \frac{t_f}{t_w} \geq 2 \quad (5.21b)$$

$$K = K_{ss} \quad \text{for } \frac{t_f}{t_w} \leq 2 \quad (5.21c)$$

Regarding the present study, Eqs.(5.21a, 5.21b and 5.21c) are used to evaluate the shear buckling coefficients for web panels.

5.3.3 Review of Failure Theories for Web Panels

The various possible failure modes of a web are illustrated by *Murray* (1984)⁽⁵⁹⁾, as shown in Fig.(5-5). The following brief review of failure theories for web panels is presented depending on various modes of failure.

Basler and *Skalout* (1971)⁽¹⁴⁾ assumed that since flange in practical plate girders under pure shear, do not possess sufficient flexural rigidity to resist the diagonal tension, the diagonal tension field does not develop near the web-flange juncture and the web collapses after development of the yield zone, as shown in Fig.(5-5a). *Rockey* and *Skalout* (1972)⁽⁵²⁾ found

that the collapse mechanism involved plastic hinges in the flanges and that these flanges often had a strong influence upon the behavior of the web panel. They assumed that for the case when the transverse shearing force acts alone (i.e., $M=0$) the plastic mechanism had the form shown in Fig. (5-5b), where it is seen that the tension field is assumed to be parallel to the diagonal of the web panel.

Porter et al. (1970)⁽¹⁰⁾ developed a failure theory for a web panel loaded in shear, based on the assumption that the flanges are able to anchor the diagonal tension field, as shown in Fig (5-5c). According to their theory, plastic hinges form after the development of the yield zone, and finally, the web panel fails in a sway mechanism.

Rockey et al. (1974)⁽¹¹⁾ proposed a design method that allowed for combined loading of shearing force and bending moment. Their method can cater for all of the collapse modes illustrated in Fig. (5-6)⁽¹¹⁾ with some modifications, and when it was compared with the test-measured collapse loads of eighty-eight girders reported by various investigators, it was found that the average value (predicted collapse load/measured collapse load) was (1.11). This method will be studied in details in the next section, and will be used in present study.

Lee and Yoo (1994)⁽¹²⁾ presented a parametric study to predict the ultimate shearing strengths of web panels subjected to pure shear by conducting nonlinear finite elements analysis using *NASTRAN* computer program. From this study, they concluded that when the plastic shearing force (V_{YW}) is greater than the elastic shear buckling (V_{CR}), the post – buckling strength (V_{PB}) is approximately equal to (40%) of the difference between (V_{YW}) and (V_{CR}). Accordingly, new design equations were proposed for the determination of the ultimate strengths of the web panels, as follows:

$$V_{pB} = 0.4(V_{yw} - V_{cr}) \quad (5.22)$$

where

$$V_{yw} = \frac{\sigma_{yw}}{\sqrt{3}} \cdot h \cdot t_w$$

in which

V_{yw} = the shearing force required to make the web fully plastic.

σ_{yw} = the yield stress of the web material.

$$V_{cr} = K \frac{\pi^2 \cdot E}{12(1 - \nu^2)} \left(\frac{t_w}{h} \right)^2 \cdot h \cdot t_w \quad (5.23)$$

The ultimate shearing strength (V_u) is obtained by adding (V_{pB}) to (V_{cr})

$$V_u = V_{cr} + V_{pB} \quad (5.24)$$

By substituting Eq. (5.22) into Eq (5.24):

$$V_u = 0.7V_{cr} + 0.4V_{yw} \quad (5.25)$$

5.3.4 Proposed interaction diagram

The parametric studies carried out by *Evans, Porter* and *Rockey* (1976) (34) have established that the interaction between the transverse shear and the bending acting on a web panel can be quite accurately represented by the interaction diagram shown in Fig (5-6). In this diagram, the transverse shearing capacity of the web is plotted on the vertical axis and the bending moment capacity is plotted horizontally. Thus, any point on the interaction diagram shows the coexistent values of shearing force and bending moment that can be sustained by the section.

The interaction diagram has three main stages, for each there is a specified limit for the web ultimate shearing capacity (V_s , V_c , and V_b) acting with their associated limits of bending moments (M_s ; M_f , and M_{ult}), respectively. These notations will be explained in the next section. The three stages may be summarized as follows:

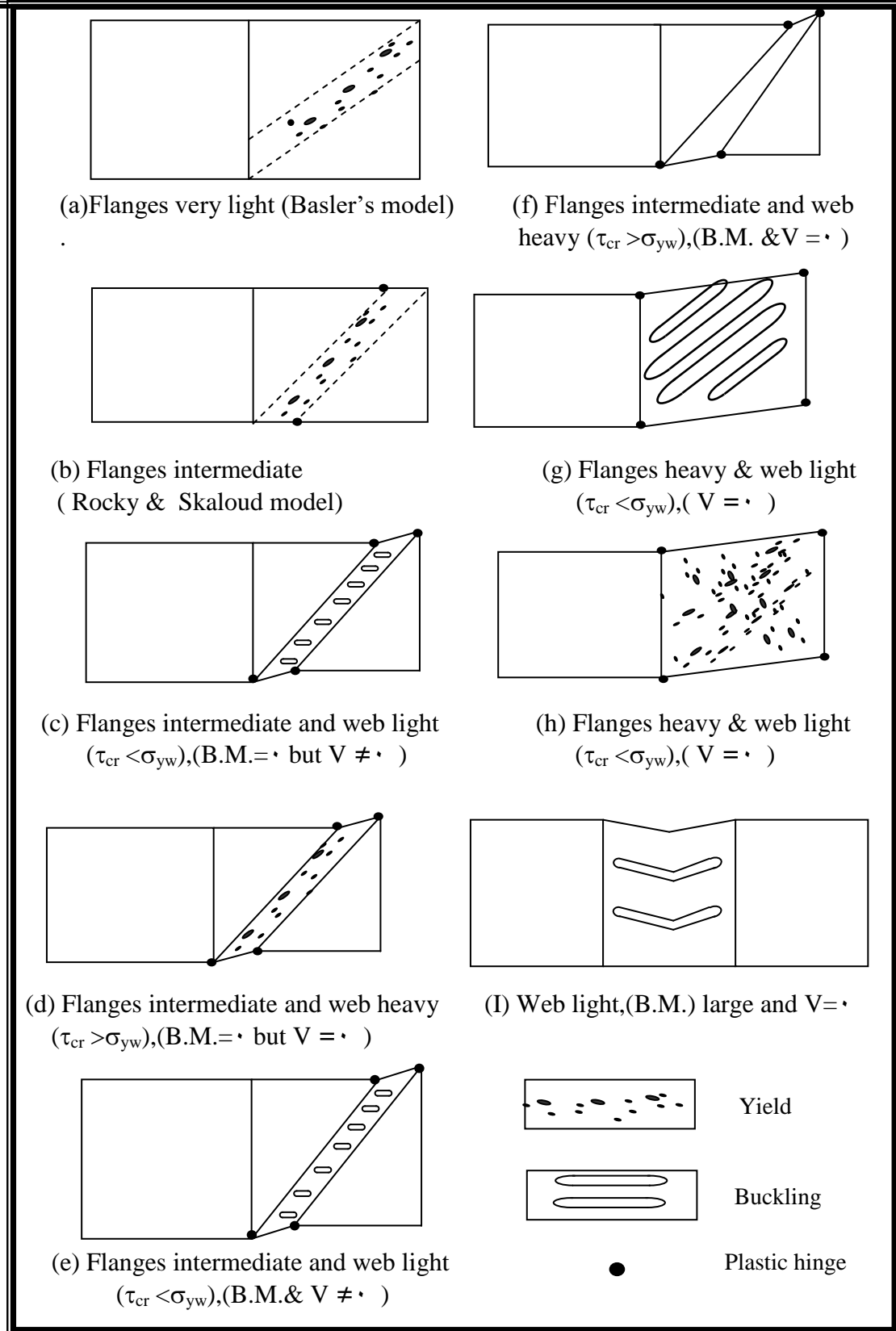
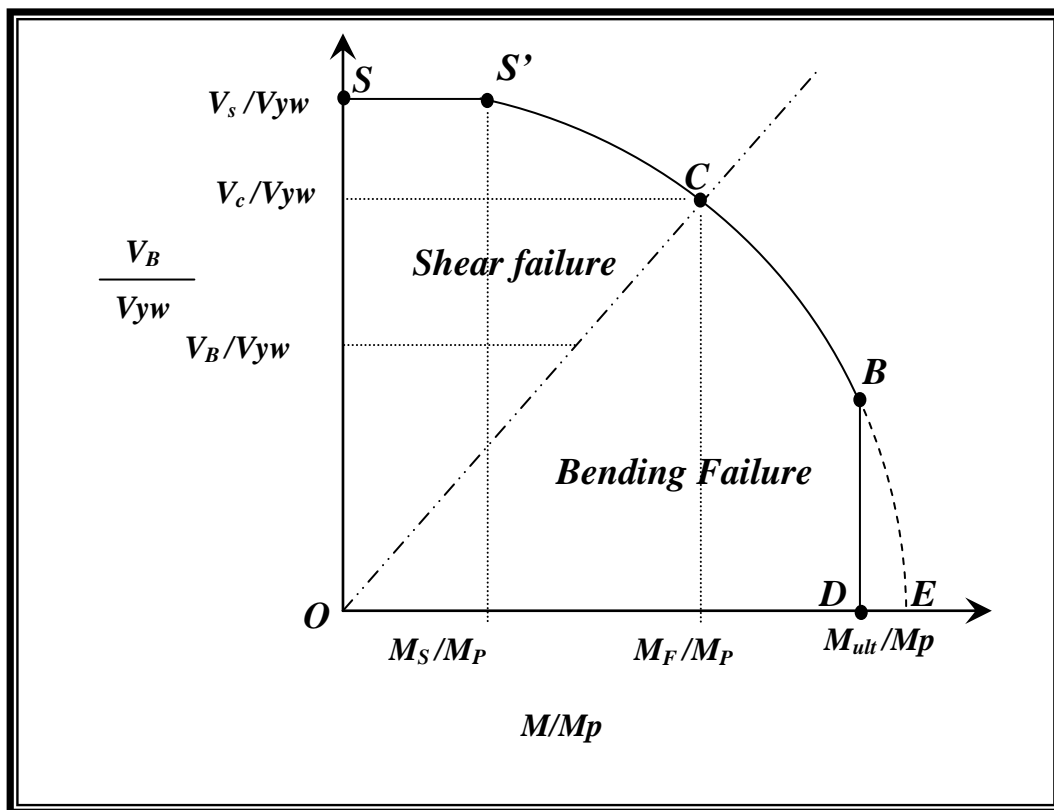


Figure (5-5) Modes of failure of plate girder ^(5A)

1-A straight line joins (S) and (S') which represents a constant value for the ultimate shearing capacity (Vs), which exists when the associated bending moment varies from zero (pure shear) to (Ms').

• A parabola with its crown at (S') is fitted between (S') and (C), and this corresponds to a bending moment value between (M_S) and (M_F) with its associated ordinates (V_S) and (V_C), respectively.

• A further reduction in the shearing capacity will exist when the bending moment exceeds (M_F). Then, the interaction diagram terminates at a shearing capacity of (V_B) associated with the ultimate bending capacity (M_{Ult}). The curve (CBE) is also a parabola with its crown at point (E). According to the simplified design method presented by *Rockey et al.* (1974)^(v), the points (S , S' , C , B and D) which construct the interaction diagram are located according to simple formulas and the curves connecting these points are either straight lines or parabolas. This method will be discussed in detail in the following section.



Figure(5-1) Interaction diagram between shear and bending effect for web

5.3.3 Rockey's Method

As mentioned in Section (5.3.3), *Rockey, Evans, and Porter* (1974) presented a simple design method for predicting the collapse behavior of

web panels subjected to combined action of transverse shearing force and bending moment. This method is considered to be the most general of the collapse mechanisms illustrated in Fig.(5-5), that is, as that shown in Fig.(5-5e), other cases can be treated as special cases of this mechanism (5-8).

According to **Rockey's** method, three stage of web behavior leading up to collapse are considerable, as follow:

I-Stage 1 (Unbuckled behavior)

When a web panel is subjected to a uniform shearing stress of magnitude (τ), equal tensile and compressive principal stresses of ($\sigma_t = \sigma_c$) of magnitude equal to τ will be developed prior to incipient buckling at (45°) and (135°), as shown in Fig.(5-6a). The web plate remains perfectly flat until the applied shearing stress (τ) reaches the critical value (τ_{cr}) at which the panel will buckle (along the diagonal of the compressive stress). This critical value (τ_{cr}) is determined as mentioned in Section (5.3.2).

II- Stage 2 (Post-buckled behavior)

When the critical stress (τ_{cr}) is reached, the web panel starts to buckle and it cannot resist any increase in compressive stress. Any additional load, beyond the buckling load, has to be supported by tension field action (or tensile membrane field), which is anchored against the top and bottom flanges and against the adjacent transverse webs on either side of the longitudinal web panel, as shown in Fig (5-6b). In this field, the tensile membrane stresses (σ_t) are inclined at an angle (θ) to the horizontal. At the start of this stage, the stresses acting on the faces of a small rectangular element obtained by a rotation through angle (θ), as shown in Fig.(5-7), may be found using **Mohr's** circle (5-9), as follows:

$$\sigma_\theta = \tau_{cr} \sin(2\theta) \quad (5.26a)$$

$$\sigma_{\theta+\pi/2} = \tau_{cr} \sin(2\theta) \quad (5.26b)$$

$$\tau_{\theta} = \tau_{cr} \cos(2\theta) \quad (5.26c)$$

As such, the total state of stresses in the web panel ($\sigma_{\theta PB}$) may be obtained by superimposing the tensile membrane stresses (σ_t) to the tensile stresses (σ_{θ}) set up when the applied shearing stress reaches its critical value (τ_{θ}). So, Eq.(5.26a) becomes:

$$\sigma_{\theta PB} = \tau_{cr} \cdot \sin(2\theta) + \sigma_t \quad (5.27)$$

Since the flanges are of finite bending (or flexural) rigidity, they begin to bend inwards under the pull exerted by the diagonal tension

III-Stage r (Ultimate load behavior);

Upon further increase of the applied shear loading, the membrane tensile stress (σ_t) (developed in the web panel) increases and a greater pull is exerted upon the flange. Eventually, the membrane tensile stress reaches such a value that when combined with that from the critical shearing stress (τ_{cr}) as in Eq.(5.27), the resulting stress ($\sigma_{\theta PB}$) reaches the yield stress (σ_{YW}) for the web material. This value of the tensile membrane stress will be denoted as (σ_t^y) and it may be determined by applying **Von Mises-Hencky** yield criterion, which is common to use in plasticity problems, as follows:

$$\sigma_y^2 = \sigma_1^2 + \sigma_2^2 - \sigma_1 \cdot \sigma_2 + 3\tau^2 \quad (5.28)$$

where

σ_y = the yield stress

σ_1, σ_2 = the direct stresses acting on two orthogonal planes

τ = the shearing stress

Thus, for the web panel:

$$\sigma_{yw}^2 = (\sigma_{\theta} + \sigma_t^y)^2 + \sigma_{(\theta+\pi/2)}^2 - (\sigma_{\theta} + \sigma_t^y) \sigma_{(\theta+\pi/2)} + 3\tau_{\theta}^2 \quad (5.29)$$

By substituting Eqs.(5.26a, 5.26b, and 5.26c) in Eq. (5.29), the value of the tensile membrane stress to produce yield (σ_t^y) is obtained in terms of

the critical shearing stress (τ_{cr}) and the inclination (θ) of the tension field, as follow:

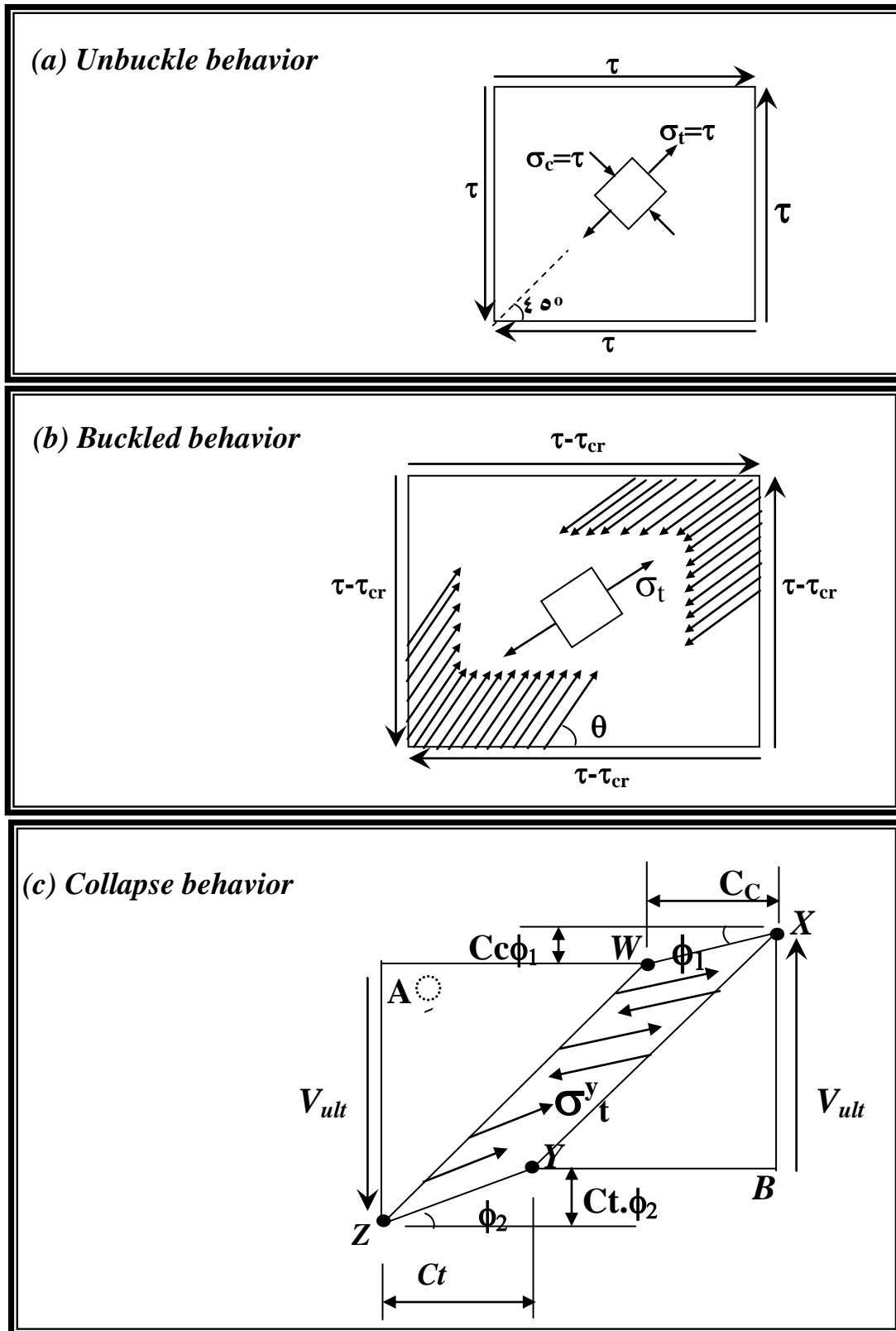
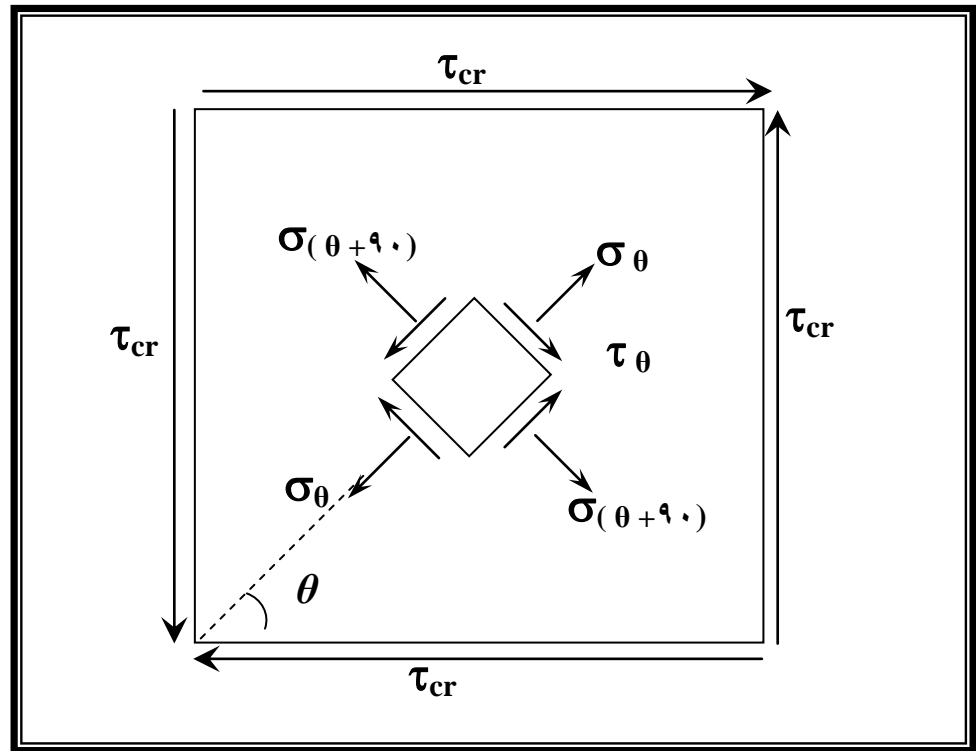


Figure (5- 1) Stages in web behavior up to collapse



Figure(5-1) State of stress in web at post-buckling stage

$$\frac{\sigma_t^y}{\sigma_{yw}} = \left[1 + \left(\frac{\tau_{cr}}{\tau_{yw}} \right)^2 (0.75 \sin^2 2\theta - 1) \right]^{1/2} - \frac{\sqrt{3}}{2} \cdot \frac{\tau_{cr}}{\tau_{yw}} \sin 2\theta \quad (5.30)$$

where:

$$\tau_{yw} = \frac{\sigma_{yw}}{3} \quad (5.31)$$

When the material in the region (WXYZ) of the web panel in Fig.(5-1c) reaches the yield stress (σ_{yw}), the panel cannot sustain any further increase in load and the final sway failure of the web will occur due to the formation of the plastic hinges in the flange panels, as shown in the same Fig (5-1c). The failure load may be determined by applying a virtual sway displacement to the web panel in its collapse stage, Fig(5-1c). It is convenient to consider the yield region (WXYZ) of the web panel to be removed and to replace its action upon the adjacent flange and regions by the membrane tensile stresses (σ_t^y).

Murray (1984)⁽²⁹⁾ proposed the following equations to determine the reduced plastic moments of the flanges (due to the influence of the normal stresses acting on the compression and tension flanges):

For the compression flange:

$$M'_{Pfc} = M_{Pfc} \left[1 - \left(\frac{\sigma_{cf}}{\sigma_{yf}} \right)^2 \right] \quad (5.32)$$

For the tension flange:

$$M'_{Pft} = M_{Pft} \left[1 - \left(\frac{\sigma_{tf}}{\sigma_{yf}} \right)^2 \right] \quad (5.33)$$

where:

M_{Pfc}, M_{Pft} = are the plastic moment capacities of the compression and tension flanges, respectively which be determined later.

σ_{cf}, σ_{tf} = are the average normal stresses in the compression and tension flanges respectively.

σ_{yf} = is the yield stress of the flange material.

Now, there is a need to determine the position of the plastic hinges (C_c, C_t) in the compression and tension flange, respectively. For this purpose, **Murray**⁽²⁹⁾ suggested that during the virtual displacement (ϕ_1) of the mechanism the compression flange, as shown in Fig (5-9c), the work done by the shearing force at (X) is equal to the energy absorbed by the plastic hinges at (X and W) and to the work done against the tension field stress (σ_t^y). It is convenient to take an average value for the membrane tensile stress, that is, (σ_t^y) at the midpoint of (WX)⁽²⁹⁾, as shown in Fig (5-9).

Thus:

$$V_X \cdot C_C \cdot \phi_1 = \sigma_t^y \cdot t_w \cdot \frac{C_C^2}{2} \cdot \sin^2 2\theta + 2M'_{PFC} \cdot \phi_1 \quad (5.34)$$

then:

$$V_X = \frac{C_C}{2} \cdot \sigma_t^y \cdot t_w \cdot \sin^2 2\theta + \frac{2M'_{PFC}}{C_C} \quad (5.30)$$

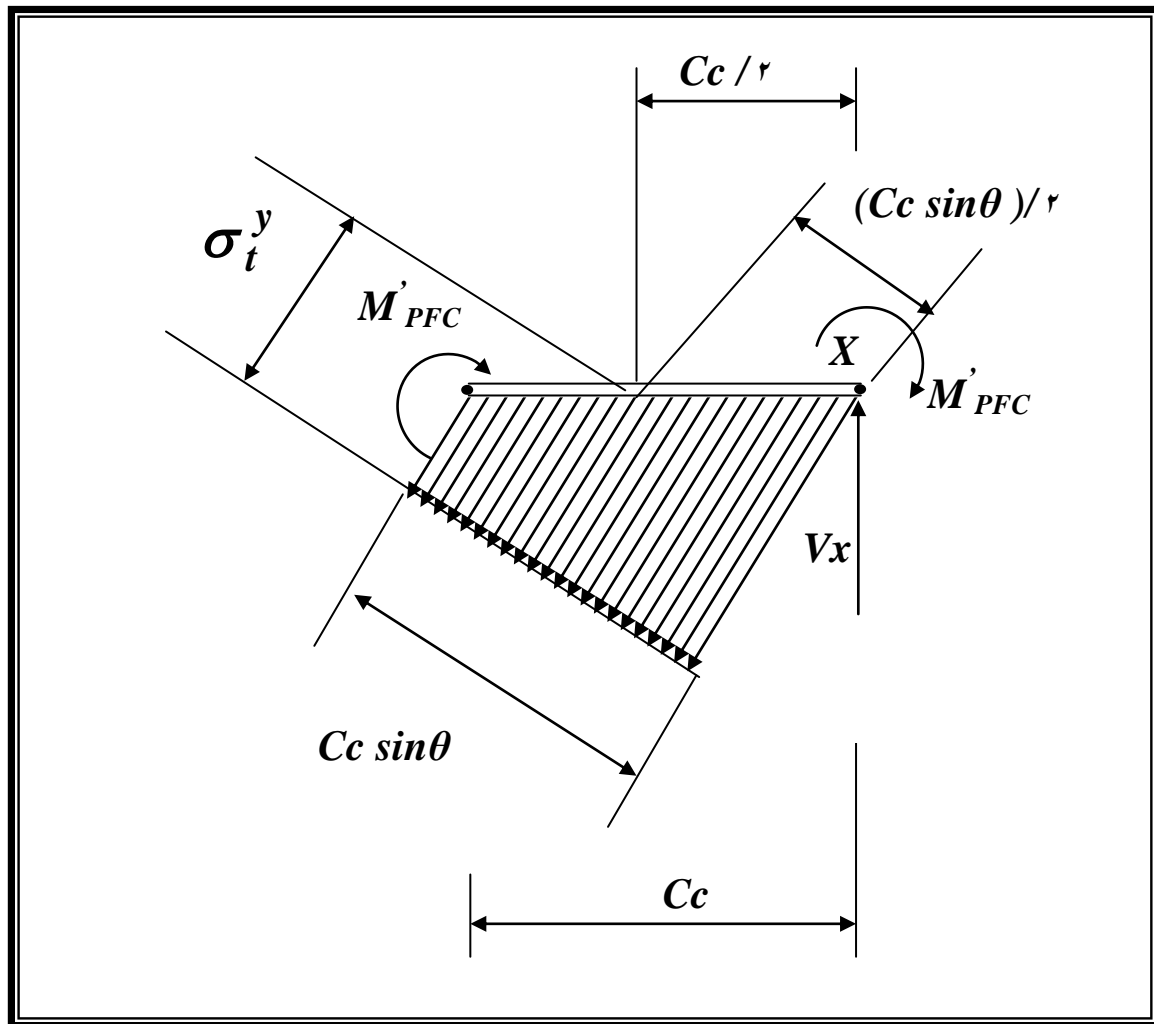


Figure (5-4): Free body diagram of compression flange.

The minimum value of (V_x) is obtained by taking the derivative of (V_x) in Eq.(5.35) with respect to (C_c) and putting this derivative equal to zero.

Thus:

$$\frac{dV_X}{dC_c} = \frac{1}{2} \cdot \sigma_t^y \cdot t_w \cdot \sin^2 2\theta - \frac{2M'_{PFC}}{C_c^2} = 0$$

Then;

$$C_c^2 \cdot (\sigma_t^y \cdot t_w \cdot \sin^2 2\theta - 4M'_{PFC}) = 0$$

from which :

$$C_c = \frac{2}{\sin\theta} \sqrt{\frac{M'_{PFC}}{\sigma_t^y \cdot t_w}} \quad (5.36)$$

Similarly for the tension flange:

$$C_c = \frac{2}{\sin\theta} \sqrt{\frac{M'_{PFT}}{\sigma_t^y \cdot t_w}} \quad (5.37)$$

These equations define the locations of the plastic hinges in the flanges, but there is a restriction that (C_c) and (C_t) must be less than (B) (unstiffened length of web)^(5.9), from Eqs. (5.36) and (5.37):

$$M_{pfc} < \frac{t_w \cdot B^2 \cdot \sin^2 \theta}{4} \cdot \sigma_t^y \quad (5.38)$$

$$M_{pft} < \frac{t_w \cdot B^2 \cdot \sin^2 \theta}{4} \cdot \sigma_t^y$$

Flanges which satisfy the criteria of Eq. (5.38) are said to be light, while those which do not are said to be heavy^(5.9). If these criteria are not satisfied then the plastic hinges would form at the four corners of the web panel, i.e., the points (A , X , B , Z) shown in Fig (5.1c), and the panel will fail like a

Vierendeel girder. In this case, the tension field occupies the whole of the web panel and ($C_c=C_t=B$), as shown in Fig.(e-o-g) and (e-o-h)^(e.3).

In order to locate the ordinate (OS) in the interaction diagram Fig. (e-6), **Rockey et al.** (1978)^[e.4] presented the following equation to determine the pure shearing load ratio (V_s/V_{yw}) for members with identical top and bottom flanges, i. e., the neutral axis is at the mid-depth of the section. Thus, ($C_c=C_t=C$) and ($M_{pfc}=M_{pft}=M_{pf}$) Accordingly, the failure mechanism for this case will be as shown in Figs.(e-o-c) and (e-o-d):

$$\frac{V_s}{V_{yw}} = \frac{\tau_{cr}}{\tau_{yw}} + \sqrt{3} \sin^2 \theta \left(\cot \theta - \frac{B}{h} \right) \frac{\sigma_t^y}{\sigma_{yw}} + 4\sqrt{3} \sin \theta \sqrt{\frac{\sigma_t^y}{\sigma_{yw}} \cdot M_p^*} \quad (e.39)$$

where:

V_{yw} = the shearing force required to make the web panel fully plastic.

$$V_{yw} = \tau_{yw} \cdot t_w \cdot h = \frac{\sigma_{yw}}{\sqrt{3}} \cdot t_w \cdot h$$

$$M_p^* = \frac{M_{pf}}{t_w \cdot h^2 \cdot \sigma_{yw}} \quad \text{and} \quad M_{pf} = \frac{1}{4} \sigma_{yf} \cdot b_f \cdot t_f^2$$

It is be noted that ($b_f=b_c=b_t$) for identical top and bottom flanges.

Mashal (1999) suggested that when a compression flange panel of a cellular plate structure buckles and after adopting the effective width concept for post-buckling, the idealized grillage member is no more symmetrical (the neutral axis moves towards the tension flange). According to this concept, he suggested new derivations by modifying Eq.(e.39), for symmetrical plate girders, to be applicable to unsymmetrical plate girders. So, the following equations were presented:

$$V_s = \tau_{cr} \cdot h \cdot t_w + \sigma_t^y \cdot t_w \cdot \sin \theta (h \cdot \cot \theta - B - C_c) + \frac{2M_{pfc}}{C_c} + \frac{2M_{pft}}{C_t} \quad (e.40)$$

in which:

$$M_{pfc} = \frac{1}{4} \cdot b_{ey} \cdot t_f^2 \cdot \sigma_{yf} \quad (5.41)$$

$$M_{pft} = \frac{1}{4} \cdot b_{ey} \cdot t_f^2 \cdot \sigma_{yf}$$

and:

b_{ey} = the effective width of the compression flange at yield.

b_t = the width of the tension flange.

By substituting Eq.(5.36) and Eq.(5.37) into Eq.(5.40) and after dividing by (V_{yw}) the final expression is:

$$\frac{V_S}{V_{yw}} = \frac{\tau_{cr}}{\tau_{yw}} + \sqrt{3} \sin^2 \theta \left(\cot \theta - \frac{B}{h} \right) \frac{\sigma_t^y}{\sigma_{yw}} + \sqrt{3} \sin \theta \sqrt{\frac{\sigma_t^y}{\sigma_{yw}}} \cdot \left(3\sqrt{M_{pc}} + \sqrt{M_{pt}} \right) \quad (5.42)$$

$$M_{pc}^* = \frac{M_{pfc}}{t_w \cdot h^2 \cdot \sigma_{yw}}$$

$$M_{pt}^* = \frac{M_{pft}}{t_w \cdot h^2 \cdot \sigma_{yw}} \quad (5.43)$$

M_{pc}^* and M_{pt}^* = are the non-dimensional flange strength parameters for the compression and tension flange, respectively.

Regarding the present study, Eq.(5.42) is used, with some modifications, to calculate (V_S) for cellular plate structures, as follows:

$$V_S = \tau_{cr} \cdot h \cdot t_w + \sigma_t^y \cdot t_w \cdot \sin \theta (h \cdot \cot \theta - B - C_c) + \frac{2\hat{M}_{pfc}}{C_c} + \frac{2\hat{M}_{pft}}{C_t} \quad (5.44)$$

where, (M_{pc}^* and M_{pt}^*) are determined from the previously mentioned equations (5.32) and (5.33). In these question (M_{pfc} , M_{pft}) are:

$$M_{pfc} = \frac{1}{4} \cdot b_{ey(av)} \cdot t_f^2 \cdot \sigma_{yf} \quad (5.45)$$

$$M_{pft} = \frac{1}{4} b_{t)av.} \cdot t_f^2 \cdot \sigma_{yf}$$

in which

$$b_{ey)av.} = \frac{b_{ey1} + b_{ey2}}{2} \quad (0.46)$$

$$b_{t)av.} = \frac{b_{t1} + b_{t2}}{2}$$

and:

b_{ey1}, b_{ey2} = the effective width, at yield, of the compression flange at the start and end of grillage member, respectively.

b_{t1}, b_{t2} = the width of the tension flange at the start and end of the grillage member, respectively.

Concerning the evaluation of (θ), the parametric studies carried out by *Evans, Porter, and Rockey (1977)*^(re) showed that (V_s / V_{yw}) has a stationary value when (θ) is approximately equal to two third of the inclination of the diagonal of the web panel, i.e.:

$$\theta = \frac{2}{3} \tan^{-1} \left(\frac{h}{B} \right) \quad (0.47)$$

The use of Eq.(0.47) will lead either to correct value or to underestimation of the collapse load^(vr). So this approximation is safe and it will be used in the present study.

The interaction diagram, Fig.(0-7) shows a constant ultimate shearing capacity (V_s) for an associated bending moment that varies from zero to ($M_{s'}$), where :

$$M_{s'} = V_s B \leq 0.5 M_f \quad (0.48)$$

The bending moment may be of such a high value that it alters the mode of failure from a shear mode to a bending mode. Point (C) on the interaction diagram is the point at which this change occurs and the line

(OC) is the dividing line between the two mode of failure. The parametric studies carried out by *Evans et al.* (1997) showed that the change in the failure modes occurs when the applied (r^e) bending moment is equal to M_f , which represents the plastic moment of resistance of flanges alone (neglecting the contribution of the web) about neutral axis. Thus, the horizontal coordinate of point (C) for a symmetrical section is calculated as follows:

$$M_f = \sigma_{yf} \cdot b_f \cdot t_f \cdot d \quad (5-49)$$

where

d = the distance between the centerline of the flange plates.

In the present study, the calculation of (M_f) for unsymmetrical grillage members (after applying the effect width concept for the compression flanges) is suggested, by taking the moments about the new position of the neutral axis, as follows:

$$M_f = \sigma_{yf} \cdot t_f (b_{ey} \cdot \lambda_y + b_t [d - \lambda_y]) \quad (5-50)$$

where

λ_y = the distance from the neutral axis to the centerline of the compression flange at yield, as shown in Fig.(5-10):

To evaluate the ultimate shearing capacity at point (C), the following empirical equation derived by the previously mentioned parametric studies are given:

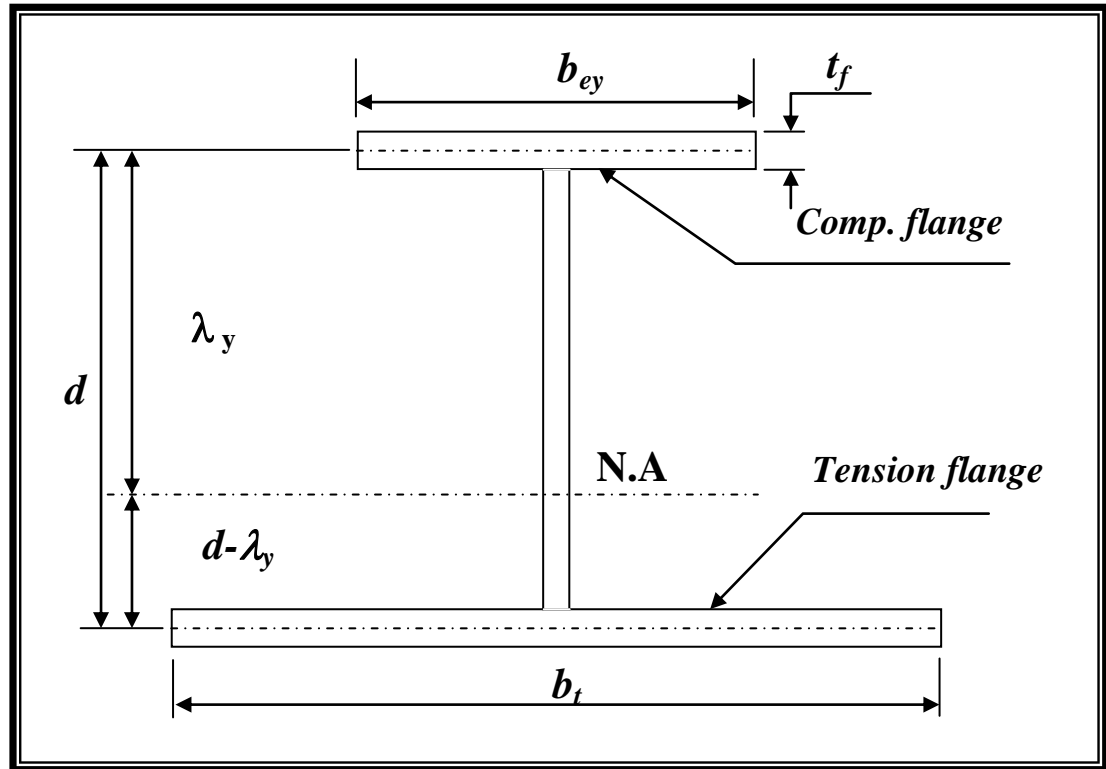
$$\frac{V_c}{V_{yw}} = \frac{\tau_c}{\tau_{yw}} + \frac{\sigma_t^y}{\sigma_{yw}} \sin 2\theta \left(0.554 + 36.8 \frac{M_{pf}}{M_f} \right) \left(2 - \left[\frac{B}{h} \right]^{1/8} \right) \quad (5-51)$$

51)

If $V_c > V_s$ then:

$$\frac{V_c}{V_{yw}} = \frac{V_s}{V_{yw}}$$

Regarding the present study it is suggested to take the parameter M_{pf} in Eq. (0.01) as $M_{pf)av.}$, where



$M_{pf)av.} = \frac{M_{pfc} + M_{pft}}{2}$ Figure (0.10) Unsymmetrical section for the grillage member

(0.02)

If a plate girder is subjected to a bending moment in excess of (M_f) then it will fail in a bending mode (γ). According to the load shedding phenomenon that was described in Section (0.3.1), the web will shed off the bending stresses that it should carry to the flanges. Thus, the cross section will be unable to develop the full plastic moment of resistance of the full section (M_p), where (M_p) is used as the denominator to the nondimensionalized horizontal coordinate of the interaction diagram. Thus:

$$M_p = M_f + M_{pw} \tag{0.03}$$

where:

M_{pw} = the plastic moment of resistance of the web plate acting alone

$$M_{pw} = \frac{1}{4} \sigma_{yw} \cdot t_w \cdot h^2$$

The section will fail by inward collapse of the compression flanges. This type of flange failure will occur at an applied moment value (M_{ult}), which

is approximately equal to the moment required to produce first yield in the extreme fiber of the compression flanges.

Schafer and *Peköz* (1991)⁽¹⁷⁾ suggested that since the web undergoes compressive stress, it is prone to buckling, and thus, its ultimate strength is governed by applying the effective width expressions, such as Eq.(5.16). They concluded that for most of the sections, the web is fully effective and the incorporation of its effective width due to buckling would a little influence on the results.

In order to determine the ultimate moment capacity (M_{ult}), *Rockey et al.* (1971)⁽¹⁸⁾ suggested to use the following empirical formula due to *Cooper* (1970, 1971)^(19,20):

$$\frac{M_{ult}}{M_y} = 1 - 0.0005 \frac{A_w}{A_f} \left(\frac{h}{t_w} - 5.7 \sqrt{\frac{E}{\sigma_{yf}}} \right) \text{ for } M_{ult} \leq M_p \quad (5-5)$$

where

M_y = the bending moment required to produce the first yield in the extreme fiber of the compression flange, assuming a fully effective web (neglecting the effect of web buckling).

A_f, A_w = the cross sectional area of the web and each of the flanges, respectively.

In the present study the parameter will be approximately taken as $A_{f(av)}$:

$$A_{f(av)} = \frac{A_{fc} + A_{ft}}{2} \quad (5-6)$$

where

A_{fc}, A_{ft} = the cross sectional area of the compression and tension flanges, respectively.

When the applied bending moment reaches the value (M_{ult}) the corresponding bending stress in the web plate is below the yield. Consequently, the web plate can support a certain amount of coexistent shear loading. This load is defined by the ordinate (V_B) in the interaction diagram Fig.(5-9). In order to calculate the shearing force (V_B), which acts with the bending moment (M_{ult}), *Rockey et al.* (1974)⁽¹⁷⁾ recommended using the following equation:

$$V_B = V_C \left(\frac{M_P - M_{ult}}{M_{pw}} \right) \quad (5-56)$$

As maintained before and according to the simple design method presented by *Rockey et al.* (1974), the curve (*CEB*) in the interaction diagram may be represented by a simple parabola. This curve will be terminated at point (**B**), as the applied bending moment reaches (M_{ult}), because the cross section cannot provide the full plastic moment of resistance (M_p) (as mentioned previously). Therefore, point (**B**) represents the terminating point of the interaction diagram. In this way the complete diagram is defined and drawn and can be programmed.

5.4 Computational Technique

In the present study, the nonlinear response of a thin walled cellular plate structure is investigated by the linear incremental approach. In this approach the load is applied as a series of small proportional increments (not necessarily equal in magnitude) and for each of these increments, the change in deformation is determined using a linear analysis, as shown in Fig.(5-11)

The magnitude of the load increment influences the accuracy of the solution. Accordingly, the load increment is chosen to be so small that a

negligible difference in the estimated collapse load will occur (existence of convergence).

A so-called tangent stiffness matrix based on geometry and internal forces existing at the beginning of any step (beginning of load increment) is constructed. The total displacement and internal forces at the end of any step are obtained by summing the incremental changes in displacement and internal forces up to that load point.

At the end of the *n*-th increment, the total applied load is given by:

$$\{P\}_n = \sum_{i=1}^n \{\Delta P\}_i \quad (5.57)$$

where:

$\{P\}_n$ = The n-th applied accumulated incremental load vector.

$\{\Delta P\}_i$ = The i-th applied incremental load vector.

Similarly, the displacements at the end of the n-th incremental are:

$$\{X\}_n = \sum_{i=1}^n \{\Delta X\}_i \quad (5.58)$$

where:

$\{X\}_n$ = The n-th accumulated incremental displacement vector.

$\{\Delta X\}_i$ = The i-th incremental displacement vector.

The tangent stiffness matrix for the i-th increment is formed for the conditions existing at the end of the previous [(i-1)-th] increment. Thus, the linearized simultaneous equations to be solved in each increment are given by:

$$[K]_{i-1} \cdot \{\Delta X\}_i = \{\Delta P\}_i \quad (5.59)$$

in which:

$$[K]_{i-1} = [K(\{P\}_{i-1}, \{X\}_{i-1})] \quad (5.60)$$

where:

$\{P\}_{i-1}$ = the vector of nodal forces at the end of the previous load increment.

$\{X\}_{i-1}$ = the vector of nodal displacement at the end of the previous load increment.

Accordingly, the stiffness matrix is nonlinear in terms of internal end forces and nodal displacements of members. The updated configuration of the structure are obtained depending on the internal forces reached by the previous load increment from the updated internal forces, the effective widths in the pre-and post-buckling ranges and the development of plastic hinges will be determined

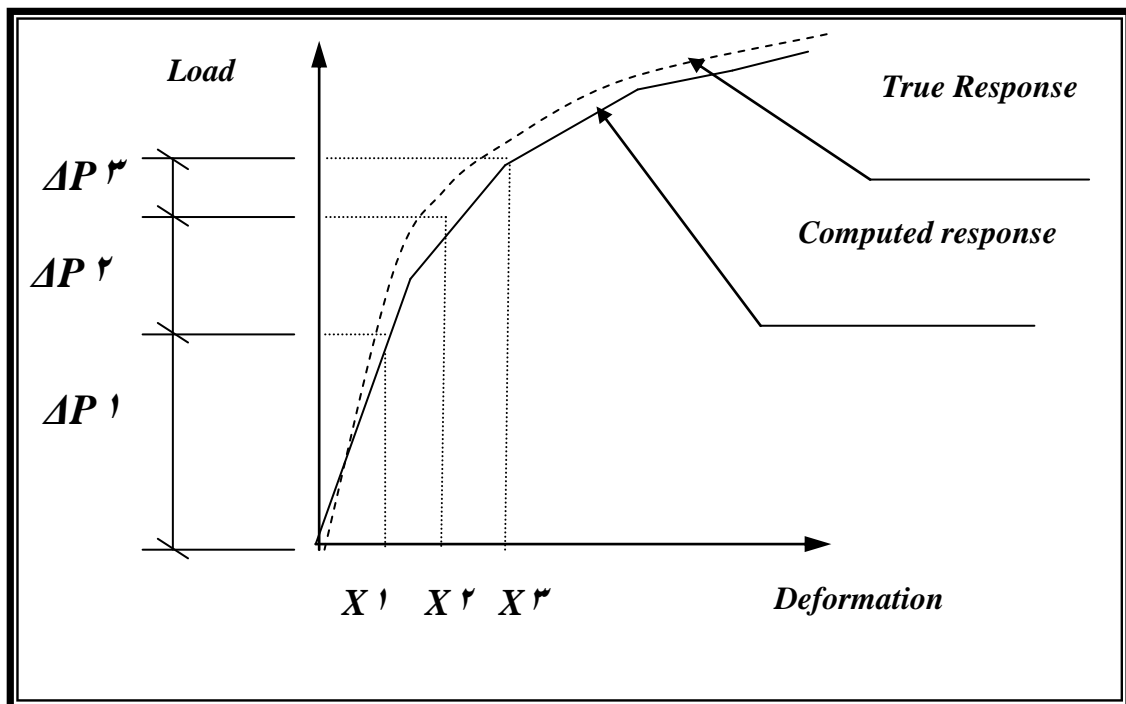


Figure (2-11) The nonlinear response of structure by incremental load approach.

2.2 Interpretation of Output

According to the suggestion for considering the shear lag only in the tension flange and the effect of post-buckling in compression flanges only, the cross section of the grillage member will be unsymmetrical.

Consequently, the neutral axis will not remain in the mid-depth of the section but moves towards the tension flanges as the applied loading increases. Thus, the second moment of area (I_y) for a certain section of a grillage member is calculated as follows:

$$I_y = \frac{1}{(1-\nu^2)} \left[t_f \cdot b_e \cdot \lambda^2 + t_f \cdot b_t (d - \lambda)^2 \right] + \frac{t_w \cdot h^3}{12} + t_w \cdot h \cdot \left(\lambda - \frac{d}{2} \right)^2 \quad (5-61)$$

where λ is the distance from the neutral axis to the centroid of the compression flange:

$$\lambda = \frac{0.5 \cdot t_w \cdot h + d \cdot b_t \cdot t_f}{(b_e + b_t) \cdot t_f + t_w \cdot h} \quad (5-62)$$

As mentioned in the previous section, the load will be applied as a series of small load increments. For each load increment (ΔP_i) the incremental (normal) stress (σ_{xi}) can be calculated from the grillage incremental bending and warping moments (M_{yi} and B_i) using the following formula :

$$\sigma_{xi} = \frac{M_{yi} \cdot Z}{I_{yi-1}} + \frac{B_i \cdot \omega}{I_w} \quad (5-63)$$

where:

Z = the distance from the neutral axis to the level at which the stress is desired.

I_{yi-1} = the second moment of area of a section at the end of the previous load increment.

ω = the sectorial area at the point where the normal stress is to be calculated

I_w = the warping moment of inertia for the whole section.

The total (accumulative) stress at the end of the load increment (i) is the sum of the previous incremental flexural stresses , as follows:

$$\sigma_x = \sum_{i=1,2,3,\dots} \sigma_{xi} \quad (5-64)$$

Regarding the compression flange, as the accumulative stress (σ_x) reaches the critical stress (σ_{cr}), the flange will buckle and the post-buckling behavior will be represented by applying the effective width concept, as mentioned previously. When (σ_x) in the compression or tension flange reaches the yield stress (σ_{yf}), the flange will fail and, accordingly, the cross section will be treated as (T-section) for further loading. At any end of the grillage member, if (σ_x) in both compression and tension flange reaches (σ_{yf}) then a plastic hinge will be inserted at this end.

5-7 Computer Program (NONLINEAR)

A computer program is coded in *FORTRAN* language to evaluate the section properties of any cellular section having n cells and with different dimensions.

A computer program NONLINEAR is written in the present study to carryout the non-linear analysis and investigate the collapse loading of steel cellular plate structure using the grillage analogy method.

The program follows the aspect of the non-linear behavior and a complete description of the program structure is given in the flow chart in appendix (A).

5-8 Summary of The Present Study

In the present study, an attempt is made to predict the non-linear behavior of non-prismatic steel cellular plate structures and to investigate the collapse loading by applying the grillage analogy. So, the following guide lines are adopted:

- 1- An incremental loading procedure is used as discussed in sec (5-4).

- ϒ- The critical stress in the compression flange panel of a straight member is evaluated by Eq.(ϑ-ϕ).
- ϒ- **Von-Karman** approach (effective width concept) is adopted to represent the post-buckling behavior of the compression flange panel. The modified **Winter's** formula Eq.(ϑ-ϕ) is used to calculate the effective width of the compression flange panel in the nonlinear range.
- ξ- During the incremental loading procedure, when the flexural stresses in the compression and tension flange reach the yield stress of the flange material (σ_{yf}) at an end of a grillage member, a hypothetical hinge (plastic hinge) will form at that end. Finally when two plastic hinges exist (one at each end of the member), the member is assumed to have failed.
- ϑ- **Rockey's** approach is adopted to represent the post-buckling tension field action of the web panel and its behavior at yield.
- ϒ- The interaction diagram Fig.(ϑ-ϒ) is programmed to investigate the ultimate shearing capacity (V_{ult}) of the web panel, with the amount of bending moment acting on the section, as follows:
- a) When member end moment ($M \leq M_{s'}$), then:
- $$V_{ult} = V_s \quad (\text{constant shear capacity})$$
- b) When ($M_{s'} < M \leq M_F$), then
- $$V_{ult} = V_S - \frac{(V_S - V_c)}{(M_F - M_{s'})^2} \cdot (M - M_{s'})^2 \quad (\varrho-60)$$
- c) When ($M_F < M \leq M_{ult}$), then:
- $$V_{ult} = \left[V_c^2 - \frac{(V_c^2 - V_B^2)}{(M_{ult} - M_F)} \cdot (M - M_F) \right]^{\frac{1}{2}} \quad (\varrho-66)$$
- ϒ- As the shearing force reaches the ultimate capacity (V_{ult}), then the grillage member is assumed to have failed.

- Λ- When the determinant of the global stiffness matrix becomes equal to zero or the deflection due to load increments increase rapidly (sudden high deformation), the structure assumed to have collapsed and the corresponding load is the collapse load.

CHAPTER SIX

APPLICATIONS AND DISCUSSION

6.1 Introduction

The grillage analogy developed and described in chapter four is used to investigate the behavior of thin-walled cellular plate structures with linear varying depth in their nonlinear post-buckling range and at ultimate strength according to the nonlinear aspects discussed in the previous Chapter. In order to assess the efficiency and accuracy of the proposed grillage analogy, a number of steel cellular plate structures are analyzed in this chapter with different loading, support conditions and structural proportions. These structures are analyzed by the present grillage analogy method.

6.2 Application (1)

Cellular Plate Structure Simply Supported at All Edges

The structure considered here is a thin-walled cellular plate simply supported on all four edges. Two different loading conditions are considered in this example. The example considers cellular plate of linear varying depth as shown in Fig. (6-1). It is analyzed in the nonlinear range up to collapse using grillage method. The dimensions, materials properties and support conditions are illustrated in Fig. (6-1). A load

increment of 10 kN. Has been adopted in this example. The interior web intersection nodes (1, 2, 3, 4, 5, 6, 7 and 8) have been loaded with equal increment loads. Each load increments is 10 kN. per node.

For the cellular plate structure, the variation of central deflection with the applied nodal load is shown in Fig (6-2). In fig. (6-2) grillage method is used to analyze cellular plate structure of linear varying depth and including the effect of warping restraints and the results are compared with results obtained from the grillage for linear varying depth without including effect the warping . Then the structure is re-analyzed using the grillage method without including effect the warping for the linear varying depth and compared the results with the results for linear varying width *Younis M.H(2001)*⁽⁹⁴⁾, the variation of central deflection with the applied nodal load is shown in Fig. (6-3).

The distribution of vertical deflections along the middle section (section A-A) for an applied load of (160) per node (load increment No.160) is shown in Fig.(6-4).

From the comparison of the results obtained from the proposed grillage method for linear varying depth with the results obtained from the grillage method for the linear varying width *Younis M.H(2001)*⁽⁹⁴⁾, the following points concerning the accuracy of the proposed method, are noticed:

- 1- The maximum vertical deflection (at center) obtained by the grillage analogy for linear varying depth with the effect of the warping is 87.07 mm at a failure load of 160 kN per node .The deflection by the grillage method for linear varying depth without the effect of the warping is 70.83 mm at a failure load of 170 KN per node as shown in Fig. (6-2).

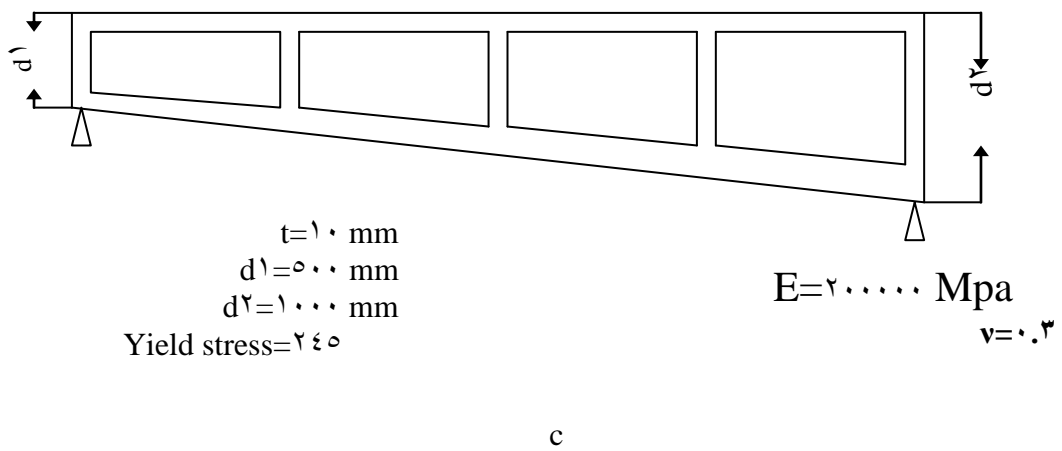
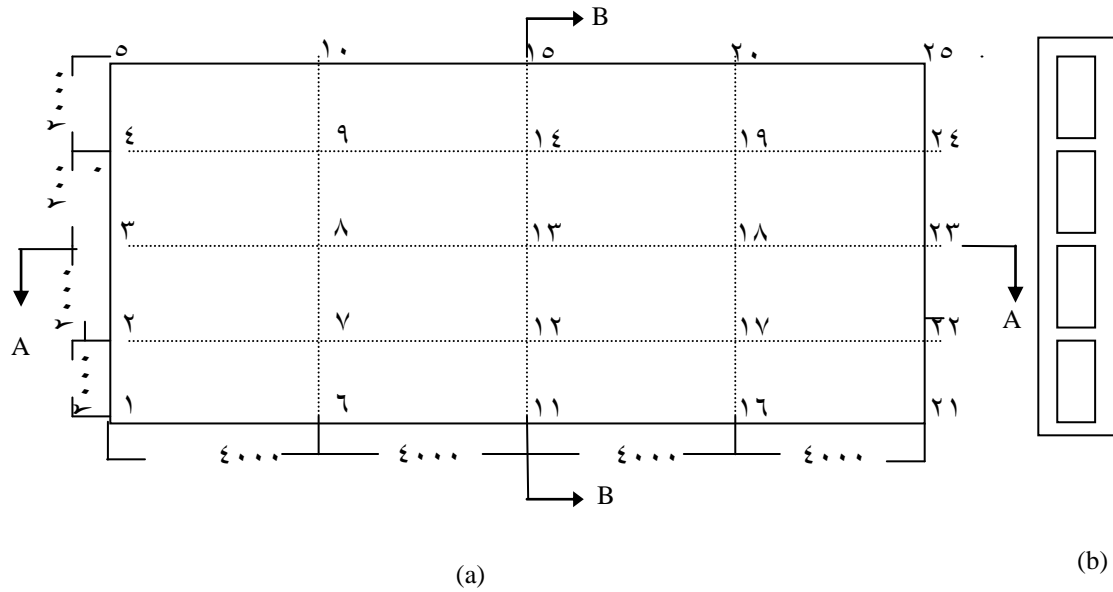
٢-The substitute grillage structure has failed by a collapse mechanism at a nodal load of ١٦٤٠ kN. This is compared well to the collapse load of ١٧٠٠ kN from the linear varying depth without the effect of the warping. This small difference for the ultimate load investigation. .

٣-The maximum vertical deflection (at center) obtained by the proposed grillage analogy for the linear varying depth without effect the warping is ٧٠.٨٣ mm at a failure load of ١٧٠٠ kN per node. The deflection by the grillage method for linear varying width *Younis M.H(٢٠٠١)^(٩٤)*, is ٥٨.٦ mm at a failure load of ١٧٠٠ KN per node . The difference for the deflection value is about ١٧.٢% .

٤-The substitute grillage structure has failed by a collapse mechanism at a nodal load of ١٧٠٠ kN. This is compared well to the collapse load of ١٧٠٠ from the liner varying width *Younis M.H(٢٠٠١)^(٩٤)*. This small difference indicates good agreement for the ultimate load investigation.

٥-As the accuracy of the proposed solution process is dependent on the chosen magnitude of the loading increment, four solutions using different increment sizes are obtained . In these successive solutions, constant increment magnitudes of ١٠ KN, ٥٠ KN, ١٠٠ KN, ٣٠٠ KN, the results are shown in Fig(٦-٤)

٦-As the accuracy of the proposed solutions using different magnitudes for the thickness of the web and thickness of the flange at the thickness equal to the ١٢ mm the deflection equal to the ٢٠.٤٣ at the collapse load equal to the ٢١٧٠ KN , at the ١٠ mm the deflection equal the ٨٧.٥٧ at the collapse load equal to the ١٦٤٠ , at the ٦ mm the deflection equal to the ٦٠.٤٥ mm at the collapse load equal to the ٥٦٠ KN shown in fig. (٦-٥) .



a-Plan b-Section (B-B) c-Section(A-A)

Figure (7.1): Cellular plate structure simply supported at all edges

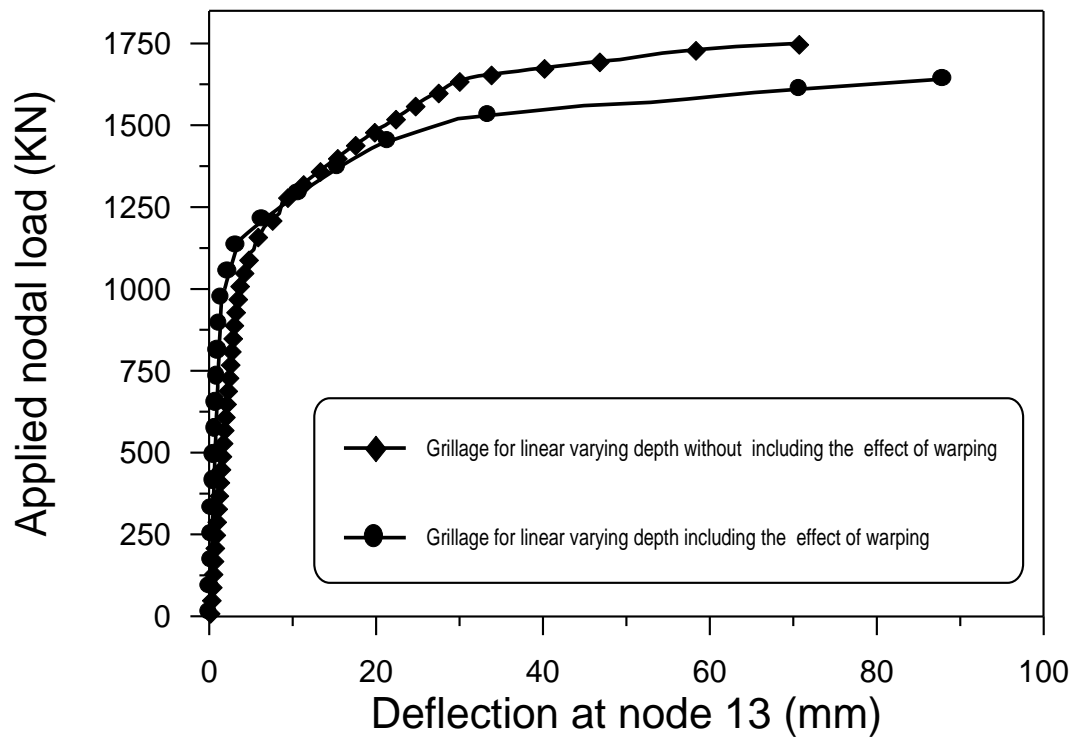


Figure (7.2): Vertical deflection at node (13) with load for a cellular plate structure simply supported at all edges.

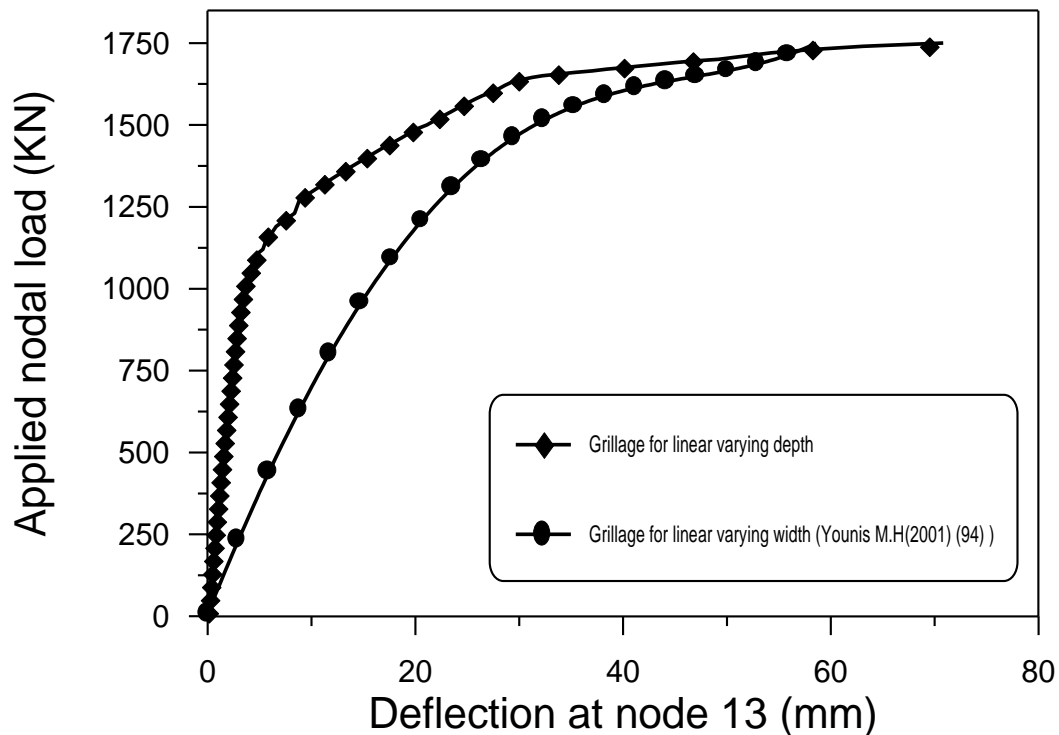


Figure (7.3): Vertical deflection at node (13) with load for a cellular plate structure simply supported at all edges.

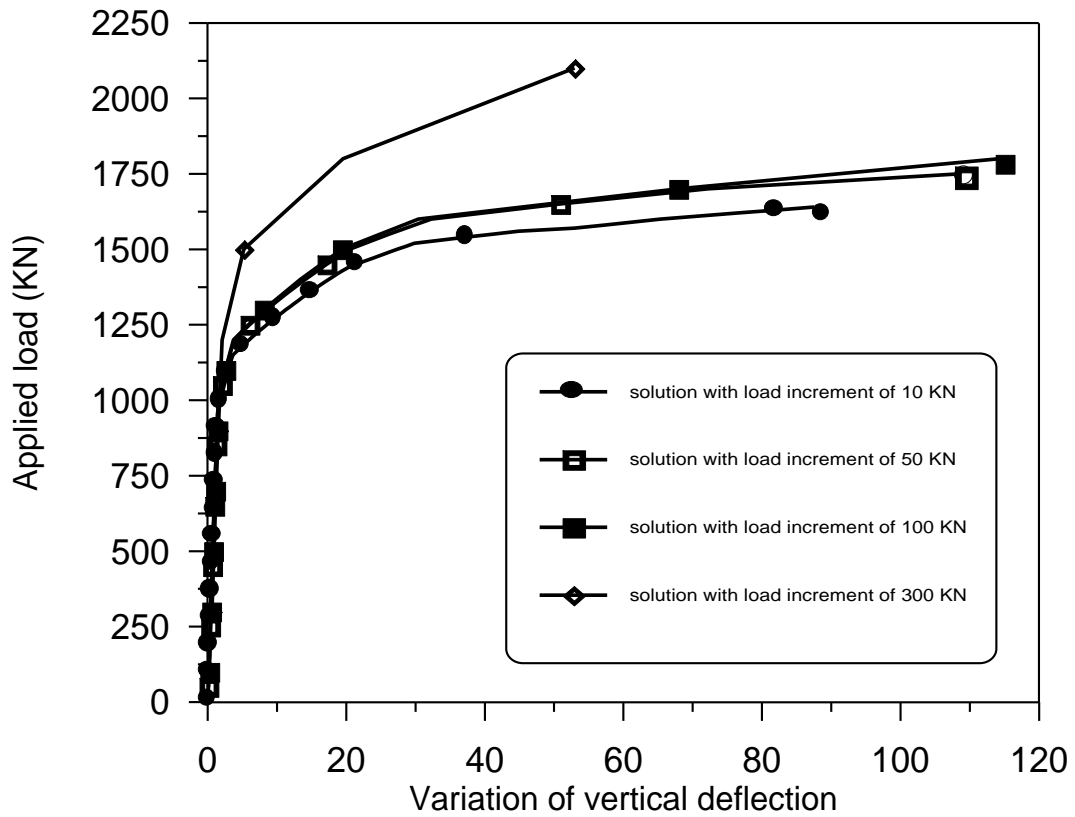


Figure (1-4): Vertical deflection at node (13) with load for a cellular plate structure simply supported at all edges for different increment load.

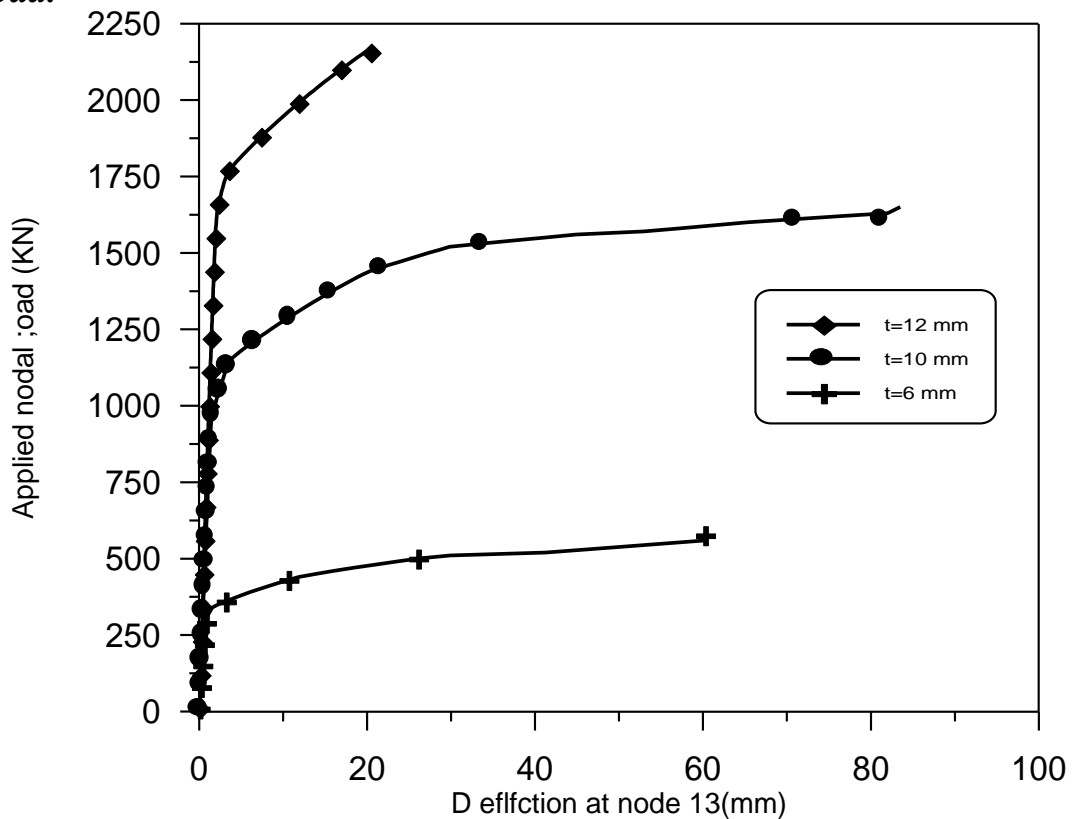
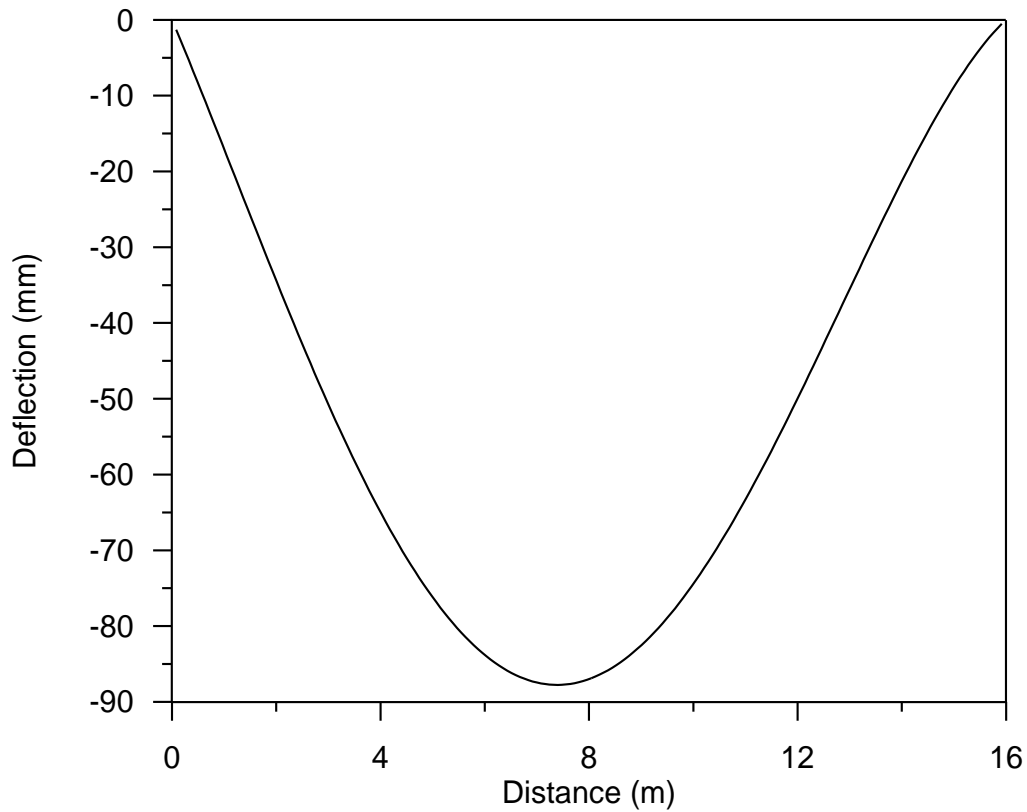


Figure (٦- ٥): Vertical deflection at node (١٢) with load for a cellular plate structure simply supported at all edges for different h_f .



Figure(٦- ٦) Vertical deflection along section (A-A) of cellular plate structure simply support all around at collapse

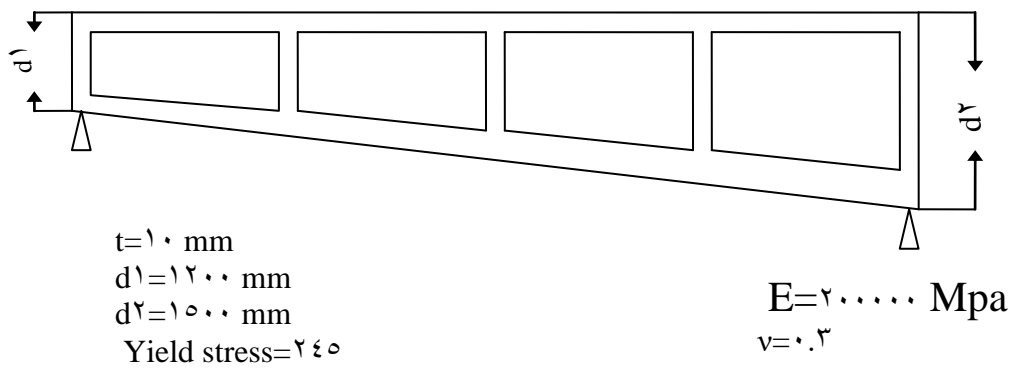
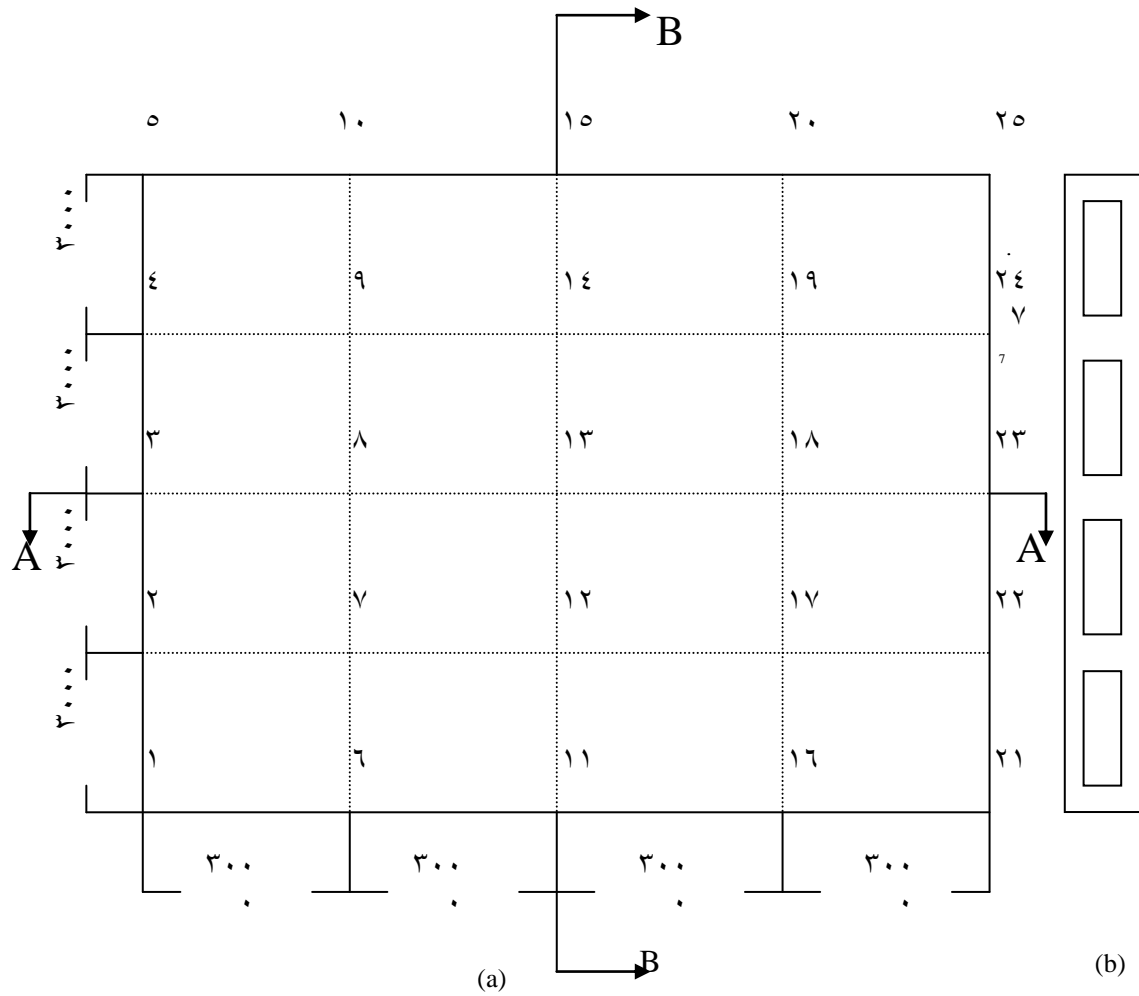
Example (2):-

The dimensions and materials properties of this application are shown in Fig. (6-7). The cellular plate structure considered here is composed of (16) rectangular cells of linearly varying depth. The loading condition considered in this application is a single load 10 kN increment at node (7, 8, 9, 12, 13, 14, 17, 18 and 19). For the cellular plate structure, the variation of maximum deflection in Fig. (6-8). In the fig. (6-8) using grillage method to analyzed cellular plate structure for linear varying depth without including the effect of warping restraints and compared the results with results obtained from the grillage for the prismatic structure *Shanmugam* and *Evans* (1981)⁽⁹⁾. The distribution of vertical deflections along the middle section (section A-A) for an applied load of (2790) per node (load increment No. 279) is shown in Fig.(6-9).

From comparisons of the results predicted for the linear varying depth the following points, connecting the accuracy of the proposed method, are noticed:

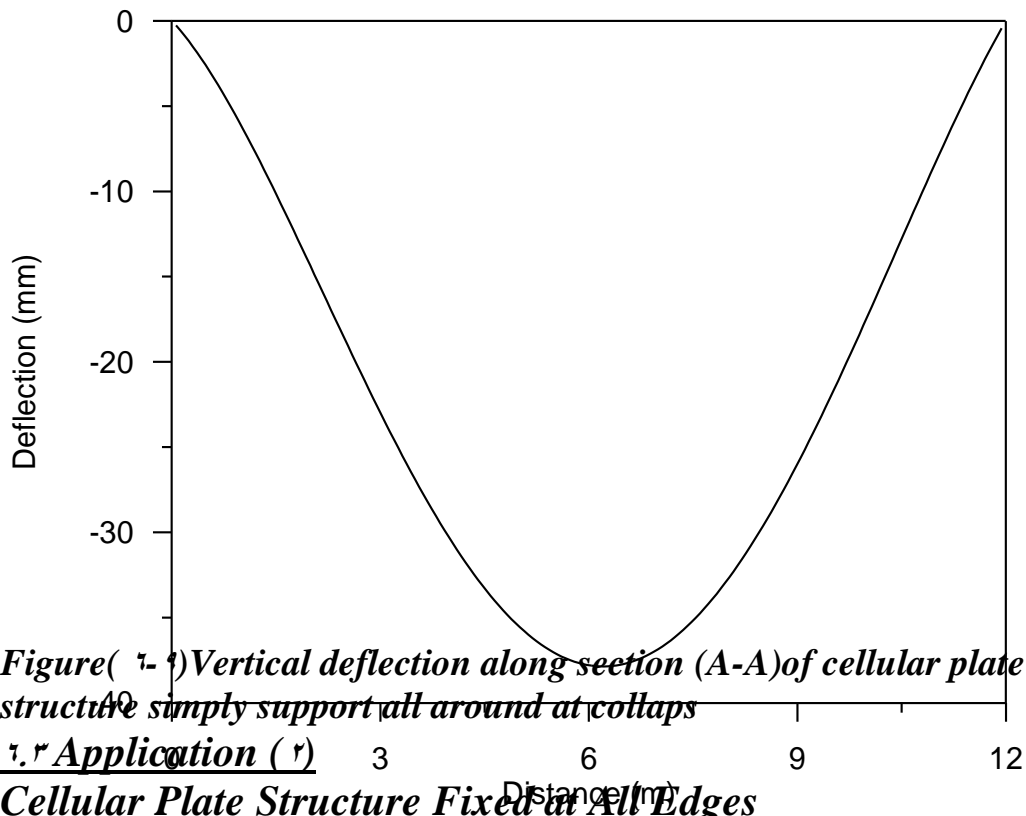
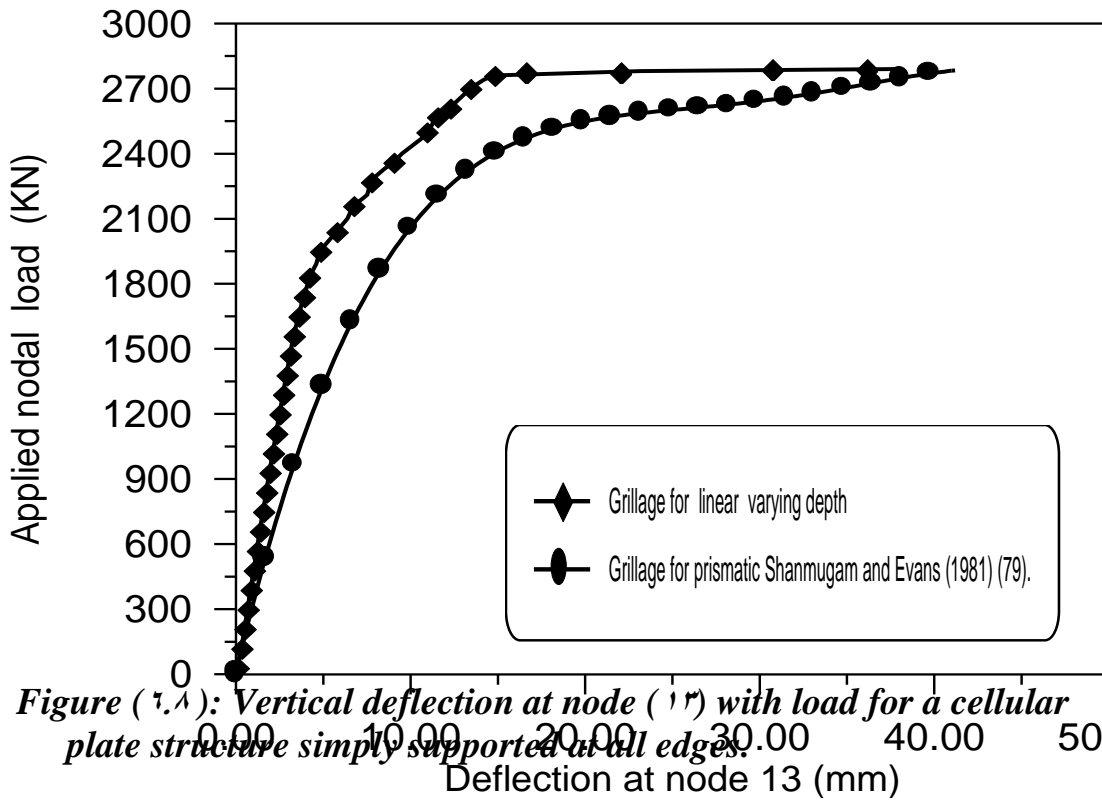
1-The maximum vertical deflections (at node 13) resulting from the grillage method for linear varying depth is 37.96 mm at a collapse load of 2790 KN, for prismatic structure analysis in the grillage method *Shanmugam* and *Evans* (1981)⁽⁹⁾ gives a maximum deflections of 41.2 mm. at a collapse load of 2780 KN. The difference for the deflection value is about 9.86% .

2-The collapse load of the substitute grillage structure is 2790 KN for linear varying depth., for prismatic structure analysis in the grillage method *Shanmugam* and *Evans* (1981)⁽⁹⁾ gives a collapse load of 2780 KN. The difference for the collapse load value is about 0.36% .



a-Plan b-Section (B-B) c-Section(A-A)

Figure (7.7): Cellular plate structure simply supported at all edges



This cellular plate structure is similar in dimension, material properties and loading condition to the structure given in the previous application. The only difference is in the boundary conditions, where here it is fixed at all edges as shown in Fig.(6-10).

The aim of this application is to study the effects of introducing fixed edges on the behavior of the cellular plate structure and also, to test the efficiency of the proposed grillage method for the analysis of cellular plate structures under this type of edge conditions. As the accuracy of the proposed solution is dependent on the chosen magnitude of the loading increment, a load increment of 10 kN. was used in the present study. The interior web intersection nodes (7,8,9,12,13,14,17,18 and 19) were loaded with equal increment loads. Each load increments is 10 kN. For the cellular plate structure, two different loading conditions are considered in this example, for the first example the variation of central node deflection (node 13) with the applied nodal loads is shown in Fig (6-11) and in Fig.(6-12). The distribution of vertical deflections along the middle section (section A-A) for an applied load of (1630) per node (load increment No.163) is shown in Fig.(6-14).

By studying the results obtained the proposed grillage method for linear varying depth including the effect of warping restraints and compared the results with results obtained from the grillage for linear varying depth without including the effect of warping restraints . Then the structure re-analyzed using the grillage method without including effect the warping for the linear varying depth and compared the results with the results for linear varying width *Younis M.H*(2001)⁽⁹⁴⁾, the variation of central deflection with the applied nodal load is shown in Fig. (6-11)and (6-12). The accuracy of the proposed method, are noticed:

1-The maximum vertical deflection (at center at node 13) obtained by the grillage analogy method for linear varying depth including the effect of

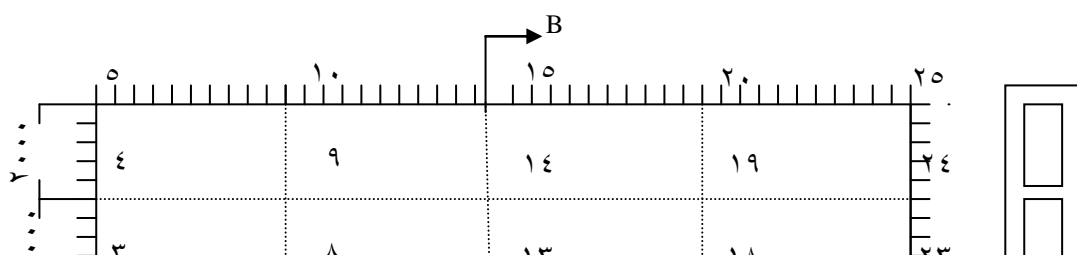
the warping is 30.90 mm, for the linear varying depth without include the effect of the warping is 21.28 mm. This deflection occurs when the applied load is 163 KN for linear varying depth , 170 KN for linear varying depth without including the effect of the warping.

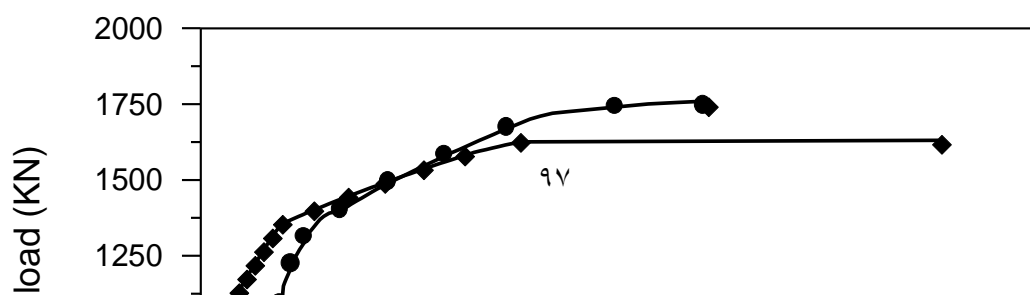
٢-The substitute grillage structure has failed by a collapse mechanism at a nodal load of 163 kN. This is compared well to the collapse load of 170 kN from linear varying depth without the effect of the warping .This small difference for the ultimate load investigation.

٣- The maximum vertical deflection (at center) obtained by the proposed grillage analogy is 21.28 mm at a failure load of 176 kN per node.The deflection by the grillage method for linear varying width *Younis M.H*(٢٠٠١)^(٩٤), is 26.6 mm at a failure load of 179 KN per node . The difference for the deflection value is about 20% .

٤-The substitute grillage structure has failed by a collapse mechanism at a nodal load of 176 kN. This is compared well to the collapse load of 179 *Younis M.H*(٢٠٠١)^(٩٤), from the liner varying width.This small difference indicates good agreement for the ultimate load investigation. . The difference for the collapse load value is about 1.67% .

٥-As the accuracy of the proposed solutions using different magnitudes for the thickness of the web and thickness of the flange at the thickness equal to the 12 mm the deflection equal to the 12.02 at the collapse load equal to the 246 KN , at the 10 mm the deflection equal the 30.90 at the collapses load equal to the 163 ,at the 6 mm the deflection equal to the 30.00 mm at the collapse load equal to the 02 KN shown in fig. (٦-١٣)





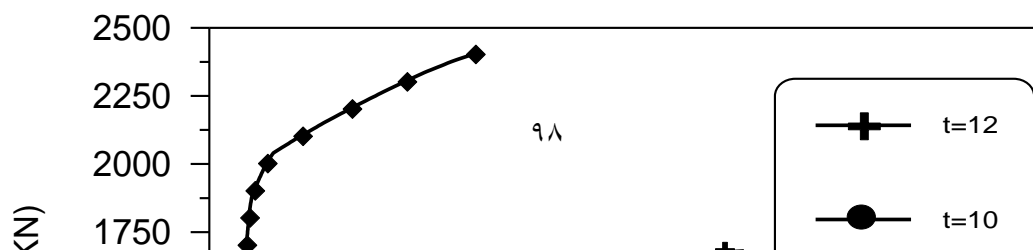
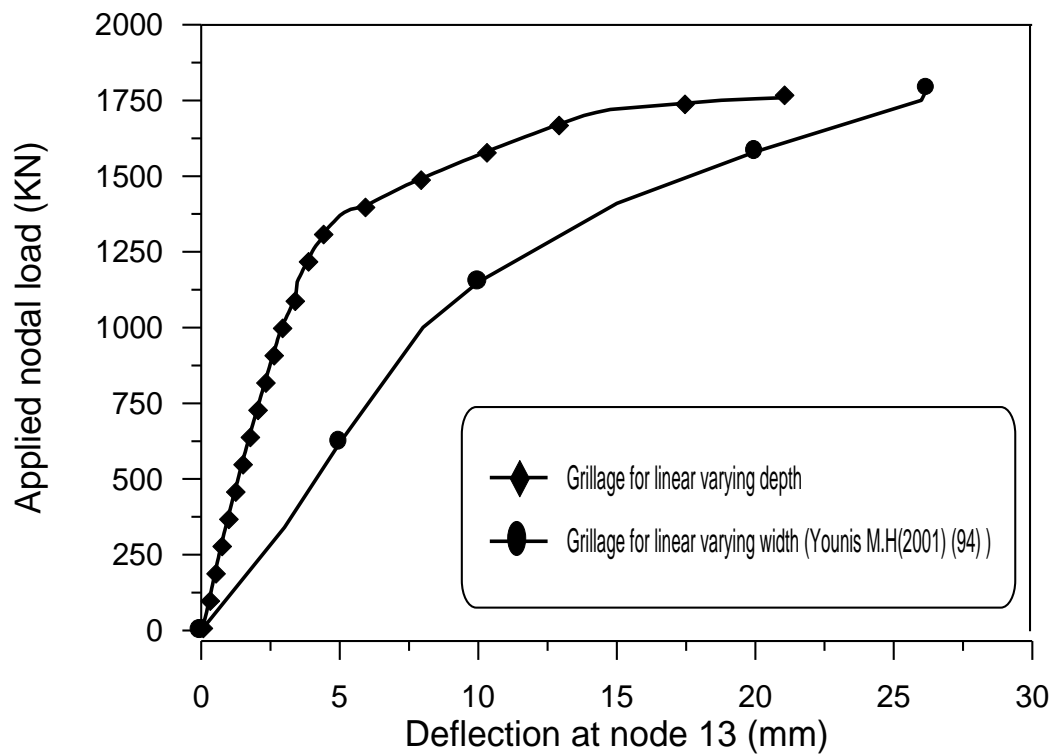
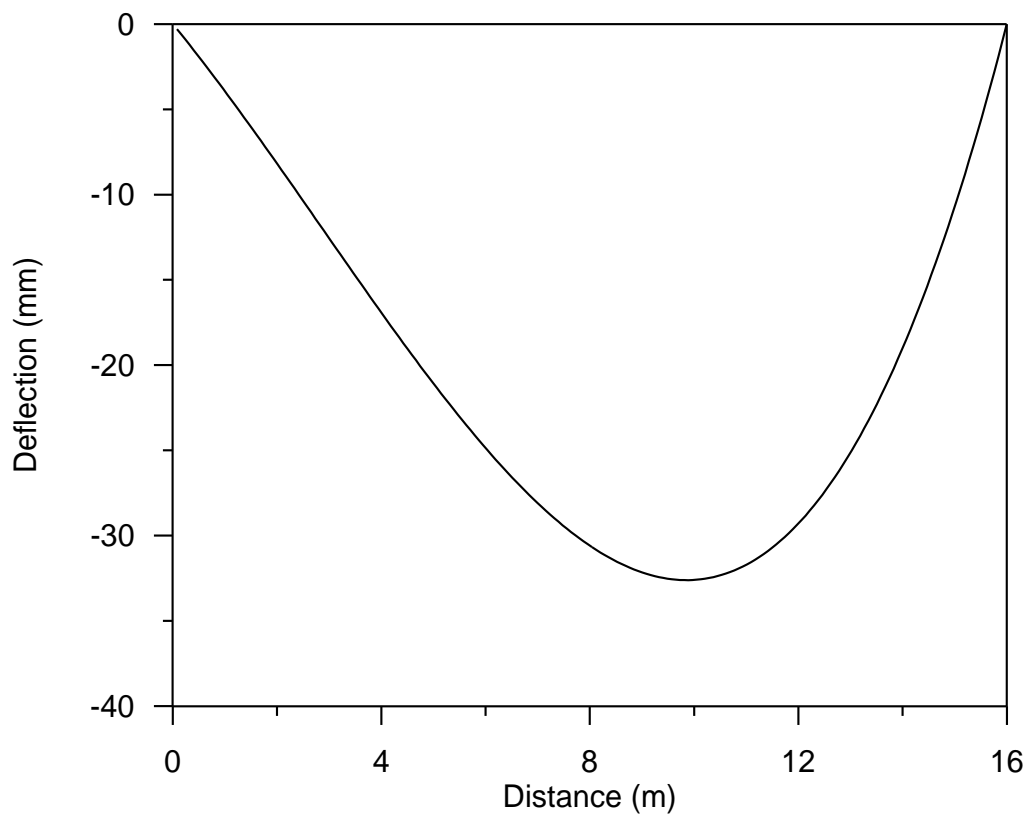


Figure (7-13): Vertical deflection at node (13) with load for a cellular plate structure fixed at all edges for different h_f .



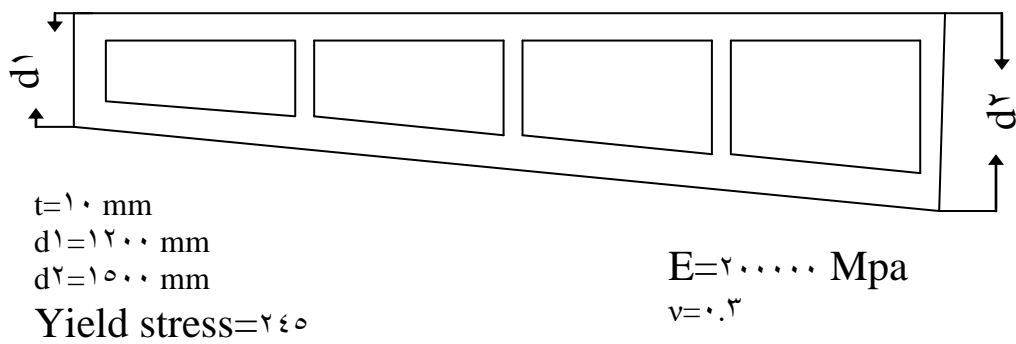
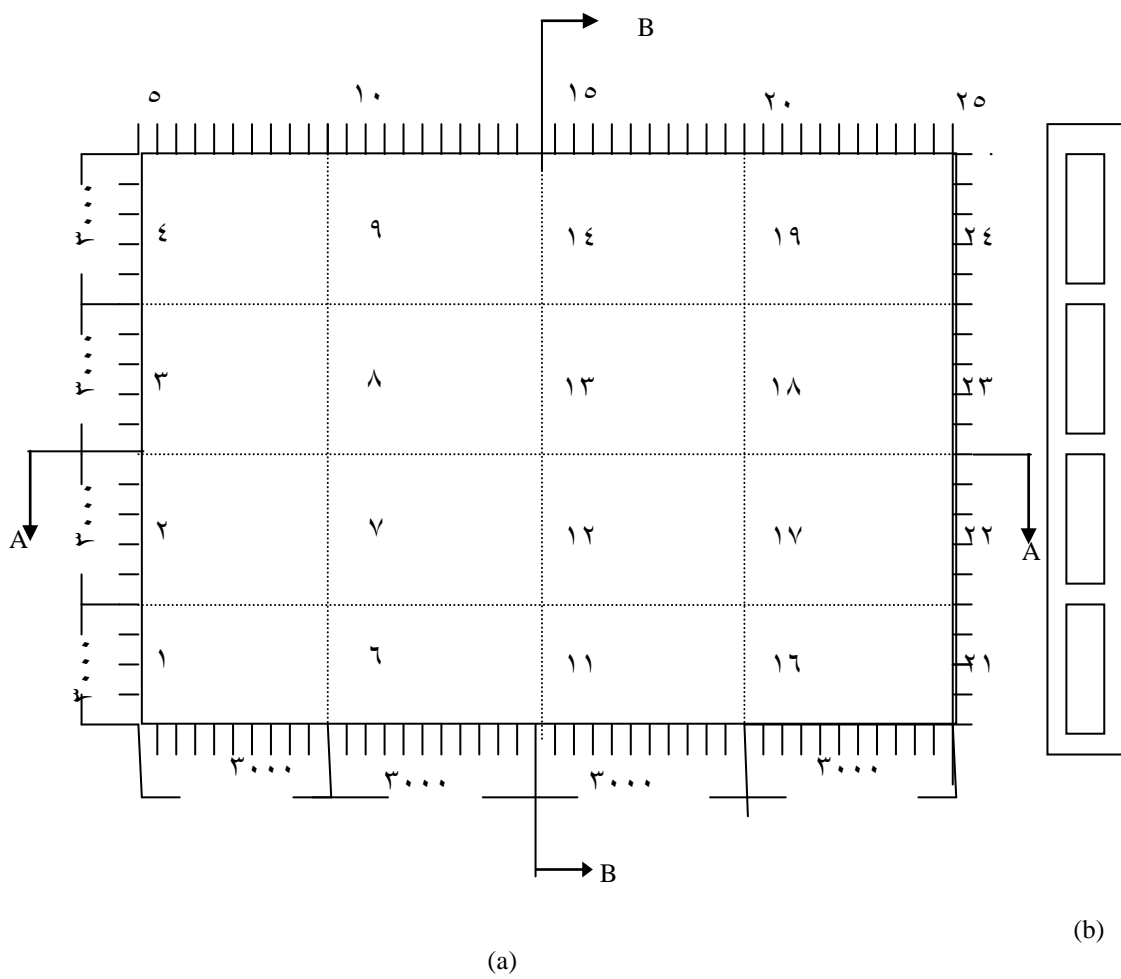
Figure(7-14) Vertical deflection along section (A-A) of cellular plate structure fixed at all around at collapse

Example (7):-

The dimensions and materials properties of this applications are shown in Fig. (6-15). The cellular plate structure considered here is composed (16) rectangular cells of linearly varying depth. The loading condition considered in this application is a single load 10kN increment at node (5,8,9,12,13,14,17,18 and 19). For the cellular plate structure, the variation of maximum deflection is shown in Fig. (6-16). In the fig. (6-16) using grillage method to analyzed cellular plate structure for linear varying depth without including the effect of warping restraints and compared the results with results obtained from the grillage and finite element methods for the prismatic structure *Mashal* (1997)⁽⁶⁷⁾. The distribution of vertical deflections along the middle section (section A-A) for an applied load of (2790) per node (load increment No.279) is shown in Fig.(6-17).

From comparisons of results predicted for the linear varying depth and for the. linear varying width.

- 1-The maximum vertical deflections (at node 13) resulting from the grillage method for linear varting depth is 10.7 mm at a collapse load of 2800 KN, for prismatic structure *Mashal* (1997)⁽⁶⁷⁾ analysis in the grillage method gives a maximum deflections of 16.7mm. at a collapse load of 2000 KN and for prismatic structure *Mashal* (1997)⁽⁶⁷⁾ analysis in the finite element method gives a maximum deflections of 18.2mm. at a collapse load of 2700 KN . The difference for the deflection with respect to the grillage value is about 6% and with respect to the finite element value is about 13.7% .
- 2-The collapse load of the substitute grillage structure is 2800 KN for linear varying depth., for prismatic structure *Mashal* (1997)⁽⁶⁷⁾ analysis in the grillage method gives a collapse load of 2000 KN and for prismatic structure *Mashal* (1997)⁽⁶⁷⁾ analysis in the finite element method gives a collapse load of 2700 KN. The difference for the collapse load with respect to the grillage value is about 9.8% and with respect to the finite element value is about 3.7% .



c

a-Plan b-Section (B-B) c-Section(A-A)

Figure (7.19): Cellular plate structure fixed at all edges

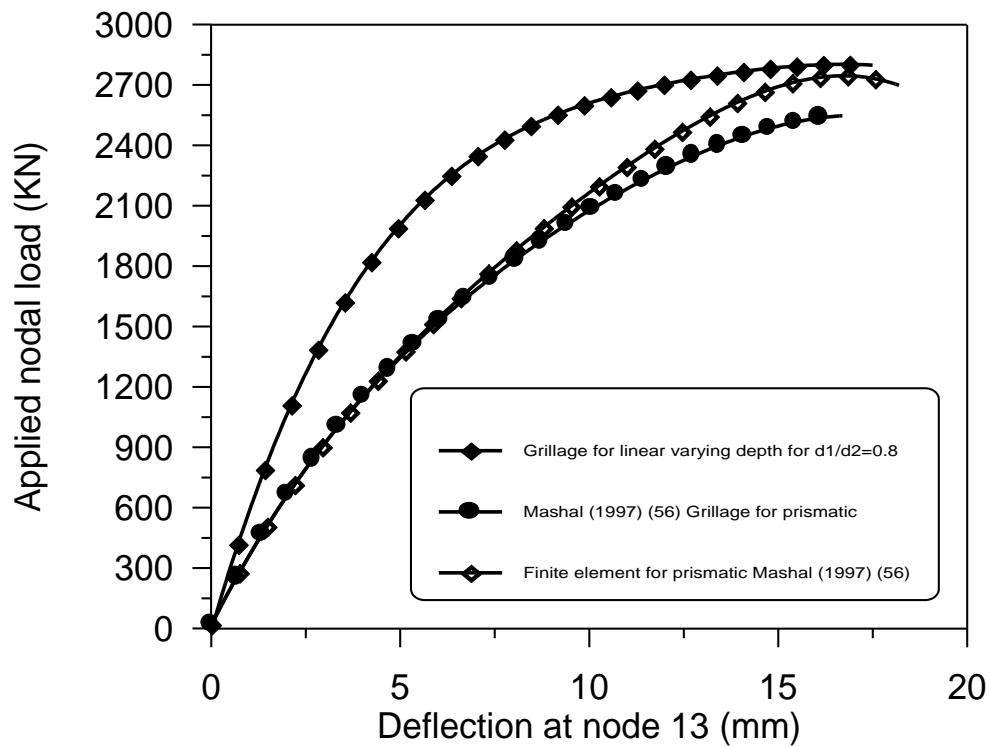
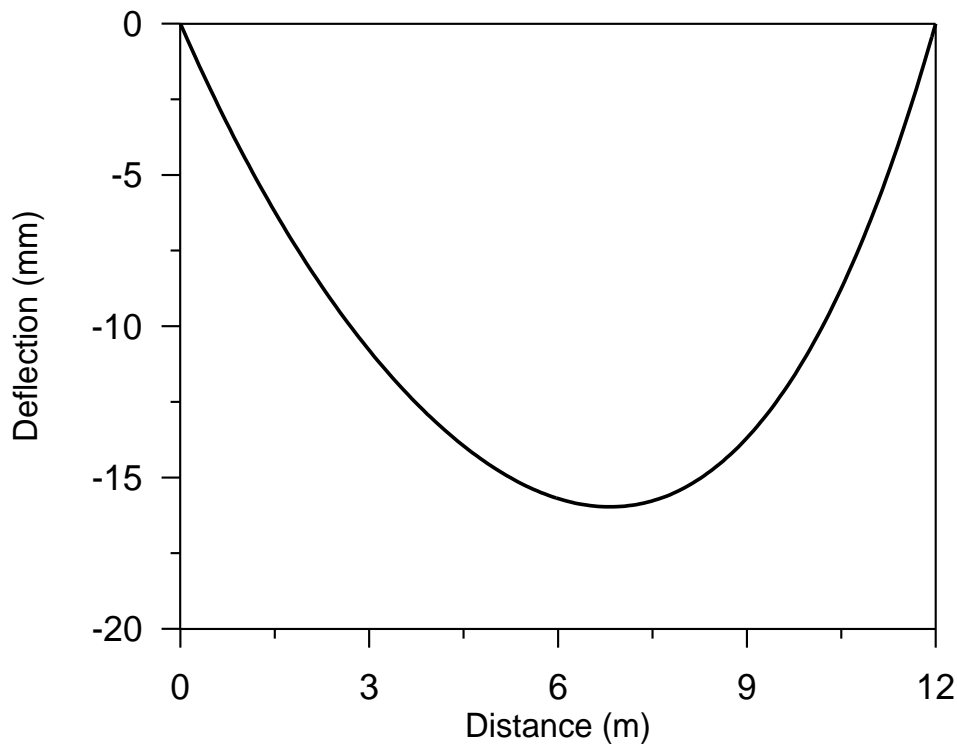


Figure (6. 16): Vertical deflection at node (13) with load for a cellular plate structure fixed at all edges.



Figure(6- 17) Vertical deflection along section (A-A) of cellular plate structure fixed at all around at collapse

6.4 Application (3)

Cantilever Cellular Plate Structure

The structure considered here is fixed at one edge (side) and the other edges are free. The support conditions are representative of those encountered in aircraft wings. These applications are considered to assess the efficiency of the proposed grillage method for cellular plate structures having high twisting and bending moments. Third different loading conditions are considered in this example. The dimensions and materials properties of this applications are shown in Fig. (6.18) for the first example.

The loading condition considered in this application is a single load 10 kN increment at the corner of the outer free edge (node 20). For the cellular plate structure, the variation of maximum deflection (corner of outer free edge) with the applied load are shown in Fig.(6.19) for the loading condition. The distribution of vertical deflections along the middle section (section A-A) for an applied load of (1210) per node (load increment No.121) is shown in Fig.(6-22).

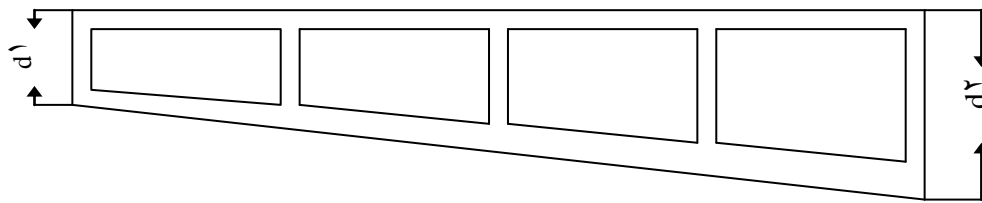
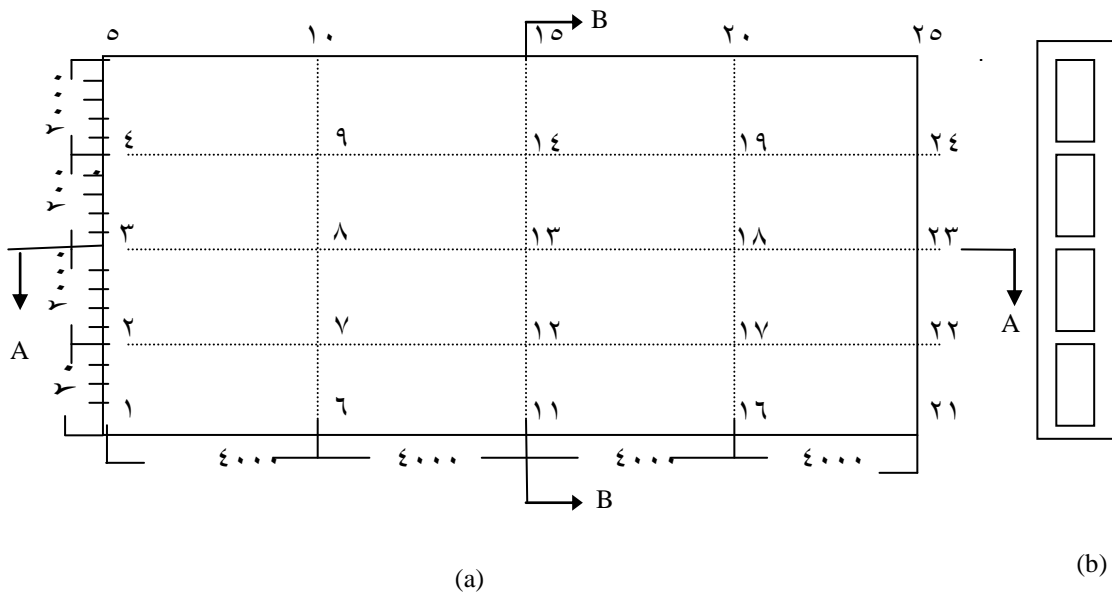
From comparisons of results predicted for the linear varying depth including the effect of warping and for the linear varying depth without including the effect of warping connecting the accuracy of the proposed method, are noticed:

1-The maximum vertical deflections (at the outer free edge at node 20) resulting from the linear varying depth for the grillage method is 142.308mm at a collapse load of 1210 kN, while the grillage method for linear varying depth without including the effect of warping analysis in the grillage method gives a maximum deflections of 92.94 mm. at a collapse load of 148 KN.

٢-The collapse load of the substitute grillage structure is 1210 KN for linear varying depth including the effect of warping, while linear varying depth without including the effect of warping gives a collapse load of 1480 kN. So, the difference in collapse load is not large

٣-As the accuracy of the proposed solutions using different magnitudes for the thickness of the web and thickness of the flange at the thickness equal to the 12 mm the deflection equal to the 148.7 mm at the collapse load equal to the 1020 KN, at the 10 mm the deflection equal to the 142.30 mm at the collapse load equal to the 1210 KN, at the 8 mm the deflection equal to the 202 mm at the collapse load equal to the 770 KN shown in fig. (٦-٢٠)

٤-As the accuracy of the proposed solutions using different magnitudes for the depth for the same example, at the first the $d^1=000$ and the $d^2=1000$ the deflection equal to the 142.308 mm at the collapse equal to the at the collapse load equal to the 1210 KN, at the second the $d^1=1000$ and $d^2=000$ the deflection equal to the 140.0 mm at the collapse load equal to the 1300 KN shown in fig. (٦-٢١)



$t=1.0 \text{ mm}$
 $d=100.0 \text{ mm}$
 $d_1=100.0 \text{ mm}$
 Yield stress= σ_{y0}

$E=200000 \text{ Mpa}$
 $\nu=0.3$

c

a-Plan b-Section (B-B) c-Section(A-A)

Figure (6.18): Cellular plate structure for cantliver

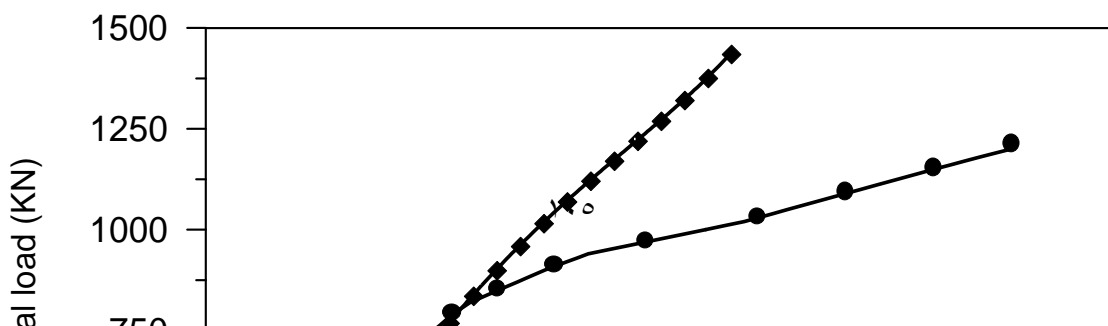


Figure (7.19): Vertical deflection at node (25) with load for cantilever

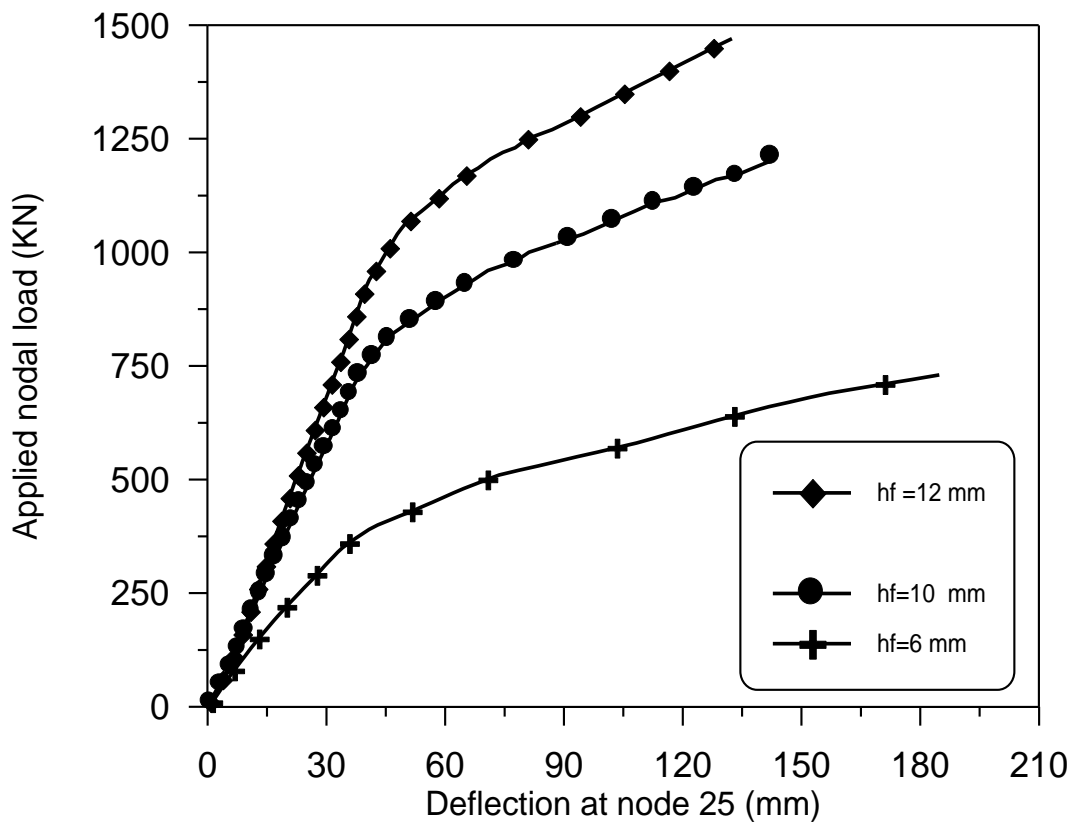


Figure (7.20): Vertical deflection at node (25) with load for cantliver for different hf.

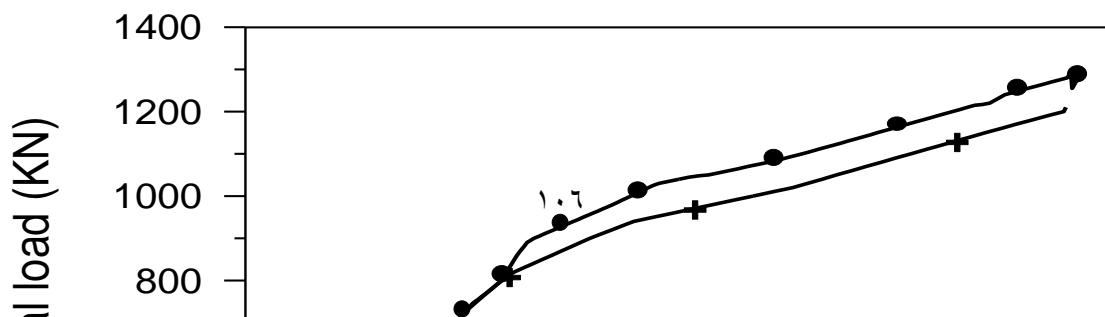
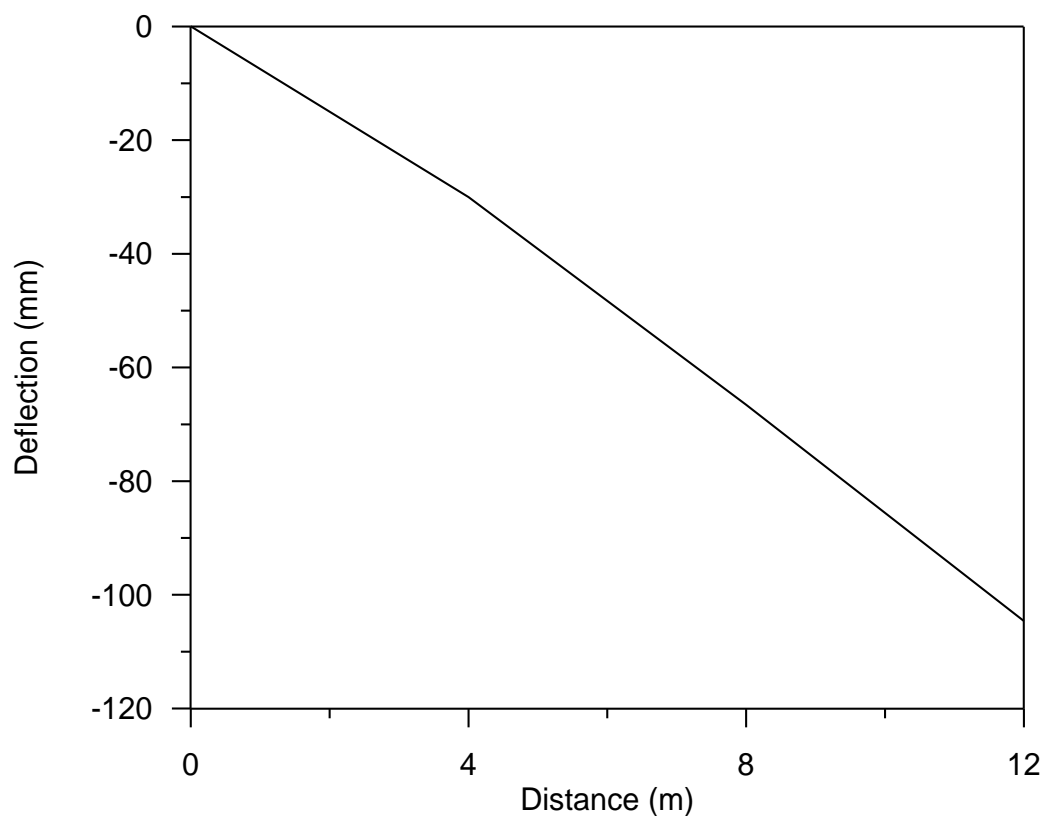


Figure (٦- ٢١): Vertical deflection at node (٢٥) with load for cantliver for different depth.



Figure(٦- ٢٢)Vertical deflection along section (A-A)of cellular plate structure for cantliever at collapse

Example (٢):-

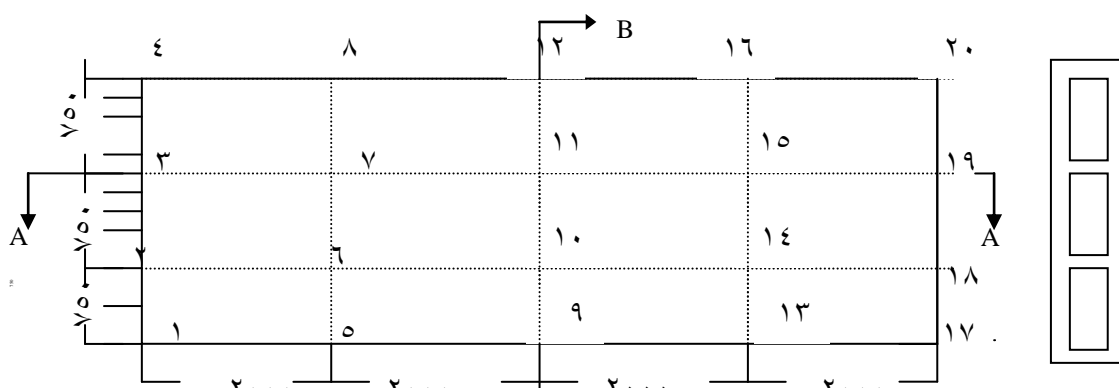
The dimensions and materials properties of this applications are shown in Fig. (٦-٢٣). The cellular plate structure considered here is coomposed of (١٢) rectangular cells of linearly varying depth. The loading condition

considered in this application is a single load ϵ kN increment at node (17). For the cellular plate structure, the variation of maximum deflection at node (17) with the applied nodal load is plotted in Fig. (6-24). The distribution of vertical deflections along the middle section (section A-A) for an applied load of (0.0) per node (load increment No. 120) is shown in Fig.(6-25).

From comparisons of results predicted for the linear varying depth and for the. linear varying width, connecting the accuracy of the proposed method, are noticed:

1-The maximum vertical deflections (at node 17) resulting from the proposed grillage method is 72.44 mm at a collapse load of 0.0 KN. The maximum deflection resulting from the grillage method for the linear varying width *Younis M.H*(2001)⁽⁹⁴⁾ is 72.07 mm,. at a collapse load of 376 KN. The difference for the deflection value is about 0.30% .

2-The collapse load of the substitute grillage structure is 0.0 KN for linear varying depth., while the linear varying width *Younis M.H*(2001)⁽⁹⁴⁾.gives a collapse load of 376 KN. The difference for the collapse load value is about 34.8%.



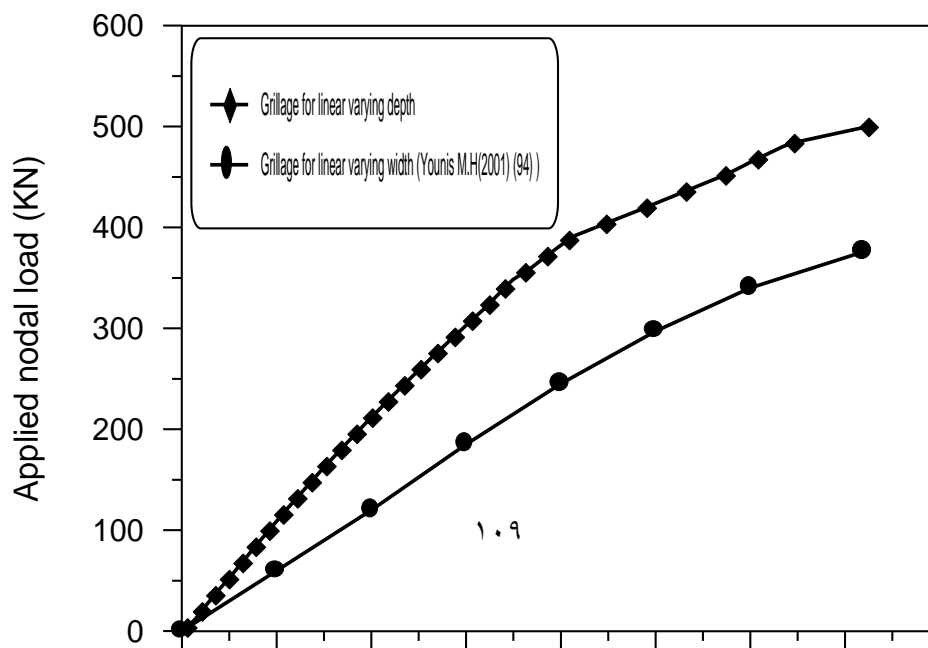
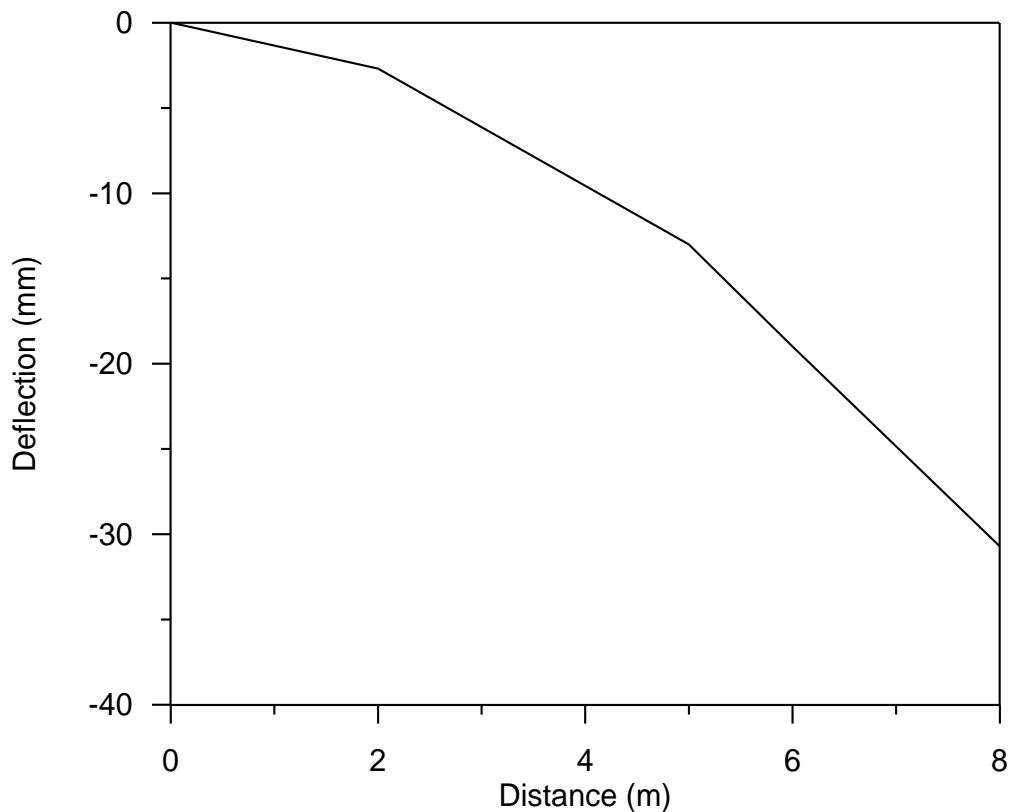


Figure (٦.٢٤): Vertical deflection at node (١٧) with load for cantilever



Figure(٦.٢٥) Vertical deflection along section (A-A)of cellular plate structure for cantliever at collapse

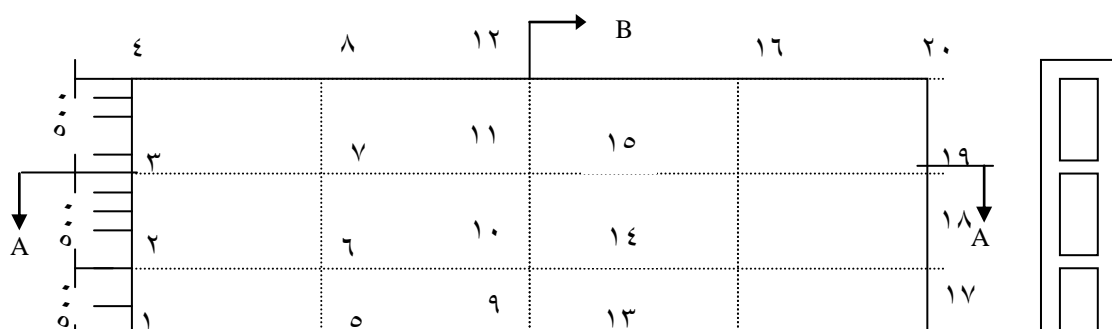
The dimensions and materials properties of this applications are shown in Fig. (٦-٢٦) for the third example. The cellular plate structure considered here is coomposed (١٢) rectangular cells of linearly varying depth. The loading condition of considered in this application is a single load ϵ kN increment at node (١٧). For the cellular plate structure, the variation of maximum deflection at node (١٧) with the applied nodal load is plotted in Fig. (٦-٢٧). The distribution of vertical deflections along the middle section

(section A-A) for an applied load of (0.0) per node (load increment No. 120) is shown in Fig.(6-28).

From comparisons of results predicted for the linear varying depth and for the. linear varying width.

1-The maximum vertical deflections (at node 17) resulting from the proposed grillage method is 38.36 mm at a collapse load of 300 KN, for the prismatic structure *Mashal* (1997)⁽⁰⁷⁾ analysis in the grillage method gives a maximum deflections of 26.02 mm. at a collapse load of 100 KN and for the prismatic structure *Mashal* (1997)⁽⁰⁷⁾ analysis in finite element method gives a maximum deflections of 34.0 mm. at a collapse load of 177.0 KN. The difference for the deflection with respect to the grillage value is about 30% and with respect to the finite element value is about 10% .

2-The collapse load of the substitute grillage structure is 300 KN for linear varying depth., while the prismatic structure *Mashal* (1997)⁽⁰⁷⁾ gives a collapse load of 100 KN and the prismatic structure *Mashal* (1997)⁽⁰⁷⁾ in finite element method gives a collapse load of 177.0 KN. The difference for the collapse load with respect to the grillage value is about 0% and with respect to the finite element value is about 40% .



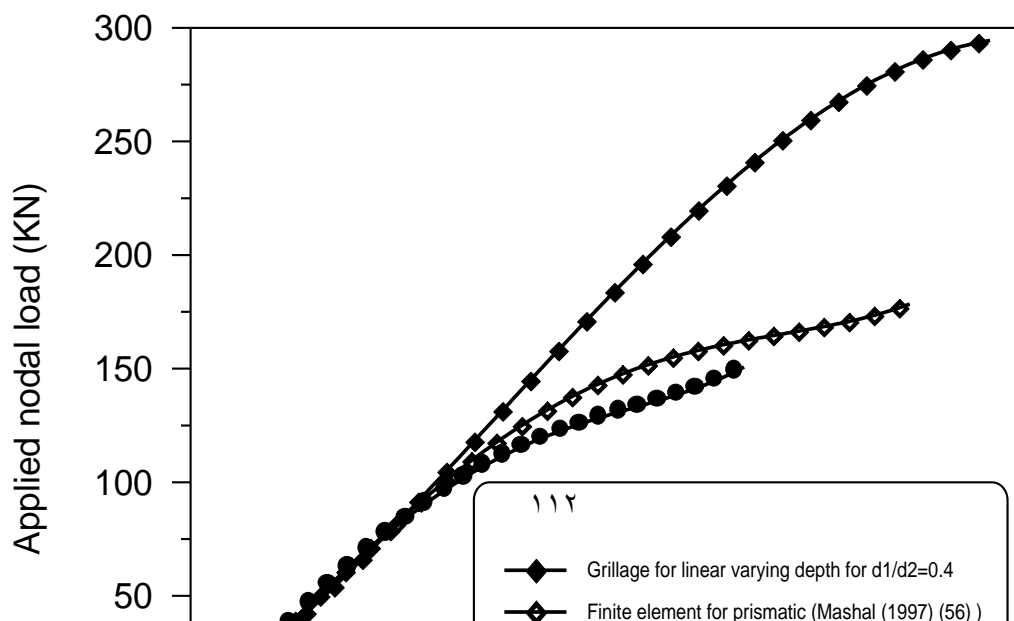
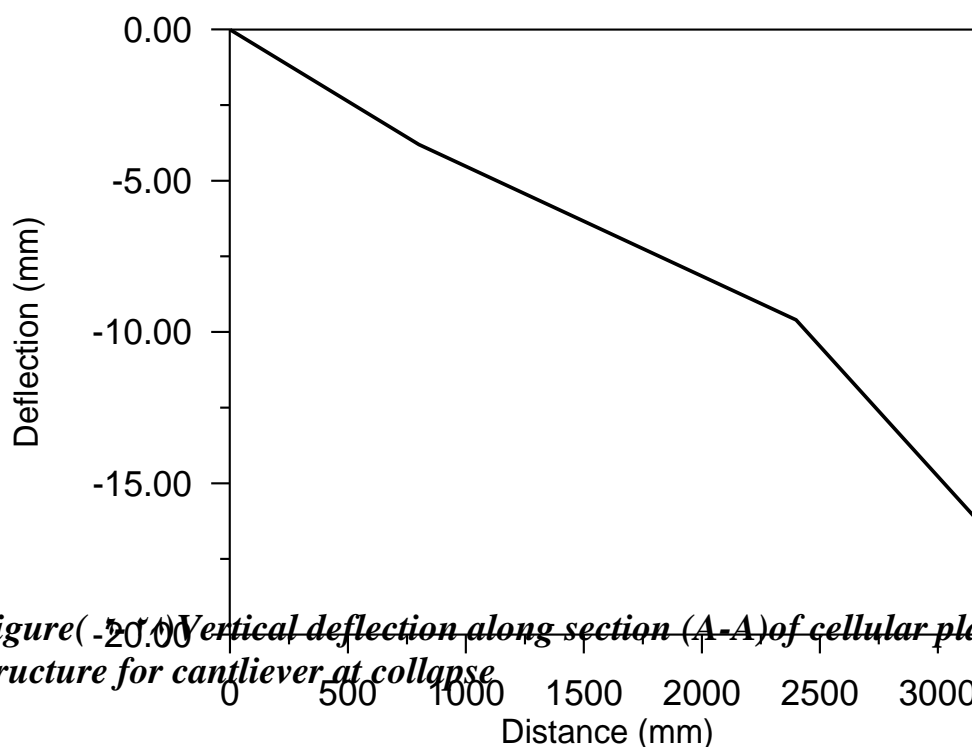


Figure (٦. ٢٧): Cellular plate structure for cantliver



Figure(٦. ٢٨) Vertical deflection along section (A-A) of cellular plate structure for cantliver at collapse

٦. ٥ Application (٤)

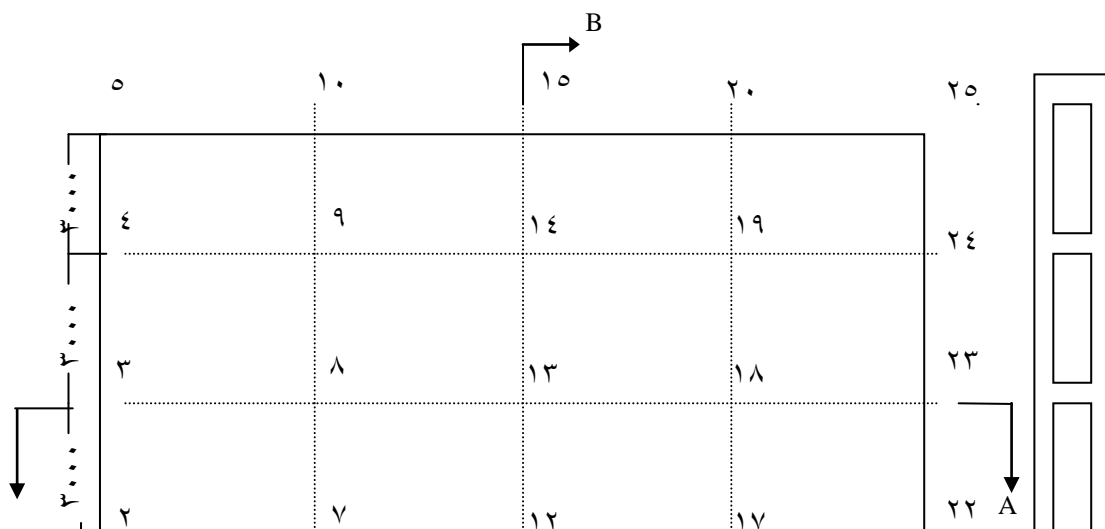
Cellular Plate Structure Simply Supported at All Edges

The structure considered here is a thin-walled cellular plate simply supported on all four edges. Threr examples are different in the shape structure. The dimensions, materials properties and support conditions are

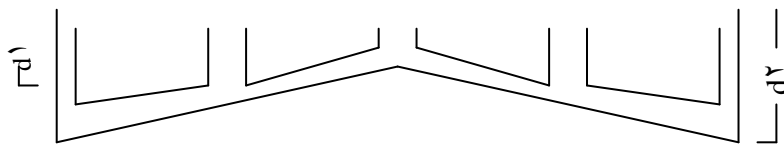
illustrated in Fig. (٦-٢٩) for example one and the dimensions, materials properties and support conditions are illustrated in Fig. (٦-٣١) for example two. It is analyzed in the nonlinear range up to collapse using grillage method. A load increment of ٣٠ kN. was adopted for the three examples. The interior web intersection nodes (٧,٨,٩,١٢,١٣,١٤,١٧,١٨ and ١٩) were loaded with equal increment loads. Each load increments are ١٠ kN. per node. The variation of central deflection with the applied nodal load is shown in Fig (٦-٣٢). In fig. (٦-٣٢) grillage method is used to analyze cellular plate structure of linear varying depth For the two example and ued grillage method for the prismatic, the variation of central deflection with the applied nodal load is shown in Fig (٦-٣٢).

١- The maximum vertical deflection (at center) obtained by the grillage analogy for the case one is ٦٤ mm at a failure load of ١٣٢٠ kN per node .The deflection by the grillage method for the case two is ٨٠.١٣ mm at a failure load of ٩٦٠ KN per node. The deflection by the grillage method for the case three is ٦٥.٦٨ mm at a failure load of ٨٥٠ KN per node. It can be easily concluded that case one represents the best among the others since it gives a higher stiffness.

٢-The substitute grillage structure has failed by a collapse mechanism at a nodal load of ١٣٢٠ kN for example one. This is compared well to the collapse load of ٩٦٠ kN for the example two . This is compared well to the collapse load of ٨٥٠ kN for the example three .



A



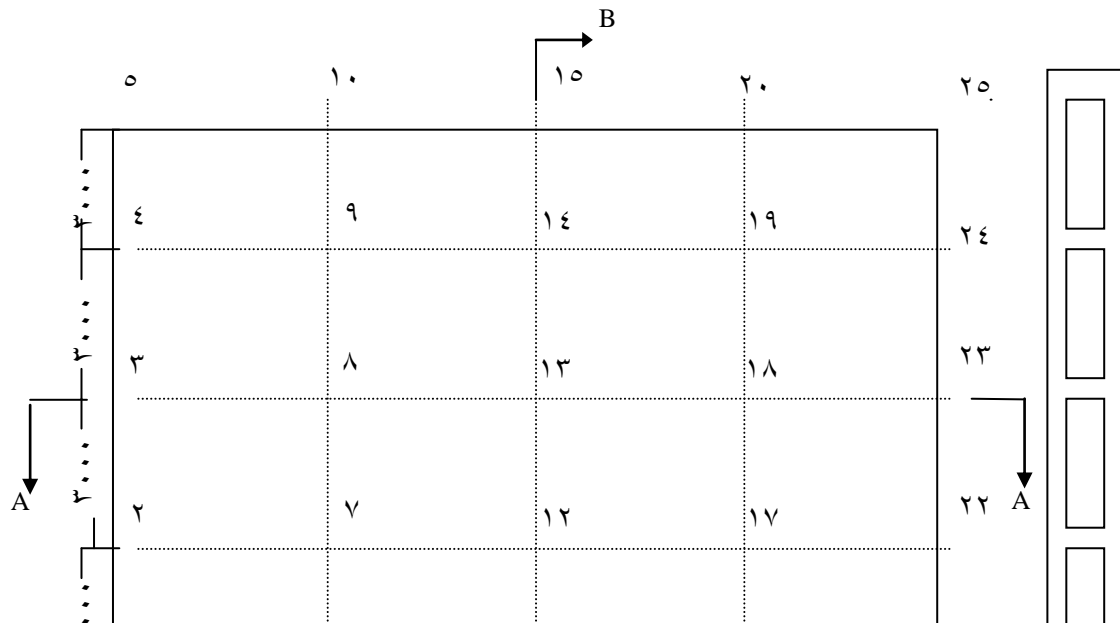
$t = 12 \text{ mm}$
 $d_1 = 1200 \text{ mm}$
 $d_2 = 1300 \text{ mm}$
 Yield stress = 240

$E = 200000 \text{ Mpa}$
 $\nu = 0.3$

c

a-Plan b-Section (B-B) c-Section(A-A)

Figure (7.30): Cellular plate structure simply supported at all edges



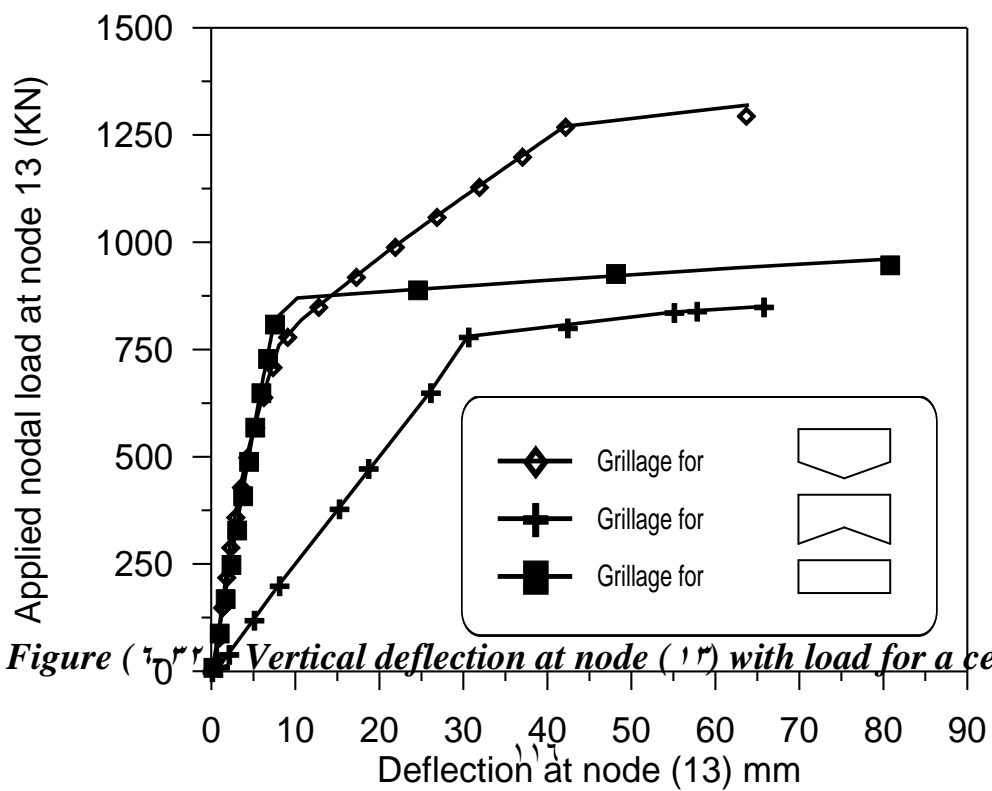


Figure 6.10 Vertical deflection at node (13) with load for a cellular

plate structure simply supported at all edges.

CHAPTER SEVEN

CONCLUSIONS AND RECOMMENDATIONS

7.1 Conclusions

The applicability and accuracy of the proposed simplified grillage method have been examined by analyzing a number of cellular plate structures linear varying depth in their nonlinear range and at ultimate load and under varieties of support and loading conditions. In no experimental work is available, extension of the grillage approach into the nonlinear post-buckling range and at ultimate load of cellular plate structures linear varying depth is successfully attained by including the effects of warping deformations and without including the effect of warping and both types of nonlinearities (geometric and material nonlinearly).

- 1- The approach grillage analogy is suitable at the design stage (especially in the nonlinear analysis) as the following advantages for the grillage method
 - i- The analysis to be performed by this method is simple and takes a very short computer time .
 - ii- The preparation of the input data requires considerably small time (as shown in Appendix B).
 - iii- The output file obtained by the proposed method requires a small memory space .
- 2- The vertical deflection (at the ultimate load) calculated by the proposed method is compared with the results for linear varying width (*Younis M.H*(1994)) and for the prismatic structure

(*Mashal* (1997)^(٥٦)) is a good agreement. From these comparisons, the differences are the percentage differences are ranging between (١.٦% to ٥.٠%) for the ultimate load and between (٦% to ٣.٠%) for the deflection. not large as the cellular plate structure is in a state of imminent failure.

- ٣- According to the grillage method, the maximum vertical deflections of the cellular plate structures are calculated at the intersecting nodes. Nevertheless, the proposed grillage method is still capable of providing reasonably good predictions of the nonlinear post – buckling behavior of cellular plate structures.
- ٤- At the collapse load, the location and the sequence of formation of all plastic hinges can be easily indicated by the proposed grillage method. Moreover, this method can predict the failing members (due to flexure or shear) during the incremental loading procedure.
- ٥- The difference corresponding for the maximum vertical deflections and at the collapse load between the cellular plate structure for the linear varying depth and for the linear varying width (*Younis M.H*(٢٠٠١)^(٩٤)) and for the prismatic structure (*Mashal* (1997)^(٥٦)) because the different between the shape of the structure and the different between the dimension (depth and width).

٧.٢ Recommendations

For further work on the nonlinear post-buckling behavior of cellular plate structures, the proposed grillage method can be extended according to the following suggested recommendations:

- ١- There is a need for further studies on the real representation of the boundary conditions of the compression flange plates in the evaluation of buckling coefficients of these plates.
- ٢- Additional work is required to study the effect of initial imperfections and residual stresses (due to welding) in the component plates.
- ٣- The present study can be developed by including the effects of openings in webs and or flanges on the behavior of cellular plate structures in their nonlinear range and at collapse.
- ٤- The suggested method can be extended to allow for the dynamic analysis of cellular plate structures curved in plan.
- ٥- The local bending and deflection behavior of the flanges directly under loads may be taken into consideration (by superimposing local effect to the general effect from the grillage analysis).
- ٦- Investigate the applicability of the method for cellular plate structures with relatively large distance between successive webs through considering interface element or factious element between them.

References

1-

AASHT

O (1 9 9 7)

“ Standard Specifications for Highway Bridges: American Association of State Highway and Transportation Officials, 16th Edition, Washington D.C., Cited in (٥٣).

٢- **Abdel Rahman , H,H,and Hinton , E. (1 9 8 7)**

“ Nonlinear Finite Element Analysis of Reinforced Concrete Stiffened and Cellular Slabs. “ Computers Structures”, Vol. ٢٣, No, ٣, Pp.٣٣٣-٣٥٠.

٣- **AISC (1 9 8 9)**

“Specification for Structural Steel Buildings, Allowable Stress Design and Plastic Design “ American Institute of Steel Construction, 9th Edition Chicago, I)) Cited in (٥٣).

٤- **AISI (1 9 9 1)**

“ Specification for Design of Cold –Formed Steel Structural Members “. American Iron Steel Institute, NW, Washington, D.C. Cited in (٥٣).

٥- **Al-Azawi , R. K. Sh. , (٢ ٠ ٠ ٠)**

“Linear and Non Linear Response of Thin – Walled Cellular and Ribbed Decks Curved in Plan “, Thesis Presented for the Doctor of Philosophy, Department of Civil Engineering University of Baghdad, Iraq.

٦- **Al-Daami,H,H. (٢ ٠ ٠ 1)**

“Linear and Non- Linear Static and Free Vibration Analysis of Thin-Walled Cellular and Ribbed Spherical Domes by Spherical Grillage Analogy ” Thesis Presented for the Degree of Doctor of philosophy, Dept. of Civil Eng., University of Baghdad, Iraq.

٧- **Al-Dosari , M.J.I. (٢ ٠ ٠ 1)**

Elastic Analysis of Cellular Plate Structures With Nonparallel Webs and Diaphragms With Inclusion of Warping “ Thesis Presented for the Degree of Master of Science, Department of Civil Engineering, University of Baghdad, Iraq.

٨- **Al-Dulaimy R.A. (٢ ٠ ٠ 1)**

Static and Free Vibration Analysis of Cellular Plate and Cellular – Hyperbolic Paraboloid Shell by Grillage Analogy “ Thesis Presented for the Degree of Doctor of Philosophy, Department of Civil Engineering, University of Baghdad, Iraq.

٩- **AL-Jowari,S.A. (٢ ٠ ٠ ٣)**

“Linear and Nonlinear Analysis and Ultimate Strength Investigation of a Horizontally Curved Cellular Duck Bridge “Thesis Presented for the Degree of Master of Science, Department of Civil Engineering, University of Bablone, Iraq.

10- *Al-Musawi, A.M.I.* (٢٠٠٠)

“Analysis and Optimum of Large Diameter Domes ” Thesis Presented for the Degree of Doctor of philosophy, Dept. of Civil Eng., University of Baghdad, Iraq.

11- *Al – Sherrawi , M.H.M.* (١٩٩٥)

“ Elastic Analysis of Steel Cellular Plate Structures with Nonparallel Webs and Diaphragms “. Thesis Presented for the Degree of Master of Science, Department of Civil Engineering, University of Baghdad, Iraq.

12- *Bakht B. Jaeger L.G. , Cheung ,M.S. and Mufti A.A.* (١٩٨١)

“ The State of the Art in the Analysis Cellular and Voided Slab Bridges “ Canadian Journal of Civil Engineering, Vol.٨, No. ٣, Pp ٣٧٦-٣٩١.

13- *Basler , K. and Thurlimann , B.* (١٩٥٩)

“ Plate Girder Research “ Proceedings of the National Engineering Conference, AISC, American Institute of Steel Construction, New York, N.Y., Cited in (٥٣).

14- *Basler , K.* (١٩٦١)

“ Strength of Plate Girders in Shear “ Journal of Structural Engineering, ASCE, Vol. ٨٧ No. St٨, Pp.١٥١-١٨٠.

15- *Basu , A. K. and Dawson , J.M.* (١٩٧٠)

Orthotropic Sandwich plates “. Supplement to Proceedings of the Institution of Civil Engineering, Pp.٨٧-١١٥, Cited in (١١).

16- *Brookhant, G.C.* (١٩٧٦)

“Circular Arc I-Type Girders”, Journal of Structural Division, ASCE Vol. ٩٣, Pp.١٣٣-١٥٩.

17- *Bradford, M.A.* (١٩٩٦)

Improved Shear Length of Webs Designed in According With LRFD Specifications “ ASIC Engrg, J. Vol.٣٣, No. ٣, Pp.٩٥-١٠٠, Cited in (٥٣).

18- *Brush,D.O. and Al- Mroth,B.O.* (١٩٧٥)

“ Buckling of Bars, Plates and Shells ”, Mc Graw Hill Company New York

19- *Chern , C. and Ostapenko , A .* (١٩٦٩)

“ Ultimate Strength of Plate Girders Under Shear “ Fritz Engineering Laboratory Report No. ٣٢٨.٧, Lehigh University, Bethlehem, Pa, Cited in (٥٣).

٢٠- *Chilver , A.H.* (١٩٦٧)

“ Thin Walled Structures “ A Collection of Papers On the Stability and Strength of Thin Walled Structural Members and Frames, Chatto and Windus, London.

٢١- *Chu,K.H. and Pinjavor,S.G.* (١٩٧١)

“ Analysis of Horizontal Curved Box Girders and Bridges “, ASCE Structural Division, Vol. ٩٧, No. St. ١٠, Pp. ٢٤٨١-٢٥٠٠.

٢٢- *Cooper, P.B.* (١٩٦٥)

“ Bending and Shear Strength of Longitudinally Stiffened Plate Girders “ Fritz Engineering Laboratory, Report No. ٣٠٤.٦, Lehigh University Cited (٥٣).

٢٣- *Cooper, P.B.* (١٩٧١)

The Ultimate Bending Moment for Plate Girders “ Proceedings of the International Association of Bridge and Structural Engineering (Iabse) Vol.٣٠, Pp. ١١٣-١٤٨. Cited in (٥٨).

٢٤- *Crisfield , M. A. , and Twemlow R.P.* (١٩٧١)

“ The Equivalent Plate Approach for the Analysis of Cellular Structures “ Civil Engineering and Public Works Review, Pp. ٢٠٩-٢٦٣.

٢٥- *Cusens A. R., and Pama , R.P. (١٩٧٥)*

“ Bridge Deck Analysis “ John Wiley and Sons, London.

٢٦- *Day, S.S. (١٩٨٠)*

“Finite Element Strip Method for Analysis of Orthotropic Curved Bridges, Decks”, Proc. Instn. Civil Eng., Part two, vol. ٦٩, June, Pp ٥١١-٥١٩.

٢٧- *Dabrowski,R. (١٩٨٨)*

“Curved Thin Walled Girders Theory and Analysis ”, Cement and Concrete Association, London Translation No. ١٤٤.

٢٨- *Dezi , L. and Mentrasti , L. (١٩٨٥) .*

Nonuniform Bending-Stress Distribution (Shear Lag) “ J. of Structural Engineering, ASCE, Vol.١١١, No. ١٢, Pp. ٢٦٧٥-٢٦٩٠.

٢٩- *Eurocode ٣, Part ١.٣ (١٩٩٠)*

“ Cold – Formed Thin Gauge Members and Sheeting “ Cited in (٤٨).

٣٠- *Evans, H. R., and Shanmugam , N.E. (١٩٧٩)*

“ An Approximate Grillage Approach to the Analysis of Cellular Structures “ Proceedings of the Institution of Civil Engineering, Part ٢, Vol.٦٧, Pp.١٣٣-١٥٤.

٣١- *Evans, H. R., and Shanmugam , N.E. (١٩٧٩)*

“The Elastic Analysis of Cellular Structures Containing Web Openings “ Proceedings of the Institution of Civil Engineers, Part ٢, Vol. ٦٧, Pp.١٠٣٥-١٠٦٣, Cited in (٣١).

٣٢- *Evans, H. R., and Shanmugam, N.E. (١٩٨٤)*

“ Simplified Analysis for Cellular Structure “ Journal of Structural Engineering, ASCE Vol.١١٠, No.٣, Pp. ٥٣١-٥٤٣.

٣٣- *Evans, H. R., Pesksa, D. O. and Taherian A.R. (١٩٨٥)*

The Analysis of the Nonlinear and Ultimate Load Behavior of Plated Structures By the Finite Element Method “ Eng. Comput., Vol.٢ , Pp.٢٧١-٢٨٤ , Cited in (٥).

٣٤- *Evans, H. R., Porter, D.M. and Rockey K.C. (١٩٧٦)*

“ A Parametric Study of the Collapse Behavior of Plate Girders “ University College, Cardiff, Report, Cited in (٧٢).

٣٥- *Fairooz , A. A. (١٩٩٧)*

“ Elastic Analysis of Steel Cellular Plate Structure Curved in Plan. “ Thesis Presented for the Degree of Master of Science, Department of Civil Engineering, University of Baghdad, Iraq.

٣٦- *Faulkner, D. (١٩٧٣)*

“ A Review of Effective Plating to Be in the Analysis of Stiffened Plating in Bending and Compression “ Massachusetts Institute of Technology, Cambridge, Mitsg ٧٣١١, Noaa ٧٣٠٧٢٣٠١.

٣٧- *Fujita,Y. and Yoshido,K. (١٩٧٧)*

“On Ultimate Collapse of Ships Structures-Researches in Japan”, Proc. Institutional Conference, Crosby Lockwood Staple, London.

٣٨- *Ghali , A. , Neville , A. M. and Cheung , Y. K. (١٩٧٧)*

“ Structural Analysis – A Unified Classical and Matrix Approach “. 2nd Edition, John Wiley and Sons, New York.

٢٩- **Hambly , E.C. , and Pennells . E. (١٩٧٥)**

“ Grillage Analysis Applied to Cellular Bridge Decks “. The Structural Engineering, Vol.٥٣, No.٧, Pp.٢٦٧-٢٧٤.

٤٠- **Harding, J. E. (١٩٩٥)**

“ Non – Linear Analysis of Components of Steel Plated Structures “ Proceedings of the 1st European Conference On Steel Structures, Athens Greece, ١٨-٢٠ May.

٤١- **Harding, J. E., Hindi, W. and Rahal, K. (١٩٩٠)**

“ The Analysis and Design of Stiffened Plate Bridge Components “ SSRC (Structural Stability Research Council), Annual Technical Session St. Louis, USA., Pp. ٢٦٧-٢٧٦ .

٤٢- **Hassan, A. F. (١٩٩٨)**

“Static and Dynamic Analysis of Spherical Domes By Method of Space Grillage“, Thesis Presented for the Doctor of Philosophy, Department of Civil Engineering University of Baghdad, Iraq.

٤٣- **Hayashikawa, T. Watanabe, N. and Ohshima, H. (١٩٨٠)**

“ On Limit Analysis of Grillage Girders “ Journal of Civil Eng. Design, Vol.٧, No.٤, Pp.٣٧٩-٣٩٠.

٤٤- **Hsu,T.T.C, (١٩٨٨)**

“ Softening Truss Model Theory for Shear and Torsion ”, ACI Journal, Vol. ٨٥, No. ٦, Nov.-Dec., Pp. ٦٢٤-٦٣٥.

٤٥- **Husain, H.M. (١٩٦٤)**

“ Analysis of Rectangular Plates and Cellular Structures “. Thesis Presented for the Degree of Doctor of Philosophy, Department of Civil Eng. University of Leeds, England.

٤٦- **Husain, H.M., Al-Ausi, M.A.A. and Al-Azawi, R. K. (١٩٩٩)**

“Torsional Stiffness of Straight and Curved Thin Walled Member with Warping Restrain” The Scientific Journal of Tekreet University, Eng. Science Section, Vol. ٦, No. ٤, Pp ١-٣٠.

٤٧- **Jaeger , L. G. and Bakht , B. (١٩٨٢)**

“ The Grillage Analogy in Bridge Analysis “ Canadian Journal of Civil Eng. , Vol.١٢ , No.١ , Pp. ٢٢٤-٢٣٥ .

٤٨- **Just,D.J (١٩٩٢)**

“ Circularly Curved Beam Under Plane Loads “ Journal of Structural Division, ASCE, Vol.١٠٨, No. St.٨ Aug., Pp. ١٨٥٨-١٨٧٣.

٤٩- **Kalyanaraman , V. and Rao , K. S. (١٩٩٨)**

“ Torsional – Flexural Buckling of Singly Symmetric Cold – Formed Steel Beam Columns “ JOURNAL of Constructional Steel Research Vol.٤٦, No.١-٣, Paper No.٣٢٨, Issn: ٠١٤٣-٩٧٤x.

٥٠- **Kuzmanovic , B.O. and Graham , H.J. (١٩٨١)**

“ Shear Lag in Box Girders “ Journal of the Structural Division, ASCE, Vol.١٠٧, No.St٩, Pp.١٧٠١-١٧١٢.

٥١- **Koniki,I. and Komatsu,S. (١٩٦٥)**

“ Three Dimensional Analysis of Curved Girders With Thin- Walled Cross Section ”, Publication International Association for Bridges and Structural Engineers ”, Vol. 20, Pp. 143-203.

٥٢- **Lamas, A.R.G., and Dowling, P. J. (1979).**

“ Effect of Shear Lag on the Inelastic Bulking Behavior of Thin – Walled Structures “. Thin – Walled Structures, Vol. 6, Pp. 100-121.

٥٣- **Lee, S.C. Davidson , J.S. , and Yoo, C.H. (1996).**

“ Coefficients of Plate Girder Web Panels “ Computer and Structures, Vol. 09, No. 0, Pp. 789-790, Cited in (٥٣).

٥٤- **Lee, S.C., and Yoo, C.H. (1998)**

“ Strength of Plate Girder Web Panels Under Pure Shear “ Journal of Structural Engineering ASCE, Vol. 124, No. 2, Pp. 184-194.

٥٥- **Marsh, C. (1998)**

“ Design Method for Buckling Failure of Plate Elements “ Journal of Structural Engineering ASCE, Vol. 124, No. 7, Pp. 800-803.

٥٦- **Mashal , Y.T. (1997)**

“ Non-Linear and Ultimate Load Investigation of Steel Cellular Plate Structures by Grillage Analogy. Thesis Presented for the Degree of Master of Science Department, Civil Engineering, University of Baghdad, Iraq.

٥٧- **Mofatt , K.R. and Dowling , P.J. (197٥)**

“ Shear Lag in Steel Box Girder Bridges. The Structural Engineering, Vol. 03, and No. 10 Pp. 749-848.

٥٨- **Mohammed, J.K. (1994)**

“ Elastic Analysis of Steel Cellular Plate Structured by Double Parallel Plates with Webs and Diaphragms “. Thesis Presented for the Degree of Master of Science Department, Civil Engineering, University of Baghdad, Iraq

٥٩- **Murray, N.W. (1984)**

“ Introduction to the Theory of Thin – Walled Structures “ Clarendon Press, Oxford.

٦٠- **Nakai, H. and Yoo, C.N. (1988)**

“ Analysis and Design of Curved Steel Bridges ”, Mc GraW Hill Book Company.

٦١- **Nastran (1994)**

“ Msc/Nastran for Windows Ver ٧ “ The Macneal – Schwendler Corporation (Msc), Enterprise Software Products, Inc., Los Angeles, California.

٦٢- **Oden ,J. T. (1977)**

“ Mechanics of Elastic Structures “, Mc GraW Hill Book Company.

٦٣- **Ova Lagerqvist (1994)**

“ Patch Loading Resistance of steel Girders Subjected to Concentrated Forces “, Thesis Presented for the Doctor of Philosophy, Department of Civil Engineering Luleå University of Technology.

٦٤- **Pavlovic , M.N., Tahan , N., and Kostovos M.D. (1998)**

“ Shear Lag Effective Breadth in Rectangular Plates with Material Orthotropy “ Part ١: Analytical Formulation, Thin –Walled Structures, Vol. 30, and Nos. 1-4, Pp. 199-213.

- ٦٥- **Proter , D.M. , Rucker , K.C. and Evans , H.R. (١٩٧٥)**
 “ The Collapse Behavior of Plate Girders Loaded in Shear “ The Structural Engineer, Vol.٥٣, No.٨, Pp.٣١٣-٣٢٥, Cited in (٥٣).
- ٦٦- **Razaqpur,A.G.) and Li ,H.G. (١٩٩٧**
 “ Analysis of Curved Multi-Cell Box Girder Assemblages ”, Journal of Structural Engineering and Mechanics, Vol. ٥, No. ١, Jan. Pp. ٣٣-٤٩.
- ٦٧- **Razaqpur,A.G. and Li ,H.G. (١٩٩٤)**
 “ Curved Thin-Walled Multi-Cell Box Girder Finite Element ”, Journal of computer and structure, Vol. ٥٣, No. ١, Pp. ١٣١-١٤٢.
- ٦٨- **Reilly,R.J. (١٩٧٢)**
 “ Stiffness Analysis of Grids Including Warping ”, Proc. American Society of Civil Engineering, St.٧, Pp. ١٥١١-١٥٢٣.
- ٦٩- **Rahal , K.N. and Harding , J.E. (١٩٩٠)**
 “ Transversely Stiffed Girder Webs Subjected to Shear Loading “ Proceedings of the Institution of Civil Engineers, Part ٢, Vol.٨٩, Pp.٦٧-٨٧.
- ٧٠- **Rahal , K.N. and Harding , J. E. (١٩٩١)**
 “Transversely Stiffed Girder Webs Subjected to Combined In-Plane Loading “ Proceedings of the Institution of Civil Engineering. Part ٢, Vol.٩١, Pp.٢٣٧-٢٥٨.
- ٧١- **Ranby , A. (١٩٩٨)**
 “ Structural Fire Design of Thin Walled Steel Sections “ Journal of Constructional Steel Research, Vol. ٤٦, No.١-٣, Paper No. ١٧٦ and ISSN: ٠١٤٣-٩٧٤x.
- ٧٢- **Reissner , E. (١٩٤١)**
 “ Least Work Solutions of Shear Lag Problems. “ Presented At the Structures Session, ٩tyh Annual Meeting, i.e., New York, Journal of the Aeronautical Sciences, Pp.٢٨٤-٢٩١.
- ٧٣- **Rockey, K.C., Evans. H. R. and Porter, D.M. (١٩٧٨)**
 “ A Design Method for Predicating the Collapse of Plate Girders “ Proceedings of the Institution of Civil Engineering, Part ٢, Vol.٦٥, Pp. ٨٥-١١٢.
- ٧٤- **Rockey, K.C. and Skaloud , M.(١٩٧٢)**
 “ The Ultimate Load Behavior of Plate Girders Loaded in Shear.” The Structural Engineering,” Vol.٥٠, No.١, Pp. ٢٩-٤٧.
- ٧٥- **Sawko , F. and Willcock , B.K. (١٩٦٧)**
 “ Computer Analysis of Bridges Having Varying Section Properties “ The Structural Engineering, Vol.٤٥, No.١١, Pp.٣٩٥-٣٩٩.
- ٧٦- **Sawko, F. and Cope, R.G. (١٩٦٩)**
 “ Analysis of Multicell Bridges Without Transverse Diaphragms – A finite Element Approach. “ The Structural Engineering”, Vol. ٤٧, No. ١١, Pp. ٤٥٥-٤٦٠.
- ٧٧- **Schafer , B.W, and Pekos , T. (١٩٩٨)**
 “ Cold – Formed Steel Members With Multiple Longitudinal Intermediate Stiffeners “ Journal of Structural Engineering, ASCE, Vol. ١٢٤, No.١٠, Pp.١١٧٥-١١٨١.
- ٧٨- **Shanmugam, N.E. and Evans, H.R. (١٩٧٩)**

“ An Experimental and Theoretical Study of the Effects of Web Openings Upon the Elastic Behavior of Cellular Structures. “ Proceedings of the Institution of Civil Engineers,” Part 2, Vol. 67, Pp. 603-676, Cited in (31).

49- **Shanmugam, N.E. and Evans, H.R.** (1981)

“ A Grillage Analysis of the Non- Linear and Ultimate Load Behavior of Cellular Plate Structures Under Bending Loads “Proceedings of the Institution of Civil Engineers, Part 2, Vol. 71, Pp. 700-719.

50- **Sharp, M.L. and Clark, J.W.** (1971)

“ Thin Aluminum Shear Web “ Journal of Structural Division, ASCE, Vol. 97, No. 5, Pp. 1021-1038, Cited in (03).

51- **Smyth, W.J.R. and Sinavasan , S.** (1971)

“ The Analysis of Multicellular Box Structure “ Proceedings of the Conference On Development of Bridge Design and Construction, Cardiff Crosby Lockwood and Sons, London, Pp. 441-453.

52- **Song, Q., and Scordelis , A.C.** (1990)

“ Formulas For Shear Lag Effect of T-, I- and Box Beams “ Journal of Structural Engineering, ASCE, Vol. 116, No. 6, Pp. 1306-1318.

53- **Song, Q., and Scordelis , A.C.** (1990)

“ Shear the Analysis of T- and I- and Box Beams “ Journal of Structural Engineering, ASCE, Vol. 116, No. 6, Pp. 1290-1300.

54- **Structural Stability Research Council (Ssrc)** (1988)

“ Guide to Stability Design Criteria for Metal Structures “ 4th Edition, T.Galambos , Ed. , John Wiley and Sons , New York , N.Y. , Cited in (03).

55- **Szilar, R.** (1974)

“ Theory and Analysis of Plates (Classical and Numerical Method) ”, Prentice Hall. Inc., N. Journal.

56- **Timoshenko, S.P. and Gere , J.M.** (1971)

“ Theory of Elastic Stability “ 2nd Edition, Mcgraw – Hill Book Company, New York.

57- **Timoshenko, S.P. and Goodier , J.N.** (1901)

“ Theory of Elasticity “ 2nd Edition, Mcgraw-Hill Book, New York.

58- **Timoshenko, S.P** (1980)

“ Strength of Material “Part 2 Advances Theory and Problem, Van Nostrand Reinhold Company, 3rd Edition.

59- **Von Karman, T., Schler , E.E and Donnell , L.H.** (1932)

“ The Strength of Thin Plates in Compression “ Trans ASME (American Society of Mechanical Engineers.) Vol. 54, Pp. 53-58, Cited in (76).

60- **Waldron, p.** (1980)

“ Elastic Analysis of Curved Thin-Walled Girders Including the effect of Warping Restraints “ Engineering Structure, Vol. 7, Apr., Pp. 93-104.

61- **Wang, C.K.** (1973)

“ General Computer for Limit Analysis “ Journal of the Structural Division, ASCE, Vol. 89, No. St 7, Pp. 101-117, Cited in (37).

62- **Winter, G.** (1947)

“ Strength of Thin Steel Compression Flanges “ Terms. ASCE, Vol. 112, Pp. 1-
5.

93- **Yang, Daily and Chang (1991)**

“ Torsional Analysis for Multi Box Cells Using Softening Truss Model “,
Journal of Structural Engineering and Mechanics, Vol. 5, No. 1, Jan. Pp. 21-32.

94- **Younis, M. H. (2001)**

“ Non Linear Analysis and Ultimate Strength Investigation of Cellular Plate
Structure with Non-Parallel Webs”, Thesis Presented for the Degree of Master
of Science, Department of Civil Engineering, University of Baghdad, Iraq.

95- **Methak, Al-Fatlawy (2001)**

“Linear Analysis and Ultimate Strength Investigation of Cellular Plate Structure
with Linear Varying Depth”, Thesis Presented for the Degree of Master of
Science, Department of Civil Engineering, University of Baghdad, Iraq.